Contributions to Regional Haze in the Northeast and Mid-Atlantic United States

Mid-Atlantic/Northeast Visibility Union (MANE-VU) Contribution Assessment

Prepared by NESCAUM
For the Mid-Atlantic/Northeast Visibility Union (MANE-VU)

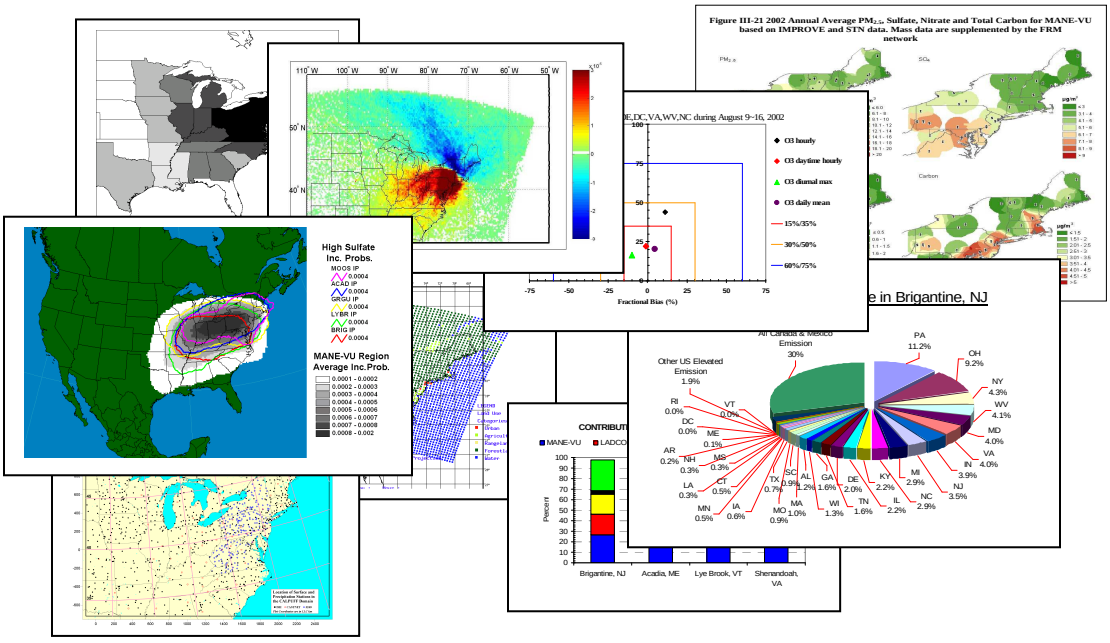

August 2006

Members of NESCAUM Board

Arthur Marin, Executive Director
NESCAUM

Anne Gobin, Bureau Chief
Connecticut Department of Environmental Protection, Bureau of Air Management

James P. Brooks, Bureau Director
Maine Department of Environmental Protection, Bureau of Air Quality

Barbara Kwetz, Director
Massachusetts Department of Environmental Protection, Bureau of Waste Prevention

Robert Scott, Director
New Hampshire Department of Environmental Services, Air Resources Division

William O'Sullivan, Director
New Jersey Department of Environmental Protection, Office of Air Quality Management

David Shaw, Director
New York Department of Environmental Conservation, Division of Air Resources

Stephen Majkut, Chief
Rhode Island Department of Environmental Management, Office of Air Resources

Richard A. Valentinetti, Director
Vermont Department of Environmental Conservation, Air Pollution Control Division

Contributions to Regional Haze in the Northeast and Mid-Atlantic United States

Mid-Atlantic/Northeast Visibility Union (MANE-VU) Contribution Assessment

Prepared by
NESCAUM

August 2006

Contributions to Regional Haze in the Northeast and Mid-Atlantic United States

Mid-Atlantic/Northeast Visibility Union (MANE-VU) Contribution Assessment

Project Director

Gary Kleiman, NESCAUM

Program Officer

Marcia Spink, U.S. EPA

Editors

John Graham, NESCAUM
Gary Kleiman, NESCAUM
Marika Tatsutani, NESCAUM
Paul Miller, NESCAUM

Principal Contributors (listed alphabetically by chapter)

Chapter 1:	Gary Kleiman, NESCAUM
Chapter 2:	Gary Kleiman, NESCAUM
Chapter 3:	George Allen, John Graham, Alan Leston, NESCAUM
Chapter 4:	Michael Borucke, John Graham, NESCAUM, Serpil Kayin, MARAMA, Jung-Hun Woo, NESCAUM
Chapter 5:	Serpil Kayin, MARAMA Iyad Kheirbek, Gary Kleiman, NESCAUM, Rich Poirot, VT DEC.
Chapter 6:	John Graham, Shan He, Emily Savelli, Jung-Hun Woo, NESCAUM
Chapter 7:	Mark Garrison, ERM, Dan Riley, Paul Wishinski, VT DEC
Chapter 8:	All of the above
Chapter 9:	Gary Kleiman, NESCAUM

Acknowledgments

NESCAUM gratefully acknowledges the support of the United States Environmental Protection Agency. Funding for this report was provided through the Mid-Atlantic/Northeast Visibility Union (MANE-VU) Regional Planning Organization (Grant No. X-983799-01-0) to the Ozone Transport Commission.

This report is the result of a joint effort by staff of the MANE-VU and its member states.

NESCAUM also thanks the following individuals and organizations for providing comments on this report:

Tom Downs, Maine Department of Environmental Protection
VISTAS
MOG
Dominion Power
AMC
Ann McWilliams, EPA Region 1

Printed: October 2006

TABLE OF CONTENTS

FIGURES

TABLES

Units, Symbols, Acronyms

Acronyms

AGL – Above Ground Level
ATAD – Atmospheric Transport and Diffusion Model
ARL – Air Resources Laboratory (NOAA)
BART – Best Available Retrofit Technology
BEIS – Biogenic Emission Inventory System
BRAVO - Big Bend Regional Aerosol and Visibility Observational study
CAIR – Clean Air Interstate Rule
CALMET – Meteorological model for developing input data for CALPUFF
CALPUFF – Lagrangian dispersion model developed by EarthTech, Inc.
CAMNET – Northeast Visibility Camera Network
CASTNet – Clean Air States and Trends Network
CEMS – Continuous Emissions Monitoring System
CENRAP – Central Regional Air Planning Association
CFR – Code of Federal Regulations
CMAQ – Community Multi-scale Air Quality Model
CMB – Chemical Mass Balance
CMU – Carnegie Mellon University
CTM – Chemical Transport Model
CWP – Clustered Weighted Probability
EDAS – Eta Data Assimilation System
EFIG – USEPA Emission Factor and Inventory Group
EGU – Electricity Generating Unit
EMAD – Emissions, Monitoring and Analysis Division
ERM – Environmental Resources Management, Inc.
FASTNET – Fast Aerosol Sensing and Tools for Natural aErosol Tracking
FNL – FiNaL run of the Global Data Assimilation System
FRM – Federal Reference Method
GIS – Geographic Information System
IMPROVE – Interagency Monitoring of Protected Visual Environments
IP – Incremental Probability
HAPS – Hazardous Air Pollutants
HYSPLIT – Hybrid Single-Particle Langrangian Integrated Trajectory model
MANE-VU – Mid-Atlantic/Northeast Visibility Union
MARAMA – Mid Atlantic Region Air Management Association
MDE – Maryland Department of the Environment
MDNR – Maryland Department of Natural Resources
MM5 – Fifth Generation Mesoscale Model
MOBILE – Mobile Source Emission Factor Model (USEPA)
MWRPO – Midwest Regional Planning Organization
NAAQS – National Ambient Air Quality Standards
NARSTO – North American Research Strategy for Tropospheric Ozone
NCAR – National Center for Atmospheric Research
NEI – National Emissions Inventory
NESCAUM – Northeast States for Coordinated Air Use Management
NET – National Emissions Trends (EPA)
NOAA – National Oceanic and Atmospheric Administration
NRC – National Research Council
NTI – National Toxics Inventory
NWS – National Weather Service
OAQPS – USEPA Office of Air Quality Planning and Standards

OAR – USEPA Office of Air and Radiation
OTC – Ozone Transport Commission
PCA – Principle Component Analysis
PM – Particulate Matter
PMF – Positive Matrix Factorization
PSCF – Potential Source Contribution Function
RAIN – Real Time Aerosol Intensive Network
REMSAD – Regulatory Modeling System for Aerosols and Deposition
RH – Relative Humidity
RPO – Regional Planning Organization
RTA – Residence Time Analysis
SIP – State Implementation Plan
SMOKE – Sparse Matrix Operator Kernel Emissions model
STN – Speciation Trends Network
TLD – Transport Layer Depth
TSC – Technical Support Committee
UMD – University of Maryland
UNMIX – Mathematical receptor model used for source attribution studies
USEPA – United States Environmental Protection Agency
USFS – United States Forest Service
USFWS – United States Fish and Wildlife Service
USNPS – United States National Park Service
VISTAS - Visibility Improvement State and Tribal Association of the Southeast
VT DEC – Vermont Department of Environmental Conservation
WRAP-Western Regional Air Partnership

Chemical Species

BC – Black Carbon
CM – coarse mass
CO – carbon monoxide
EC – elemental carbon
HC – hydrocarbons
H_2SO_4 – sulfuric acid
HNO_3 – nitric acid
NO_X – oxides of nitrogen (NO_2 and NO)
NO – nitric oxide
NO_2 – nitrogen dioxide
NO_3^- – nitrate
NH_3 – ammonia
NH_4 – ammonium
NH_4HSO_4 – ammonium bisulfate
$(NH_4)_2SO_4$ – ammonium sulfate
(NH_4NO_3) – ammonium nitrate
O_3 – ozone
OC – organic carbon
OMC – organic mass from carbon
$PM_{2.5}$ – particle matter up to 2.5 μm in size
PM_{10} – particle matter up to 10 μm in size
Se – selenium
SOA – secondary organic aerosol
SO_2 – sulfur dioxide
SO_4^{2-} – sulfate
VOC – volatile organic compounds

Symbols

b_{ext} – light extinction coefficient (Mm^{-1})
C_i – constant for wind sector i
d – distance
E x UP – emissions times upwind probability
f(RH) – relative humidity adjustment factor
I – impact
Q – annual emissions
R^2 – correlation coefficient

Units

Length

m – meter
μm – micrometer (0.000001m; 10^{-6}m)
km – kilometer (1,000 x m; 10^{3} m)
Mm – Megameter (1,000,000 x m; 10^{6} m)

Area

m^2 – square meter
km^2 – square kilometer

Volume

L – liter
m^3 – cubic meter

Concentration

$\mu g/m^3$ – micrograms per cubic meter
ng/m^3 – nanograms per cubic meter
ppb – parts per billion
ppm – parts per million

Scattering Efficiency

m^2/g – square meters per gram

Visibility

dv – deciview

Executive Summary

Regional haze State Implementation Plans (SIPs) due in December 2007 must include a contribution assessment and pollution apportionment analysis as part of the long-term emissions management strategy for meeting visibility improvement objectives in Class I areas subject to USEPA's 1999 Regional Haze Rule. The Mid-Atlantic/Northeast Visibility Union (MANE-VU) Technical Support Committee (TSC) has adopted a weight-of-evidence approach as a first step toward meeting these obligations and in an effort to better understand the causes of visibility impairment at Class I areas within the MANE-VU region. The weight-of-evidence approach relies on several independent methods for assessing the contribution of different emissions sources and geographic source regions to regional haze in the northeastern and mid-Atlantic portions of the United States.

The preliminary findings described in this report draw from the considerable body of work that has already been developed concerning the nature and extent of visibility impairment in the MANE-VU region. This work has produced a conceptual model of regional haze in which sulfate emerges as the most important single constituent of haze-forming fine particle pollution and the principle cause of visibility impairment across the region. Sulfate alone accounts for anywhere from one-half to two-thirds of total fine particle mass on the 20 percent haziest days at MANE-VU Class I sites. Even on the 20 percent clearest days, sulfate generally accounts for the largest fraction (40 percent or more) of total fine particle mass in the region. Sulfate has an even larger effect when one considers the differential visibility impacts of different particle constituents. It typically accounts for 70–82 percent of estimated particle-induced light extinction at northeastern and mid-Atlantic Class I sites.

While substantial visibility impairment is common across the region, it is most severe in the southern and western portions of MANE-VU that are closest to large power plant sources of sulfur dioxide (SO_2) emissions located in the Ohio River and Tennessee Valleys. Summertime visibility is driven almost exclusively by the presence or absence of regional sulfate, whereas wintertime visibility depends on a combination of regional *and* local influences coupled with local meteorological conditions (inversions) that can lead to the concentrated build-up of emissions from local sources.

These findings suggest that an effective emissions management approach would rely heavily on broad-based regional SO_2 control efforts in the eastern United States aimed at reducing summertime fine particulate matter ($PM_{2.5}$) concentrations. MANE-VU is investigating additional measures to reduce in-region emissions of SO_2 and organic carbon (OC), which is typically the next most important contributor to overall fine particle mass throughout the region. Nearby SO_2 reductions can help reduce wintertime PM concentrations, while OC reductions can help reduce total PM concentrations year-round. For areas with high wintertime PM levels, strategies aimed at reducing ambient levels of nitrogen oxides (NO_X) may also be effective.

Available monitoring data provide strong evidence that regional SO_2 reductions have yielded, and will continue to yield, reductions in ambient secondary sulfate levels with subsequent reductions in regional haze and associated light extinction. They indicate that reductions in anthropogenic primary particle emissions will also result in visibility

improvements, but that these will not have a zone of influence as large as those of the secondary aerosols.

Given the dominant role of sulfate in the formation of regional haze in the Northeast and Mid-Atlantic region — and the likelihood that SO_2 reductions will therefore need to play a central role in achieving near-term visibility improvements — this report focuses on early efforts to assess the regional sulfate contribution to ambient fine particle levels experienced at the (primarily rural) MANE-VU Class I areas. The primary objective of this report is to identify and describe the suite of analytical tools and techniques that are presently available for: (1) understanding the causes of sulfate-driven visibility impairment at Class I areas in MANE-VU and nearby regions, as well as the relative contribution of various emissions sources and geographic source regions; and (2) describe how these tools and techniques will be applied in future MANE-VU SIP work.

The analytical and assessment tools discussed in this report include Eulerian (grid-based) source models, Lagrangian (air parcel-based) source dispersion models, as well as a variety of data analysis techniques that include source apportionment models, back trajectory calculations, and the use of monitoring and inventory data. A range of methodological approaches characterize these tools, which Table ES-1 summarizes. The tools rely on different data sources and entail varying degrees of sophistication and uncertainty. Thus, it is important to emphasize that these methods have been extensively reviewed, updated, and refined over the past year to ensure that the highest quality results are now available for the SIP development process. The overall coherence and consistency of results that emerges from application of these tools and techniques suggest that what is known about the causes of sulfate pollution in the MANE-VU region is sufficiently robust to provide a useful and appropriate basis for design of future control programs and for consultations between different regional organizations charged with planning for compliance with the Regional Haze Rule.

Figure ES-1 provides one illustration of the high degree of correspondence in the results. The figure shows rankings of state contributions to sulfate mass at Brigantine Wilderness Area in New Jersey derived from several of the techniques listed in Table ES-1.[1] There is substantial consistency across a variety of analysis methods using techniques based on disparate chemical, meteorological and physical principles. Taken together, these findings create a strong weight-of-evidence case for the preliminary identification of the most significant contributors to visibility impairment in the MANE-VU Class I areas.

Similar results for other sites demonstrate that highly simplified, empirical approaches for identifying source contributions are consistent with more sophisticated approaches. Therefore, a firm basis exists for addressing contributions to regional transport of sulfate, and the range of variability between these techniques suggests the precision of these estimates.

[1] As described in Chapter 8, REMSAD is the only analysis platform used to quantify "out of domain" contributions to sulfate. Thus, the REMSAD calculated contribution for the "out of domain" sources (17% at Brigantine, NJ) was used to calculate the percent contribution shown in Figure ES-1 for all other methods.

We have further aggregated these results by regional planning organization (RPO) using state-by-state sulfate mass contributions (in $\mu g/m^3$) derived by the REMSAD, CALPUFF, emissions/distance, and emissions times (×) upwind probability methods.[2] Figure ES-2 shows these results in terms of their absolute contribution (displayed within the bars shown in the graphic) and in terms of their proportional contribution relative to other RPOs.[1]

Table ES-1. Summary of technical approaches for attributing state contributions to observed sulfate in MANE-VU Class I areas.

Analytical technique	Approach
Emissions/distance	Empirical
Incremental probability	Lagrangian trajectory technique
Cluster-weighted probability	Lagrangian trajectory technique
Emissions × upwind probability	Empirical/trajectory hybrid
Source apportionment approaches	Receptor model/trajectory hybrid
REMSAD tagged species	Eulerian source model
CALPUFF with MM5-based meteorology	Lagrangian source dispersion model
CALPUFF with observation-based meteorology	Lagrangian source dispersion model

Figure ES-1. Comparison results using different techniques for ranking state contributions (in units of percent of in-domain contribution) to sulfate levels at Brigantine Wilderness Area, New Jersey.

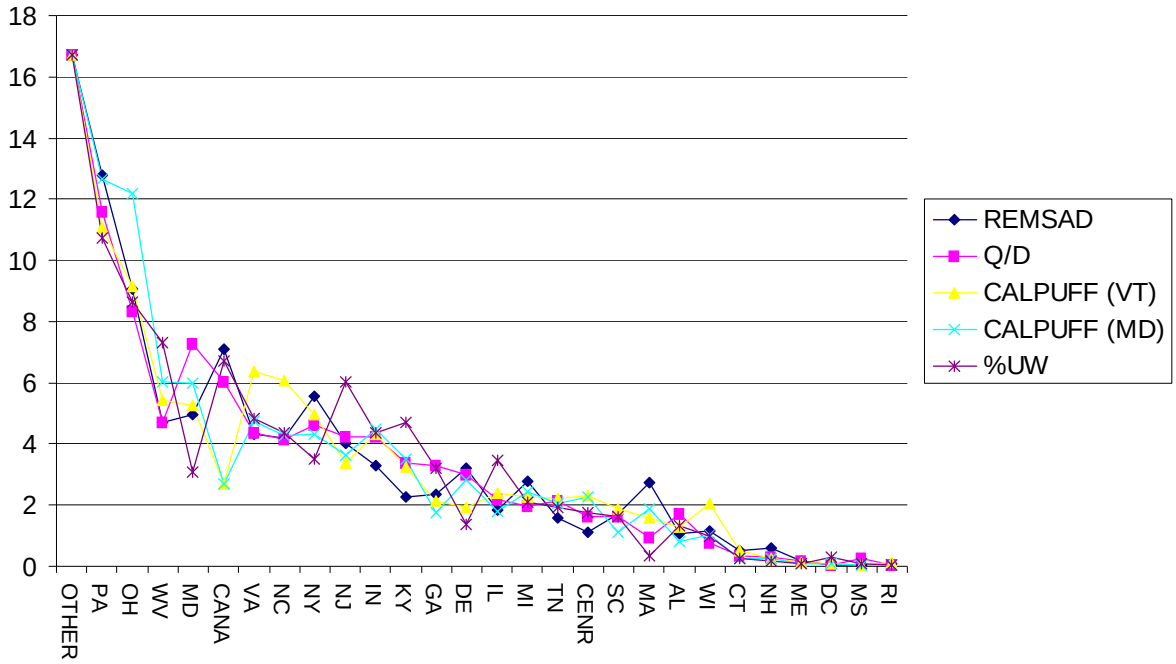

[2] See Chapter 4 for an explanation of how the emissions divided by distance technique is expressed as a sulfate mass concentration and the associated assumptions for the emissions × upwind probability method.

Notwithstanding small differences in precisely which states were included within each assessment technique, estimates obtained from averaging over the five quantitative assessment techniques indicate that MANE-VU states account for about 25-30 percent of the sulfate in the Acadia, Brigantine, and Lye Brook Class I areas. The Midwest RPO (MWRPO) and Visibility Improvement State and Tribal Association of the Southeast (VISTAS) states each account for about 15 percent of the total sulfate contribution at Acadia and about 25 percent each at Brigantine and Lye Brook. The Central states Regional Air Partnership (CENRAP) states, Canada, and an "out of domain" contribution add the remainder.[3] Although variation exists across estimates of contributions for different sites and using different techniques, the overall pattern is generally consistent.

Figure ES-2. Estimated RPO contributions to sulfate concentrations at Class I areas using different assessment techniques

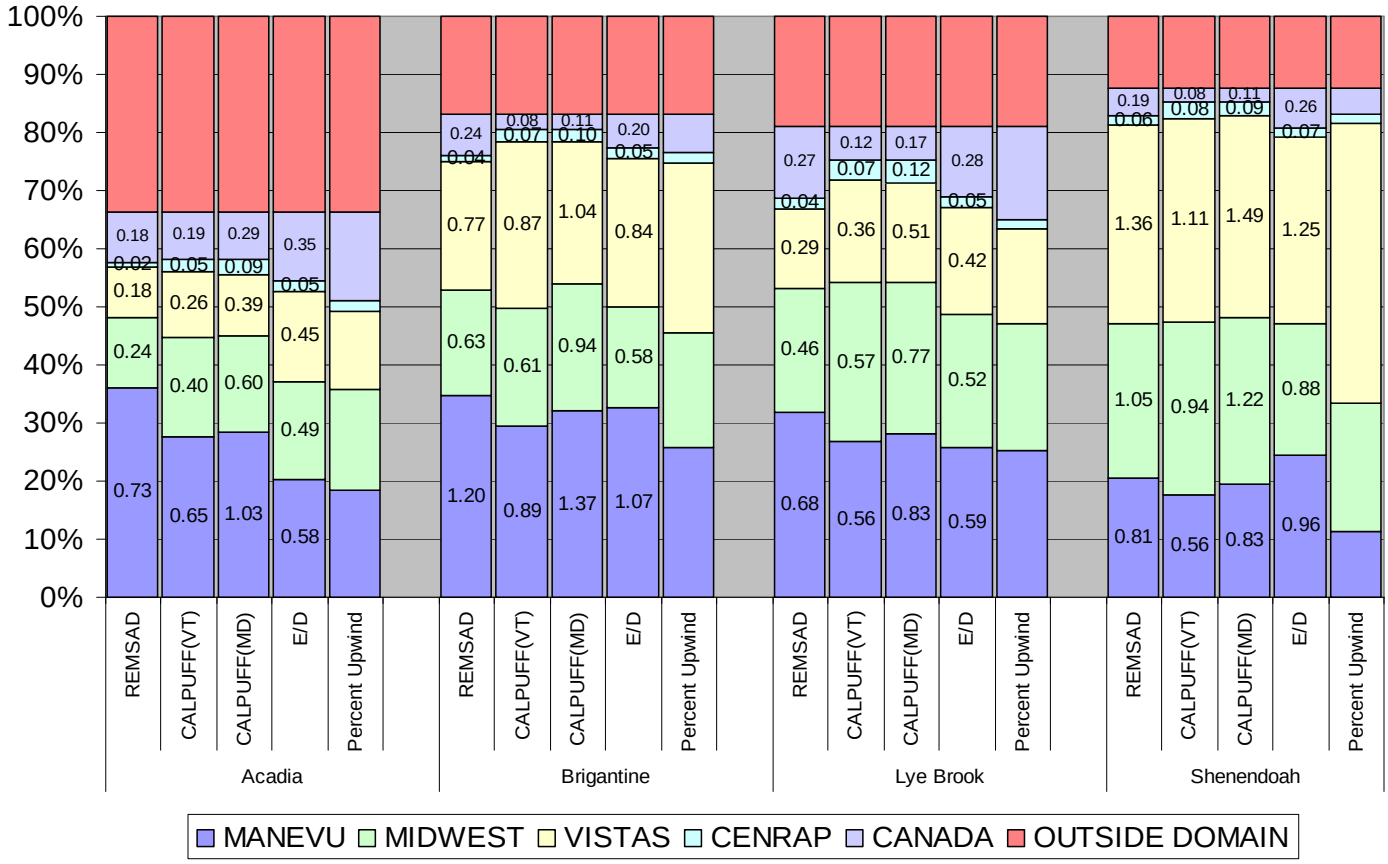

Shenandoah National Park, Virginia, which is a VISTAS Class I area, has a somewhat reversed order of relative contributions. There, VISTAS and MWRPO states account for roughly 30 percent of overall sulfate each, with MANE-VU states contributing roughly 15-20 percent and CENRAP states, Canada and "out of domain" accounting for the remainder.

[3] Note here that the contribution representing out of domain sources was – in all cases – derived solely by the REMSAD platform and that this value has been applied to the other analysis techniques to provide a consistent estimate of the total contributions to sulfate pollution at each site.

Other qualitative analysis methods have been developed that reinforce the findings shown above. These include trajectory methods and source apportionment techniques. These receptor-based methods provide compelling support for the more quantitative attribution methods discussed previously. Figure ES-3 (left panel) shows the source region associated with a "coal combustion/secondary sulfate" source profile observed at Brigantine Wilderness in New Jersey and (right panel) the predominant meteorological pathways associated with the highest sulfate observations at Brigantine. The meteorological transport regime most common during high sulfate observations (shown on the right) directly connects the most likely source region with the receptor site (shown on the left), which reinforces the large quantitative contributions of source states determined for the Brigantine receptor in Chapter 8.

Finally, we note that while sulfate is the most important particle constituent for designing near-term control strategies, reductions in other local and distant pollutant emissions are important. Additional measures will be necessary in the long term to address public health impacts of ambient fine particle concentrations and to achieve long-term regional haze goals to restore pristine visibility conditions year-round in the nation's Class I wilderness areas. This is especially true during winter months, when planners need to give particular consideration to reducing urban and mobile sources of NO_X and OC as well as sources of SO_2.

Figure ES-3. Geographic regions associated with "coal combustion/secondary sulfate" sources (left) and sulfate transport (right) for Brigantine Wilderness Area, NJ.

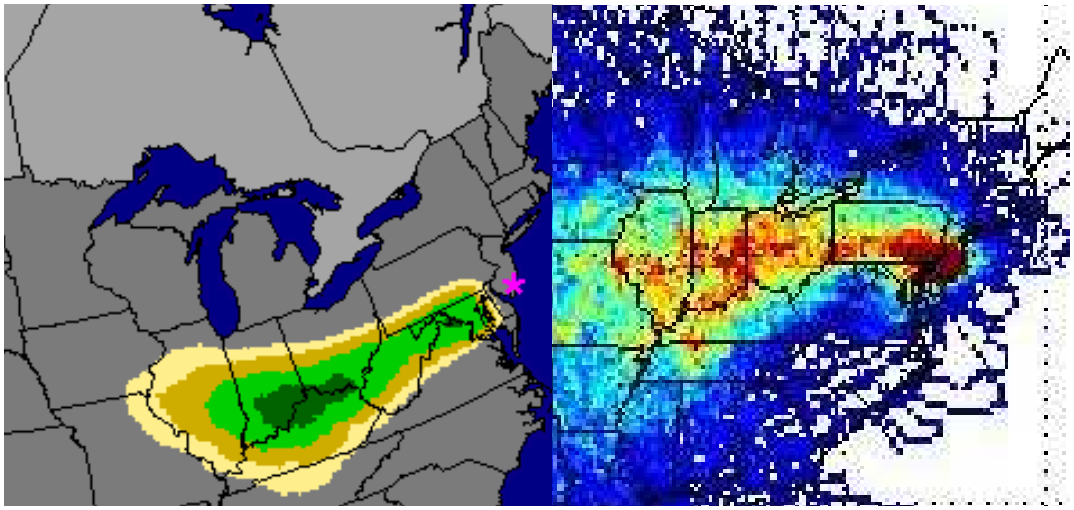

Note: This figure is the consistency of interpretation between the "coal-combustion/secondary sulfate" source region and receptor site shown in the left hand panel being directly connected by the predominant meteorological transport pathway on high observed sulfate days at Brigantine, shown in the right hand panel.

1. INTRODUCTION

The 1999 Regional Haze Rule (hereafter, the Haze Rule) requires States and Tribes to submit State Implementation Plans (SIPs) to the U.S. Environmental Protection Agency (USEPA) for approval by January 2008 at the latest. The haze SIPs must include a "contribution assessment" to identify those states or regions that may be influencing specially protected federal lands known as Federal Class I areas.[4] These states or regions would then be subject to the consultation provisions of the Haze Rule. The Haze Rule also requires a "pollution apportionment" analysis as part of the long-term emissions management strategy for each site.

In 2004, Congress harmonized the timeline for SIP submissions, including SIPs for meeting federal fine particulate matter ($PM_{2.5}$) and regional haze requirements.[5] One effect of this change is that the "regional planning SIP" or "committal SIP" — originally due one year after PM designations — will now be due along with all other SIP products in late 2007 or early 2008.

The Haze Rule originally would have applied a very low threshold test to determine whether a state would be part of a regional planning process, As a result of the congressional harmonization, however, the requirement for a contribution assessment is now, in effect, part of the "pollution apportionment" analysis used to determine which sources must be included in a long-term emissions management strategy. This is subject to a somewhat higher threshold of evidence since it forms the basis for judging whether long-term strategies are adequately addressing the causes of haze in protected areas.

To adequately determine the degree to which specific geographic regions or areas are contributing to visibility impairment at MANE-VU Class I areas, the MANE-VU Technical Support Committee (TSC) has adopted a weight-of-evidence approach that relies on several independent methods of attribution. These include Eulerian (grid-based) source models, Lagrangian (air pollution-based) source dispersion models, and a variety of data analysis techniques that include source apportionment models, back trajectory calculations, and the use of monitoring and inventory data.

---

[4] The Class I designation applies to national parks exceeding 6,000 acres, wilderness areas and national memorial parks exceeding 5,000 acres, and all international parks that were in existence prior to 1977. In the MANE-VU area, this includes: Acadia National Park, Maine; Brigantine Wilderness (within the Edwin B. Forsythe National Wildlife Refuge), New Jersey; Great Gulf Wilderness, New Hampshire; Lye Brook Wilderness, Vermont; Moosehorn Wilderness (within the Moosehorn National Wildlife Refuge), Maine; Presidential Range – Dry River Wilderness, New Hampshire; and Roosevelt Campobello International Park, New Brunswick.

[5] In the Omnibus Appropriations Act of 2004 [Consolidated Appropriations Act for Fiscal Year 2004, Pub. L. 108–199, January 23, 2004], Congress harmonized both designations and regional haze SIP deadlines. EPA promulgated $PM_{2.5}$ designations for all areas of each state on December 17, 2004. The Omnibus Appropriations Act provides that regional haze SIPs for each state as a whole are then due not later than three years after promulgation of the $PM_{2.5}$ designations. Thus, all components of the regional haze SIPs are now due no later than December 17, 2007 (three years after the USEPA issued the official designations). The USEPA has suggested informally that they will accept Regional Haze SIPs in April 2008 when $PM_{2.5}$ SIPs are due.

While we already know much about visibility impairment and its causes in the MANE-VU region (see NESCAUM, 2001; NESCAUM, 2002), significant gaps in understanding remain with respect to the organic component of fine particulate pollution. While we expect continuing research activities to substantially benefit future SIP efforts, the MANE-VU members have determined that sufficient information exists to design effective emission control strategies to meet visibility goals through 2018.

Reducing sulfur emissions offers particular leverage for achieving near-term visibility goals. It is the sulfate fraction of airborne fine particle matter that dominates light extinction on the 20 percent worst visibility days in the Northeast and Mid-Atlantic region. This is important because improving visibility on the 20 percent worst days is a near-term regulatory objective under the Regional Haze rule. In addition, many tools are available for assessing sulfate contributions. Therefore, this document focuses to a large extent on assessing sources and source regions for the sulfate fraction of haze-causing particles.

To lay a foundation for the analyses described in later chapters of this report, Chapter 2 provides a conceptual model of visibility impairment in the eastern United States. Chapter 3 presents a summary of available monitoring data and observations that we use to support the conceptual model and to validate models and data analyses. In fact, measured data — far from being used merely to support modeling analyses — serve as the primary basis for several of the receptor techniques presented in later chapters. There is thus no substitute for a robust monitoring network to understand the causes of fine particle pollution and visibility impairment.

Later chapters reinforce the notions introduced in Chapters 2 and 3 in using emission inventories (Chapter 4), receptor-based approaches including the use of back trajectories, trajectory clustering techniques and source apportionment models (Chapter 5), Eulerian chemical transport models (Chapter 6), and Lagrangian dispersion models (Chapter 7). We synthesize and interpret these various techniques in Chapter 8 and present conclusions in Chapter 9. We discuss technical aspects of the analyses in several of these later chapters in greater detail in a series of appendices.

As a general matter throughout this report, the focus is on assessing the contribution of all sources within broad geographical areas (i.e., whole states) whose combined emissions are likely to contribute to regional haze. As cited in Watson (2002), the National Research Council (NRC) has concluded that:

> (1) "…a program that focuses solely on determining the contribution of individual emission sources to visibility impairment is doomed to failure. Instead, strategies should be adopted that consider many sources simultaneously on a regional basis, although assessment of the effect of individual sources will remain important in some situations;" (2) "…there are (and will probably continue to be) considerable uncertainties in ascertaining a precise relationship between individual sources and the spatial pattern of regional haze;" and (3) "…the best approach for evaluating emission sources is a nested progression from simpler and more direct models to more complex and detailed methods" (Watson, 2002).

Watson (2002) goes on to point out that, "Part of the modeling conundrum is the focus of modeling efforts on demonstrating attainment rather than gaining a better understanding of the situation. Although USEPA emphasizes the construction of a conceptual model and evaluation of the weight of evidence in its introduction, the modeling details contained in the guidance are business as usual: seeking a quantitative comparison of present and future design values with a numerical goal."

Consistent with the NRC's admonition and USEPA's stated desire to incorporate weight-of-evidence approaches to improve conceptual models, MANE-VU has attempted wherever possible to incorporate qualitative analyses in sensible ways so as to increase confidence in its quantitative estimates of the contribution of various emissions sources and source regions to regional haze.

References

NESCAUM, *Regional Haze and Visibility Impairment in the Northeast and Mid-Atlantic United States*, Northeast States for Coordinated Air Use Management, Boston, MA, January, 2001.

NESCAUM, *Updated Visibility Statistics for the MANE-VU Region Technical Memorandum #1*, Northeast States for Coordinated Air Use Management, Boston, MA February, 2002.

Watson, J., "Visibility: Science and Regulation," *JAWMA* 52:628-713, 2002.

2. CONCEPTUAL MODEL OF REGIONAL HAZE IN THE MANE-VU REGION

Developing a conceptual model of regional haze requires combining experience and atmospheric-science expertise with multiple data sources and analysis techniques. This includes measured data on ambient pollutant concentrations as well as emission inventory and meteorological data, chemical transport modeling, and observationally based models (NARSTO, 2003). Here, we begin with a conceptual model based on the existing scientific literature concerning fine particles and their effect on visibility. This includes numerous review articles and reports on the subject. Most past assessments of fine particle pollution and visibility impairment have tended to be national in scope. For purposes of this discussion, we have selectively reviewed the literature in order to present a distinctly Eastern focus.

Because the uncertainties involved in any particular method of analysis are usually large or ill-defined, it is preferable to develop visibility and fine particle management strategies with inputs from multiple analyses using multiple approaches. The MANE-VU TSC has adopted this approach, which leads to the diversity of data analyses and model results that follow. Later chapters of this report use original contributions and analyses developed by MANE-VU researchers to bolster and support the concepts presented in these introductory chapters. MANE-VU has combined the outputs and integrated them into a final conceptual model that explains the formation and transport mechanisms for fine particulate matter in the eastern United States.

2.1. Visibility Effects of Particulate Matter (PM)

Visibility impairment in the eastern United States is largely due to the presence of light-absorbing and light-scattering fine particles in the atmosphere. The USEPA has identified visibility impairment as the best understood of all environmental effects of air pollution (Watson, 2002). A long-established physical and chemical theory relates the interaction of particles and gases in the atmosphere with the transmission of visual information along a sight path from object to observer.

Visibility-impairing particle-light interactions are sensitive to the chemical composition of the particles involved, and also depend strongly on ambient relative humidity. Secondary particles, which form in the atmosphere through chemical reactions, tend to fall within a size range that is most effective at scattering visible light (NARSTO, 2003). These particles are generally smaller than one micrometer (µm) or one one-millionth of a meter. The particles that contribute most to visibility impairment also are a concern under the health-based National Ambient Air Quality Standard (NAAQS) for fine particulate matter, defined as including all particles with an aerodynamic diameter less than 2.5 µm ($PM_{2.5}$).

2.2. Chemical Composition of Particulate Matter in MANE-VU

Sulfate alone accounts for anywhere from one-half to two-thirds of total fine particle mass on the 20 percent haziest days at all MANE-VU Class I sites. Even on the 20 percent clearest days, sulfate generally accounts for the largest fraction (40 percent or more) of total fine particle mass in the region (NESCAUM, 2001). Sulfate accounts for a

major fraction of $PM_{2.5}$, not only in the Northeast but across the eastern United States (NARSTO, 2003).

After sulfate, organic carbon (OC) consistently accounts for the next largest fraction of total fine particle mass. Its contribution typically ranges from 20 to 30 percent of total fine particle mass on the haziest days. The fact that the contribution from organic carbon can be as high as 40 percent at the more rural sites on the 20 percent clearest days is likely indicative of the role played by organic emissions from vegetation (so-called "biogenic hydrocarbons" (HC)). Relative contributions to overall fine particle mass from nitrate (NO_3), elemental carbon, and fine soil are all smaller (typically under 10 percent), but the relative ordering among the three species varies with location. Nitrate plays a noticeably more important role at urban sites compared to northeastern and mid-Atlantic Class I locations, perhaps reflecting a greater contribution from vehicles and other urban pollution sources (NESCAUM, 2001).

Almost all particle sulfate originates from sulfur dioxide (SO_2) oxidation and typically associates with ammonium (NH_4) in the form of ammonium sulfate ($(NH_4)_2SO_4$), 95 percent of SO_2 emissions are from anthropogenic sources (primarily from fossil fuel combustion), while the majority of ammonium comes from agricultural activities and, to a lesser extent, from transportation sources in some areas (NARSTO, 2003).

Two major chemical pathways produce sulfate from SO_2 in the atmosphere. In the gas phase, production of sulfate involves the oxidation of SO_2 to sulfuric acid (H_2SO_4), ammonium bisulfate (NH_4HSO_4), or ammonium sulfate, depending on the availability of ammonia (NH_3). In the presence of small wet particles (typically much, much smaller than rain drops or even fog), a highly efficient aqueous phase process can oxidize SO_2 to sulfate extremely quickly (~10 percent per hour).

Not only is sulfate the dominant contributor to fine particle mass in the region, it accounts for anywhere from 60 percent to almost 80 percent of the difference between fine particle concentrations on the clearest and haziest days at northeastern and mid-Atlantic Class I sites. Notably, at urban locations such as Washington, DC, sulfate accounts for only about 40 percent of the difference in average fine particle concentrations for the 20 percent most versus least visibility impaired days (NESCAUM, 2001). We discuss this further in the next section of this chapter.

Some of the dominant components of total fine particle mass have an even larger effect when considering the differential visibility impacts of different particle species. Sulfate typically accounts for over 70 percent of estimated particle-induced light extinction at northeastern and mid-Atlantic Class I sites. Organic carbon continues to be the second most important contributor to particle-induced light extinction at rural sites on the most impaired days, but slips to third behind nitrate in Washington, DC (NESCAUM, 2001).

2.3. Geographic Considerations and Attribution of PM/Haze Contributors

In the East, an accumulation of particle pollution often results in hazy conditions extending over thousands of square kilometers (km^2) (NARSTO, 2003). Substantial

visibility impairment is a frequent occurrence in even the most remote and pristine areas of the Northeast and Mid-Atlantic region (NESCAUM, 2001).

Both annual average and maximum daily fine particle concentrations are highest near heavily industrialized areas and population centers. Not surprisingly, given the direct connection between fine particle pollution and haze, the same pattern emerges when one compares measures of light extinction on the most and least visibility impaired days at parks and wilderness areas subject to the Haze Rule in the Northeast and Mid-Atlantic region (NESCAUM, 2001).

Contributions to fine particle mass concentrations at rural locations include long-range pollutant transport as well as non-anthropogenic background contributions. Urban areas generally show mean $PM_{2.5}$ levels exceeding those at nearby rural sites. In the Northeast, this difference implies that local urban contributions are roughly 25 percent of the annual mean urban concentrations, with regional aerosol contributing the remaining, and larger, portion (NARSTO, 2003).

This rural versus urban difference in typical concentrations also emerges in a source apportionment analysis of fine particle pollution in Philadelphia (Chapter 10, NARSTO, 2003) using two different mathematical models, UNMIX and Positive Matrix Factorization (PMF). (We describe these models in greater detail in Chapter 5 and Appendix B.) This analysis provides additional insight concerning sources of fine particle pollution in urban areas of the densely populated coastal corridor between Washington D.C. and New England. Specifically, this analysis found the following apportionment of $PM_{2.5}$ mass in the study area:

- Local SO_2 and sulfate: ~ 10 percent
- Regional sulfate: ~ 50 percent
- Residual oil: 4-8 percent
- Soil: 6–7 percent
- Motor vehicles: 25–30 percent

The analysis does not account for biogenic sources, which most likely are embedded in the motor vehicle fraction (NARSTO, 2003). The Philadelphia study suggests that both local pollution from near-by sources and transported "regional" pollution from distant sources contribute to the high sulfate concentrations observed in urban locations along the East Coast on an annual average basis. Summertime sulfate and organic carbon are strongly regional in eastern North America. Typically 75–95 percent of the urban sulfate concentrations and 60–75 percent of the urban OC concentrations arise from cumulative region-wide contributions (NARSTO, 2003).

While these statistics provide some preliminary context for attributing responsibility for the region's particulate matter and visibility problems, they say nothing about the relative efficiency of a state's or region's emissions in causing or contributing to the problem. It is clear that distance from the emissions source matters. Local, near-by sources are exceedingly important and sources within about 200 kilometers (km) are much more efficient (on a per ton emitted basis) at producing pollution impacts at eastern Class I sites such as Shenandoah National Park than emissions sources farther away (USNPS, 2003). In general, the "reach" of sulfate air pollution resulting from SO_2

emissions is longest (650-950 km). The reach of ammonia emissions or reduced nitrogen relative to nutrient deposition is the shortest (around 400 km), while oxides of nitrogen and sulfur — in terms of their impacts with respect to acidic deposition — have a reach between 550–650 km and 600–700 km, respectively (USNPS, 2003).

Monitoring evidence indicates that non-urban visibility impairment in eastern North America is predominantly due to sulfate particles, with organic particles generally second in importance (NARSTO, 2003). This makes sense, given the "long reach" of SO_2 emissions once they are chemically transformed into sulfate and given the ubiquitous nature of OC sources in the East.

The poorest visibility conditions occur in highly industrialized areas encompassing and adjacent to the Ohio and Tennessee River Valleys. These areas feature large coal-burning power stations, steel mills, and other large emissions sources. Average visibility conditions are also poor in the highly populated and industrialized mid-Atlantic seaboard but improve gradually northeast of New York City (Watson, 2002).

A review of source apportionment and ensemble trajectory analyses conducted by USEPA (2003) found that all back trajectory analyses for Eastern sites associated sulfate with the Ohio River Valley area. Studies also frequently associated other types of industrial pollutants with known source areas. Several studies in the USEPA review noted transport across the Canadian border, specifically sulfates from the midwestern United States into Canada, and smelter emissions from Canada into the northeastern United States.

A recent, comprehensive analysis of air quality problems at Shenandoah National Park conducted by the U.S. National Park Service (USNPS, 2003) focused on contributions to particulate pollution and visibility impairment south of the MANE-VU region. In descending order of importance, the National Park Service analysis determined that Ohio, Virginia, West Virginia, Pennsylvania, and Kentucky comprise the top five of thirteen key states contributing to ambient sulfate concentrations and haze impacts at the park. West Virginia, Ohio, Virginia, Pennsylvania, and Kentucky comprise the top five contributing states with respect to sulfur deposition impacts at the park. Finally, Virginia, West Virginia, Ohio, Pennsylvania, and North Carolina were found to be the top five states contributing to deposition impacts from oxidized nitrogen at the park (USNPS, 2003).

In summary, the National Park Service found that emission sources located within a 200 kilometer (125 mile) radius of Shenandoah cause greater visibility and acidic deposition impacts at the park, on a per ton basis, than do more distant emissions sources (USNPS, 2003). When mapping deposition and concentration patterns for all three pollutants using contour lines, the resulting geographic pattern shows a definite eastward tilt in the area of highest impact. This is the result of prevailing wind patterns, which tend to transport most airborne pollutants in an arc from the north-northeast to the east.[6] The Park Service found, for example, that emissions originating in the Ohio River Valley end up three times farther to the east than to the west (USNPS, 2003).

[6] The prevailing winds are eastward to northeast. This leads to greater pollution transport to the east-northeast relative to other directions.

We note that several MANE-VU states may themselves be contributing to fine particle mass concentrations observed at Shenandoah. According to the Park Service analysis, sources in Pennsylvania contribute on the order of 10 percent of observed ambient sulfate mass at the park, while sources in Maryland, New York and Delaware contribute 3.5, 1.7 and 0.5 percent respectively (USNPS, 2003).

2.4. Seasonal differences

Eastern and western coastal regions of the United States and Canada show marked seasonality in the concentration and composition of fine particle pollution, while central interior regions do not (NARSTO, 2003). While the MANE-VU domain extends inland as far as the Pennsylvania and Ohio border, the majority of Class I areas in MANE-VU cluster along the East Coast and thus typically show strong seasonal influences. Maximum $PM_{2.5}$ concentrations occur during the summer over most of the Northeast, with observed summer values for rural areas in the region, on average, twice those of winter. Winter nitrate concentrations, however, are generally higher than those observed in summer and, as mentioned above, urban concentrations typically exceed rural concentrations year-round. In addition, local mobile source carbon grows in importance during wintertime. Hence, in some large urban areas such as Philadelphia and New York City, peak concentrations of $PM_{2.5}$ can occur in winter.

The conceptual models that explain elevated regional $PM_{2.5}$ peak concentrations in the summer differ significantly from models that explain the largely urban peaks observed during winter. On average, summertime concentrations of sulfate in the northeastern United States are more than twice that of the next most important fine particle constituent, OC, and more than four times the combined concentration of nitrate and black carbon (BC) constituents (NARSTO, 2003). Episodes of high summertime sulfate concentrations are consistent with stagnant meteorological flow conditions and the accumulation of airborne sulfate (via atmospheric oxidation of SO_2) through long-range transport of sulfur emissions from industrialized areas within and outside the region.

National assessments (NARSTO, 2003) have indicated that in the winter, sulfate levels in urban areas are almost twice as high as background sulfate levels across the eastern U.S., indicating that the local urban contribution to wintertime sulfate levels is comparable in magnitude to the regional sulfate contribution from long-range transport. MANE-VU's network analysis for the winter of 2002 suggests that the local enhancement of sulfate in urban areas of the OTR is somewhat less with ranges from 25 to 40% and that the long range transport component of PM sulfate is still the dominant contributor in most eastern cities.

In the winter, urban OC and sulfate each account for about a third of the overall $PM_{2.5}$ mass concentration observed in Philadelphia and New York City. Nitrate also makes a significant contribution to urban $PM_{2.5}$ levels observed in the northeastern United States during the winter months. Wintertime concentrations of OC, sulfate, and NO_3 in urban areas can be twice the average regional concentrations of these pollutants, indicating the importance of local source contributions (NARSTO, 2003). This is likely because winter conditions are more conducive to the formation of local inversion layers that prevent vertical mixing. Under these conditions, emissions from tailpipe, industrial

and other local sources become concentrated near the Earth's surface, adding to background pollution levels associated with regionally transported emissions.

It is worth noting that while sulfate plays a significant role in episodes of elevated particle pollution during summer and winter months, the processes by which sulfate forms may vary seasonally. Nearly every source apportionment study reviewed by USEPA (2003) identified secondary sulfate originating from coal combustion sources as the largest or one of the largest contributors to overall fine particle mass in the region. It often accounted for more than 50 percent of $PM_{2.5}$ mass at some locations during some seasons. In a few cases, source apportionment studies identified a known local source of sulfate, but most assessments (in conjunction with back trajectory analysis) have pointed to coal-fired power plants in the Midwest as an important source for regional sulfate. Studies with multiple years of data have also tended to identify a distinguishable chemical "signature" for winter versus summer sources of sulfate, with the summer version typically accounting for a greater share of overall fine particle mass. Researchers have speculated that the two profiles represent two extremes in the chemical transformation processes that occur in the atmosphere between the source regions where emissions are released and downwind receptor sites. We note that while coal combustion is often referred to as the "sulfate source" because of the dominance of its sulfate contribution, coal combustion is usually the single largest source of selenium (Se) and other heavy metal trace elements (USEPA, 2003).

Visually, hazy summer days in the Northeast can appear quite different from hazy winter days. The milky, uniform visibility impairment shown in Figure 2-1 is typical of summertime regional haze events in the Northeast. During the winter, by comparison, reduced convection and the frequent occurrence of shallow inversion layers often creates a layered haze with a brownish tinge, as shown in Figure 2-2. This visual difference suggests seasonal variation in the relative contribution of different gaseous and particle constituents during the summer versus winter months (NESCAUM, 2001). Rural and inland areas tend not to experience these layered haze episodes as frequently due to the lack of local emission sources in most rural areas (valleys with high wood smoke contributions are an exception).

Overall (regional) differences in summer versus winter particle mass concentrations and corresponding visibility impairment (as measured by light extinction) are largely driven by seasonal variation in sulfate mass concentrations. This is because winter meteorological conditions are less conducive to the oxidation of sulfate from SO_2 (as borne out by the previously cited source apportionment studies). In addition, seasonal differences in long-range transport patterns from upwind SO_2 source regions may be a factor.

The greater presence of nitrate during the cold season is a consequence of the chemical properties of ammonium nitrate. Ammonia bonds more weakly to nitrate than it does to sulfate, and ammonium nitrate tends to dissociate at higher temperatures. Consequently, ammonium nitrate becomes more stable at lower temperatures and hence contributes more to overall light extinction during the winter months (NESCAUM, 2001).

Figure 2-1. Summer time at Mt Washington

Clean Day **Typical Haze Event**

Figure 2-2. Wintertime in Boston

Clean Day **Typical Haze Event**

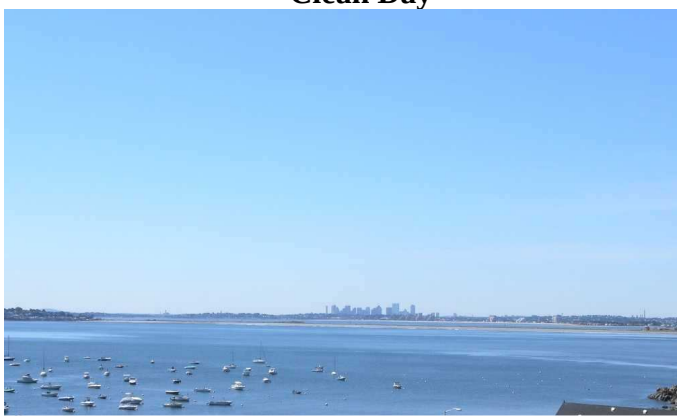

2.5. Implications for control strategies

A 2003 assessment of fine particulate matter by NARSTO[7] notes that, "[c]urrent air-quality management approaches focusing on reductions of emissions of SO_2, NO_X, and VOCs are anticipated to be effective first steps towards reducing $PM_{2.5}$ across North America, noting that in parts of California and some eastern urban areas VOC (volatile organic compounds) emissions could be important to nitrate formation."

This conclusion seems to be well supported by the historical record, which documents a pronounced decline in particulate sulfate concentrations across the eastern United States during the 1990s. The timing of this observed decline suggests that this is linked to reductions in SO_2 emissions resulting from controls implemented under the federal Acid Rain Program beginning in the early to mid 1990s. From 1989 to 1998, SO_2

[7] NARSTO was formerly an acronym for the "North American Research Strategy for Tropospheric Ozone." More recently, the term NARSTO became simply a wordmark signifying a tri-national, public-private partnership for dealing with multiple features of tropospheric pollution, including ozone and suspended particulate matter. For more information on NARSTO see http://www.cgenv.com/Narsto/.

emissions in the eastern half of the country — that is, including all states within a region defined by the western borders of Minnesota and Louisiana — declined by about 25 percent. This decline in SO_2 emissions correlated with a decline of about 40 percent in average SO_2 and sulfate concentrations, as measured at Clean Air States and Trend Networks (CASTNet) monitoring sites in the same region over the same time period. In fact, at prevailing levels of atmospheric SO_2 loading, the magnitudes of the emissions and concentration changes were not statistically different. This finding suggests that regional reductions in SO_2 emissions have produced near-proportional reductions of particulate sulfate in the eastern United States (NARSTO, 2003). Reductions since 1990 in precursor SO_2 emissions are likely also responsible for a continued decline in median sulfate concentrations in the northeastern United States. Nevertheless, the fact that episodes of high ambient sulfate concentrations (with peak levels well above the regional median or average) continue to occur, especially during the summertime when regional transport from the Ohio River Valley is also at its peak, suggests that further reductions in regional and local SO_2 emissions would provide significant further air quality and visibility benefits (NARSTO, 2003).

For urban areas of the northeastern and southeastern United States, an effective emissions management approach may be to combine regional SO_2 control efforts aimed at reducing summertime $PM_{2.5}$ concentrations with local SO_2 and OC control efforts. Local SO_2 reductions would help reduce wintertime PM concentrations, while OC reductions can help reduce overall PM concentrations year-round. For areas with high wintertime PM levels, strategies that involve NO_X reductions may also be effective (NARSTO, 2003).

Further support for this general approach may be found in a review of several studies by Watson (2002) that concluded SO_2 emission reductions have in most cases been accompanied by statistically significant reductions in ambient sulfate concentrations. One study (Husar and Wilson, 1993) shows that regionally averaged light extinction closely tracks regionally averaged SO_2 emissions for the eastern United States from 1940 through the mid-1980s. Another study by Malm et al. (2002) shows that regionally averaged emissions and ambient concentrations decreased together from 1988 through 1999 over a broad region encompassing the states of Connecticut, Delaware, Illinois, Indiana, Kentucky, Maine, Massachusetts, Maryland, Michigan, New Hampshire, New Jersey, New York, Ohio, Pennsylvania, Rhode Island, Vermont, Virginia, Wisconsin, and West Virginia (Watson, 2002).

These studies and available data from the IMPROVE (Interagency Monitoring of Protected Visual Environment) monitoring network provide strong evidence that regional SO_2 reductions have yielded, and will continue to yield, reductions in ambient secondary sulfate levels with subsequent reductions in regional haze and associated light extinction. They indicate that reductions in anthropogenic primary particle emissions will also result in visibility improvements, but that these will not have a zone of influence as large as those of the secondary aerosols (Watson, 2002).

Watson (2002) notes that during the 65 years in which the regional haze program aims to reach its final visibility goals, several opportunities to revise this basic control approach will arise through the decadal SIP cycle. This enables new scientific results to continue to exert a positive influence as states implement new regulatory control

programs for SO_2, NO_X and VOCs, and as ambient concentrations of these pollutants change relative to each other and relative to ambient ammonia levels. As these relationships between species change, atmospheric chemistry may dictate a revised control approach to those previously described. Further research on these issues should be a priority for supporting 2018 SIP submissions. They include the possibility that:

- Reduction of sulfate in a fully neutralized atmosphere (excess ammonia) could encourage ammonium nitrate formation.
- Ever greater emissions reductions could be required to produce a given level of improvement in ambient pollutant concentrations because of non-linearities in the atmospheric formation of sulfate.
- Changes in ambient conditions favoring the aqueous oxidation of sulfate (this pathway largely accounts for the non-linearity noted above) may have implications for future emissions control programs. Causes of changing ambient conditions could include, for example, climate change.

West et al. (1999) examine a scenario for the eastern United States where $PM_{2.5}$ mass decreases linearly with ammonium sulfate until the latter is fully neutralized by ammonia. Further reductions would free ammonia for combination with gaseous nitric acid that, in turn, would slightly increase $PM_{2.5}$ until all of the nitric acid is neutralized. At that point, further sulfate reductions would once again be reflected in lower $PM_{2.5}$ mass. This is an extreme case that is more relevant to source areas (e.g., Ohio) where nitric acid (HNO_3) is more abundant than in areas with lower emissions (e.g., Vermont) (Watson, 2002).

In most situations with non-neutralized sulfate (typical of the eastern United States), ammonia is a limiting agent for the formation of nitrate but will not make any difference until sulfate is reduced to the point where it is completely neutralized. At that point, identifying large sources of ammonia emissions will be important. This point is likely to be many years in the future, however (Watson, 2002).

Based on analyses using the Community Multi-Scale Air Quality (CMAQ) model, the aqueous phase production of sulfate in the Northeast appears to be very oxidant limited and hence non-linear. Thus, conditions that are conducive to a dominance of the gas-phase production pathway drive the summer peaks in ambient sulfate levels. Nonetheless, the expected reduction in ambient sulfate levels resulting from a given reduction in SO_2 emissions is less than proportional overall due to the non-linearity introduced by the aqueous pathway for sulfate formation (NARSTO, 2003). These non-linearity effects are more pronounced for haze than for sulfate deposition, especially at higher sulfate air concentrations (USNPS, 2003).

Finally, we note that because visibility in the clearest areas is sensitive to even minute increases in particle concentrations, strategies to preserve visibility on the clearest days may require stringent limits on emissions growth. In this context, even the dilute emissions from distant sources can be important (NARSTO, 2003).

2.6. Summary

The presence of fine particulate matter in ambient air significantly obscures visibility during most parts of the year at sites across the MANE-VU region. Particle pollution generally, and its sulfate component specifically, constitute the principle driver for regional visibility impacts. While the broad region experiences visibility impairment, it is most severe in the southern and western portions of MANE-VU that are closest to large power plant SO_2 sources in the Ohio River and Tennessee Valleys.

The presence or absence of regional sulfate almost exclusively drives summer visibility impairment, whereas winter visibility depends on a combination of regional and local influences coupled with local meteorological conditions (inversions) that lead to the concentrated build-up of pollution.

Sulfate is the key particle constituent from the standpoint of designing control strategies to improve visibility conditions in the northeastern United States. Significant further reductions in ambient sulfate levels are achievable, though they will require more than proportional reductions in SO_2 emissions.

Long-range pollutant transport and local pollutant emissions are important, especially along the eastern seaboard, so one must also look beyond the achievement of further sulfate reductions. During the winter months, in particular, consideration also needs to be given to reducing urban sources of SO_2, as well as NO_X and OC (NARSTO, 2003).

References

Husar, R.B. and Wilson, W.E., "Haze and Sulfur Emission Trends in the Eastern United States," *Environ. Sci. Technol. 27* (1), 12-16, 1993.

NARSTO, *Particulate Matter Science for Policy Makers: A NARSTO Assessment*, EPRI 1007735, February, 2003.

NESCAUM, *Regional Haze and Visibility Impairment in the Northeast and Mid-Atlantic United States*, Northeast States for Coordinated Air Use Management, Boston, MA, January, 2001.

Malm, W. C., Schichtel, B. A., Ames, R.B., and Gebhart, K.A., "A 10-year spatial and temporal trend of sulfate across the United States," *J. Geophys. Res. 107(D22):4627*, doi:10.1029/2002JD002107, 2002.

USEPA, *COMPILATION OF EXISTING STUDIES ON SOURCE APPORTIONMENT FOR $PM_{2.5}$, Second Draft*, Emissions, Monitoring, and Analysis Division, Office of Air Quality Planning and Standards, Research Triangle Park, NC, August, 2003.

USNPS, *Assessment of Air Quality and Related Values in Shenandoah National Park*, Technical Report NPS/NERCHAL/NRTR-03/090, U.S. Department of the Interior, National Park Service, Northeast Region, Philadelphia, Pennsylvania, May, 2003.

Watson, J., "Visibility: Science and Regulation," *JAWMA* 52:628-713, 2002.

West, J.J., Ansari, A.S., and Pandis, S.N., "Marginal $PM_{2.5}$: Nonlinear Aerosol Mass Response to Sulfate Reductions in the Eastern United States," *JAWMA* 49:1415-1424, 1999.

3. OVERVIEW OF MONITORING RESULTS

SIP developers use monitoring data in three important ways to support regional haze SIP activities. Section 3.1 presents measurements from the IMPROVE network needed in establishing SIP requirements. Following USEPA guidance (USEPA, 2003a; USEPA, 2003b), we use these data to preview the uniform progress goals that SIP developers must consider for each Class I area.

Section 3.2 reviews a recent NESCAUM report (NESCAUM, 2004b) to demonstrate how available monitoring data support and validate the conceptual model presented in Chapter 2.

Section 3.3 presents early results from the MANE-VU Real-Time Aerosol Intensive Network (RAIN). These suggest some of the ways MANE-VU is preparing to extend and improve understanding of visibility issues across the region. We anticipate this aspect of the MANE-VU monitoring strategy to be critical for future status reports and SIP updates.

3.1. Baseline Conditions

The Haze Rule requires states and tribes to submit plans that include calculations of current and estimated baseline and natural visibility conditions. They will use monitoring data from the IMPROVE program as the basis for these calculations. Table 3-1 presents the five-year average[8] of the 20 percent worst day mass concentrations in six Class I areas. Five of these areas are in MANE-VU and one (Shenandoah) is nearby but located in a neighboring regional planning organization (RPO) region.[9] Table 3-2 gives the corresponding worst day contributions to particle extinction for the six Class I areas. Each of these tables show the relative percent contribution for all six Class I sites. Sulfate and organic carbon dominate the fine mass, with sulfate even more important to particle extinction.

To guide the states in calculating baseline values of reconstructed extinction and for estimating natural visibility conditions, USEPA released two documents in the fall of 2003 outlining recommended procedures (USEPA 2003a; USEPA 2003b). These proposed methods were used, along with the data in Table 3-1 and Table 3-2 to create Table 3-3, which provides detail on the 20 percent worst conditions for the six Class 1 areas.

The first column of data in the Table 3-3 gives the default natural background levels for the worst visibility days at these six sites. Although debate continues with regard to some assumptions underlying the USEPA default approach for estimating natural background visibility conditions, MANE-VU has decided to use this approach, at least initially, for 2008 SIP planning purposes (NESCAUM, 2004a). The second column shows the baseline visibility conditions on the 20 percent worst visibility days. These values are based on IMPROVE data from the official five-year baseline period (2000-

[8] Great Gulf calculations are based on four years of data (2001-2004).

[9] Note that values presented for Shenandoah, a Class I area in the Visibility Improvement State and Tribal Association of the Southeast (VISTAS) region, are for comparative purposes only. VISTAS will determine uniform rates of progress for areas within its region.

2004). Using these baseline and natural background estimates, we derive the uniform rate of progress shown in the third column.[10] The final column displays the interim 2018 progress goal based on 14 years of improvement at the uniform rate.

Table 3-1. Fine mass and percent contribution for 20% worst days

20% Worst-day fine mass ($\mu g/m^3$) / % contribution to fine mass					
Site	SO_4	NO_3	OC	EC	Soil
Acadia	6.3 / 60%	0.8 / 8%	2.5 / 23%	0.4 / 4%	0.5 / 5%
Brigantine	11.5 / 59%	1.8 / 9%	4.5 / 23%	0.7 / 4%	1.0 / 5%
Great Gulf	7.3 / 63%	0.3 / 3%	2.9 / 25%	0.4 / 3%	0.6 / 5%
Lye Brook	8.5 / 62%	1.1 / 8%	3.0 / 22%	0.5 / 3%	0.6 / 5%
Moosehorn	5.7 / 58%	0.7 / 7%	2.6 / 27%	0.4 / 4%	0.4 / 4%
Shenandoah	13.2 / 72%	0.7 / 4%	3.3 / 18%	0.6 / 3%	0.7 / 4%

Table 3-2. Particle extinction and percent contribution for 20% worst days

20% Worst-day particle extinction (Mm^{-1}) / % contribution to extinction						
Site	SO_4	NO_3	OC	EC	Soil	CM
Acadia	66.0 / 73%	8.1 / 9%	10.1 / 11%	4.4 / 5%	0.5 / 1%	1.8 / 2%
Brigantine	106.2 / 69%	16.1 / 10%	18.3 / 12%	7.1 / 5%	1.0 / 1%	5.2 / 4%
Great Gulf	66.5 / 76%	3.0 / 3%	10.6 / 13%	3.8 / 4%	0.5 / 1%	2.9 / 3%
Lye Brook	76.7 / 73%	9.3 / 9%	12.1 / 11%	4.7 / 5%	0.7 / 1%	1.8 / 2%
Moosehorn	56.1 / 70%	6.3 / 8%	10.5/ 13%	4.4 / 5%	0.4 / 0%	2.1 / 3%
Shenandoah	132.5 / 82%	5.8 / 4%	13.2 / 8%	5.7 / 4%	0.8 / 0%	2.6 / 2%

Table 3-3. Natural background and baseline calculations for select Class I areas

Site	Natural Background (dv)	Baseline 2000-04 (dv)	Uniform Rate (dv/year)	Interim Progress Goal 2018 (dv)
Acadia	11.45	22.34	0.18	19.80
Brigantine	11.28	27.60	0.27	23.97
Great Gulf	11.30	22.25	0.18	19.69
Lye Brook	11.25	23.70	0.21	20.80
Moosehorn	11.36	21.18	0.16	18.89
Shenandoah	11.27	27.88	0.28	24.00

The regional haze rule calls for steady improvement of visibility on the 20 percent worst visibility days. States are to consider this uniform rate of progress, and if reasonable measures can be identified to meet or exceed this rate while ensuring no degradation of visibility on the best days, then it should be adopted as a Federal Class I

[10] We calculate the rate of progress as (baseline – natural background)/60 to yield the annual deciview (dv) improvement needed to reach natural background conditions in 2064, starting from the 2004 baseline.

area's *reasonable* progress goal. A number of instructive analyses are presented below using each area's uniform progress goal as an example, but these should not be interpreted as constituting MANE-VU recommendations on reasonable progress goals.

As a practical means of analyzing uniform progress goals, we have examined the components of observed fine particle pollution that substantially contribute to visibility degradation. This analysis shows that certain species dominate the extinction budget while others play virtually no role on the worst haze days.

As demonstrated in Table 3-2, the inorganic constituents of fine particles (sulfates and nitrates) are the dominant contributors to visibility impairment, accounting for about 80 percent of total particle extinction. Within the MANE-VU sites, the relative split between these two components is about eight to one sulfate to nitrate (at Shenandoah, the average 20 percent worst day contribution of sulfates is even more dominant). Carbonaceous components account for the bulk of the remaining particle extinction, ranging from 12 to nearly 20 percent, mostly in the form of organic carbon. The remaining components add little to the extinction budget on the worst days, with a few percent attributable to coarse mass and around a half percent from fine soil.

One approach to designing control strategies for achieving reasonable progress goals is to reduce all components of $PM_{2.5}$ in equal proportion. Achieving the 2018 uniform progress goals (expressed in Mm^{-1} in the second column of Table 3-4) requires between a 29 and 36 percent reduction in each component of the six haze components of fine particle extinction if their relative percent contributions to the current worst baseline conditions are kept constant (see the third column of Table 3-4). Given the dominant role of sulfate and nitrate, however, and the difficulty in obtaining 29 to 36 percent reductions in some of the other categories such as soil or course mass, sulfate- and nitrate-based control programs are likely to offer more reasonable emission reduction opportunities.

Table 3-4. Percent particle B_{ext} reduction needed to meet uniform progress[11]

Site	Particle Extinction Decrease (Mm^{-1})	Uniform Reduction (%)	Sulfate/Nitrate Reduction (%)	OC/EC Reduction (%)
Acadia	27.7	31	38	194
Brigantine	55.3	36	46	218
Great Gulf	30.6	33	42	195
Lye Brook	35.4	34	41	210
Moosehorn	23.4	29	38	158
Shenandoah	57.1	36	42	303

[11] We derive the information in this table from the results of Table 3-3. First, we converted the baseline and interim goal levels from dv to Mm^{-1} units, thus avoiding the logarithmic nature embedded into the deciview calculations. The first column of the table gives the difference between baseline and interim goal. The ratio of this difference to the baseline yields the uniform rate of reduction tabulated in the second column. We generate the paired species reduction percentages by using the wet and dry aerosol extinction coefficients. We determine f(RH) values by dividing the five-year B_{ext} average by the dry extinction coefficient, giving a weighted average value of the f(RH) during the worst 20% of days. Similarly, in Table 3-5, we calculate mass values using the relative contributions of the species to be reduced and their wet and dry efficiencies.

The fourth column of Table 3-4 displays the results if a sulfate and nitrate focused control approach were taken to meet uniform progress goals. For these two inorganic species, a greater reduction would be necessary on the 20 percent worst days if the other four components showed no change relative to baseline levels. The last column shows that the contribution of the carbonaceous species is too small to meet the entire required 2018 progress goal on its own (i.e. the percent reduction is greater than 100) if a carbon-only control approach were attempted.

Since it is easier to understand the implications of requisite mass reductions, rather than extinction, Table 3-5 tabulates the corresponding mass changes required for meeting uniform progress goals on the 20 percent worst days. On an absolute mass basis, the changes across sites are more varied than they are when viewed from a percentage change perspective. That in part is a function of the relative pollution levels at each site, in addition to the logarithmic nature of the deciview (dv). This table (along with Table 3-6) can aid planners to gauge the potential impact that meeting uniform progress goals under the Regional Haze program will have on regional fine particle mass levels.

Table 3-5. Mass reductions required on 20% worst days based on extinction estimates in Table 3-4

	20% Worst Day Mass Reduction ($\mu g/m^3$)							
	Uniform Percent Change All Species				Only Inorganic		Only Carbonaceous	
Site	SO_4	NO_3	OC	EC	SO_4	NO_3	OC	EC
Acadia	1.95	0.25	0.76	0.13	2.38	0.31	4.80	0.85
Brigantine	4.14	0.65	1.64	0.26	5.22	0.82	9.92	1.56
Great Gulf	2.42	0.11	0.97	0.13	3.06	0.14	5.74	0.76
Lye Brook	2.85	0.36	1.02	0.16	3.49	0.44	6.36	1.00
Moosehorn	1.68	0.20	0.77	0.13	2.14	0.26	4.12	0.69
Shenandoah	4.78	0.24	1.19	0.21	5.57	0.28	9.94	1.74

Table 3-6 provides an estimate of mass decreases that might be expected on an average day. It assumes using either a uniform rate of change in *all* species, or a uniform rate of change in the *sulfate and nitrate* component of fine particulate, to achieve the progress toward the 2018 goals, respectively. These values are likely a lower bound to the annual average change at Class I areas anticipated from current conditions to 2018 as they are based on the assumption that on the best days, no change occurs and the percent reduction on the middle days is half of what is predicted on the worst.[12]

[12] We derived the values tabulated in Figure 3-6 as follows: We multiplied half of the percentage change expected on the worst 20% of days by the average mass concentration of each species for the middle 20% of days. Note that if we apply a 25% reduction on the cleaner remaining quintile and 75% reduction on the dirtier remaining quintile, the annual average reduction would presumably be greater than that on the middle days given the skew in the distribution of all days. For example, in the inorganic-only case at Acadia, the average of the worst 20% change and best 20% is (2.69 + 0)/2 or 1.35 $\mu g/m^3$, which is nearly four times greater than the middle day. Further, given the large reduction on the worst days, it is reasonable to expect some small improvement on the best days.

Table 3-6. Estimated Mass Reduction on an Average Day

	Estimated Average Day Mass Reduction ($\mu g/m^3$)					
	Uniform Percent Change All Species				Only Inorganic	
Site	SO_4	NO_3	OC	EC	SO_4	NO_3
Acadia	0.25	0.05	0.16	0.02	0.31	0.06
Brigantine	0.80	0.19	0.38	0.08	1.01	0.25
Great Gulf	0.28	0.04	0.19	0.03	0.36	0.05
Lye Brook	0.29	0.07	0.17	0.03	0.36	0.09
Moosehorn	0.25	0.05	0.19	0.03	0.32	0.06
Shenandoah	0.79	0.24	0.28	0.05	0.92	0.28

3.1.1. Preview of revised IMPROVE Algorithm for aerosol extinction

Recently, the IMPROVE Steering Committee accepted an alternative approach for calculating visibility metrics based on measured aerosol concentrations. The new algorithm improves the correspondence between the reconstructed extinction and directly measured light scattering at the extremes of the visibility range. These extremes form the basis for determining the uniform progress "glide path."

The new equation revises or adds to the original version. The most significant changes include:

- revision of the dry aerosol extinction coefficients for sulfate, nitrate and organic carbon,
- splitting sulfate, nitrate and organic mass into small and large size fractions based on total species mass,
- revised f(RH) curves for inorganic species,
- inclusion of sea salt mass and associated f(RH) growth factor,
- use of a *site-specific* Rayleigh scattering term, and
- revision of the organic mass multiplier.

The VIEWS website provides the revised dataset for all IMPROVE data, allowing the calculation of the baseline period with the new algorithm. Natural background calculation methods that mirror many of the changes adopted as an alternative for baseline calculations have been suggested; however, none have been formally adopted by the IMPROVE Steering Committee at this time.

As a first step toward assessing the implications of the algorithm revisions, we compare the baseline visibility levels from the old and new approaches. The new calculation approach results in between one and two deciview increase in the 20 percent worst visibility conditions during the baseline period for the six sites considered. Extinction changes are observed for all components, with increases ranging from 6 to 42 percent depending on species. The greatest overall percentage change occurs for organic

carbon and the least for fine soil. Changes in the baseline 20 percent best days were much less with the absolute contribution of a component to visibility degradation increasing in some cases and decreasing in others. On average, the values decrease by 0.1 deciview. Table 3-7 and Table 3-8 summarize the species-specific changes for worst and best days' aerosol extinction.

Table 3-7. Aerosol extinction by specie for 20% worst days

20% worst-day particle extinction (Mm^{-1}) New Algorithm / Old Algorithm							
Site	SO_4	NO_3	OC	EC	Soil	Coarse	Salt
Acadia	76.4 / 66	8.6 / 8.1	12.5 / 10.1	4.8 / 4.4	0.6 / 0.5	2.1 / 1.8	1.4 / 0
Brigantine	134.2 / 106.2	18.1 / 16.1	25.9 / 18.3	7.9 / 7.1	1.0 / 1.0	6.5 / 5.2	0.7 / 0
Great Gulf	79.6 / 66.5	3.4 / 3.0	14.8 / 10.6	4.3 / 3.8	0.6 / 0.5	3.1 / 2.9	0.1 / 0
Lye Brook	94.4 / 76.7	10 / 9.3	17.1 / 12.1	5.3 / 4.7	0.7 / 0.7	2.1 / 1.8	0.1 / 0
Moosehorn	64 / 56.1	7 / 6.3	13.4 / 10.5	5.1 / 4.4	0.4 / 0.4	2.5 / 2.1	1.1 / 0
Shenandoah	169.6 / 132.5	7.9 / 5.8	18.2 / 13.2	6.5 / 5.7	0.8 / 0.8	3.0 / 2.6	0.1 / 0

Table 3-8. Aerosol extinction by specie for 20% best days

20% best-day particle extinction (Mm^{-1}) New Algorithm / Old Algorithm							
Site	SO_4	NO_3	OC	EC	Soil	Coarse	Salt
Acadia	6.8 / 7.4	1.1 / 1.2	2.3 / 2.4	0.9 / 0.9	0.1 / 0.1	0.7 / 0.7	0.4 / 0
Brigantine	5.7 / 6.2	1.0 / 1.1	2.0 / 2.1	0.9 / 0.9	0.1 / 0.1	0.9 / 0.7	0.2 / 0
Great Gulf	5.7 / 6.2	1.0 / 1.1	2.0 / 2.1	0.9 / 0.9	0.1 / 0.1	0.9 / 0.7	0.2 / 0
Lye Brook	4.5 / 5.0	1.2 / 1.2	1.3 / 1.4	0.6 / 0.6	0.1 / 0.1	0.5 / 0.5	0.0 / 0
Moosehorn	6.8 / 7.3	1.0 / 1.2	3.1 / 3.1	1.0 / 1.0	0.1 / 0.1	1.1 / 1.1	0.3 / 0
Shenandoah	11.4 / 12.8	4.2 / 4.4	2.9 / 3.0	1.6 / 1.6	0.2 / 0.2	1.1 / 1.1	0.1 / 0

Figure 3-1and Figure 3-2 graphically compare the old and new algorithm for six sites. The left-hand side of the figures presents the old contribution of aerosol extinction while the right-hand side shows the new calculations. Relatively small differences are apparent, with slight relative decreases in sulfate contribution offset by small increases in nitrate, organic carbon and the addition of sea salt.

The potential impact of these changes on the uniform rate of progress slope cannot be determined at this time, since revisions in natural background calculations remain incomplete. A preliminary assessment, however, suggests that natural background estimates for MANE-VU may increase by about 10 percent. This translates to a change of just over one deciview. This estimate combined with the average increase of 1.5 deciview in baseline conditions would not likely change the slope of the uniform progress curve in any significant way. Nonetheless, the actual mass reductions required could change given the logarithmic nature of the haze index, where marginal mass changes are larger at higher deciview levels. It is not a straightforward exercise to estimate the potential effect of such changes given the increased complexity of the new algorithm relative to the old equation.

Figure 3-1. Comparison of Old and New Algorithms for Baseline Worst Days

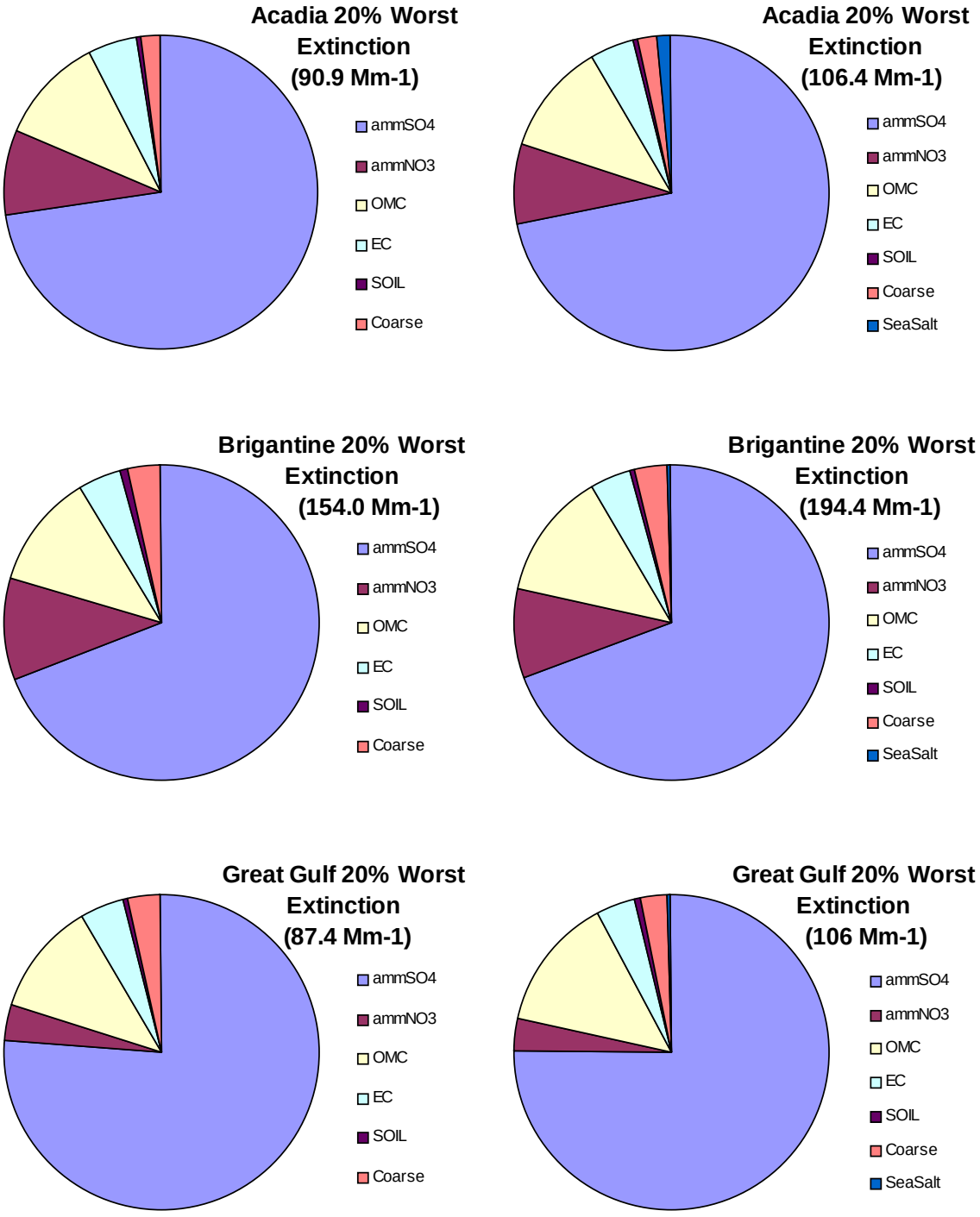

Figure 3-2. Comparison of Old and New Algorithms for Baseline Worst Days

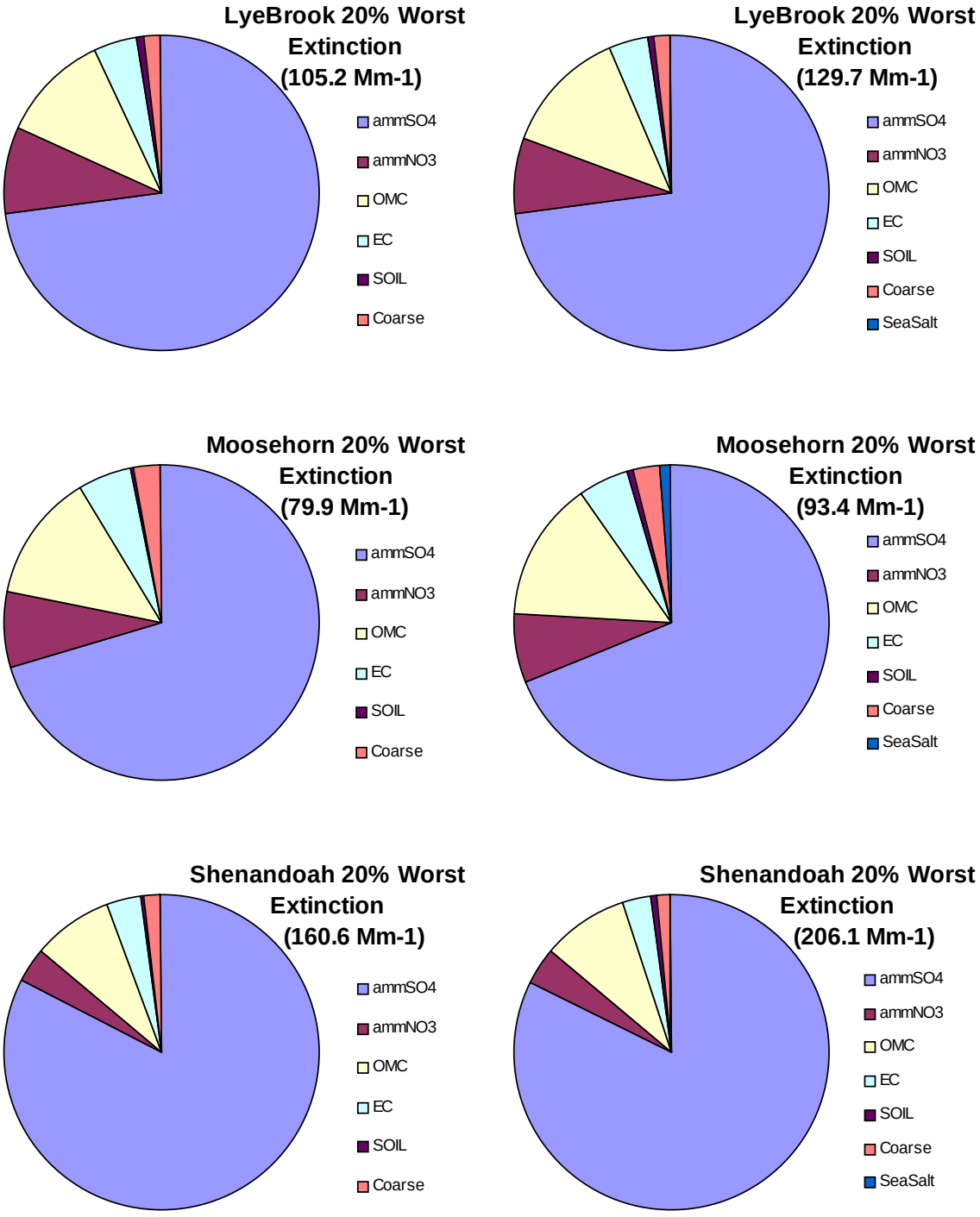

3.2. 2002 Monitoring Data

The recent MANE-VU report "2002 Year in Review" (NESCAUM, 2004b) provides a comprehensive review of monitoring data available to support SIP development in the MANE-VU region, including data on fine particle composition, as well as temporal and spatial distributions. The data in this study support the conceptual model in several important ways. They show that: (1) the single largest component of fine particle mass is sulfate; (2) the largest sulfate-generating emissions sources that affect the MANE-VU region lie to the south and west of the region; (3) fine particle concentrations are bi-modal with peaks in the summer and winter; and (4) summer and winter peak concentrations are generally caused by different chemical and physical processes in the atmosphere (i.e., summer peaks are strongly related to regional sulfate transport whereas winter peaks result from the sum of regionally-generated sulfate and locally generated sulfate, as well as organics and nitrate that build up during local stagnation events).

3.2.1. Sulfate

Data from several monitoring programs indicate that sulfate (on an annual basis) is the single largest component of fine particle mass in the MANE-VU region. Figure 3-3 displays sample data from two Speciation Trends Network (STN) sites in New Jersey. This shows that sulfate accounts for roughly half of fine particle mass on an annual average basis at background sites and about a third at the urban site. During summer, sulfate comprises over half the fine particle mass at rural background sites and two-fifths of fine particle mass at the urban site. When considering the different light-extinguishing properties of various fine particle constituents, sulfate is responsible for an even greater fraction of visibility impairment. It accounts for between three-quarters and four-fifths of overall light extinction on the 20 percent worst- visibility days (Table 3-2).

Figure 3-3. New Jersey Urban Area Compared to an Upwind Background Site

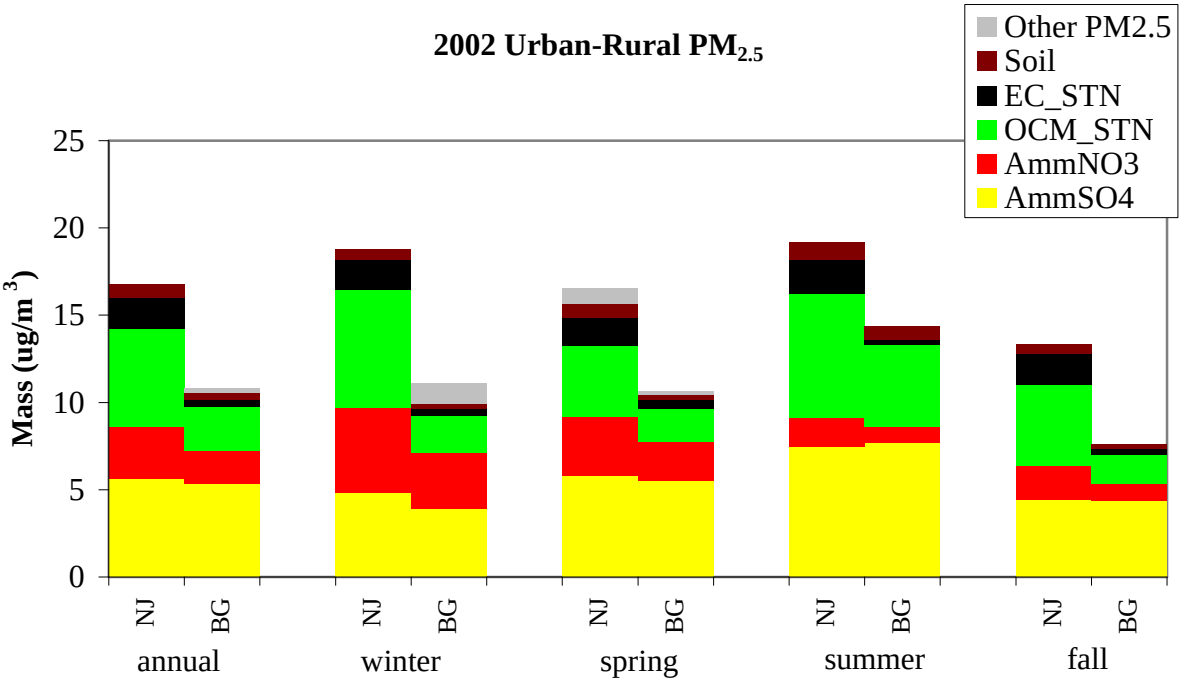

3.2.2. Southwest-Northeast Gradient

Figure 3-4 shows that $PM_{2.5}$ mass declines fairly steadily along a southwest to northeast transect of MANE-VU. This decline is consistent with the existence of large fine particle emissions sources (both primary and secondary) to the south and west of the MANE-VU region.

This trend in $PM_{2.5}$ mass is primarily due to a marked southwest-to-northeast gradient in ambient sulfate concentrations during three seasons of the year as illustrated in Figure 3-5. Wintertime concentrations, by contrast, are far more uniform across the entire region. Figure 3-6 shows that on an annual basis, both total PM and sulfate mass are highest in the southwestern portions of MANE-VU (note the different scales for each pollutant). High concentrations of nitrate and organic particle constituents, which play a role in localized wintertime PM episodes, tend to be clustered along the northeastern urban corridor and in other large urban centers.

Sulfate is a secondary pollutant, meaning that it forms in the atmosphere from precursor emissions. The formation of sulfate from SO_2 emissions requires time in an oxidizing environment. Therefore, it is likely that a substantial portion of the sulfate observed in the MANE-VU region is from sulfur emitted from south and west of the region. Modeled meteorological (trajectory) data presented in Chapter 5 support this conclusion by showing that the dominant wind direction over the MANE-VU region during periods of high sulfate concentrations is from the southwest.

Figure 3-4. MANE-VU FRM $PM_{2.5}$ statistics along a southwest to northeast axis

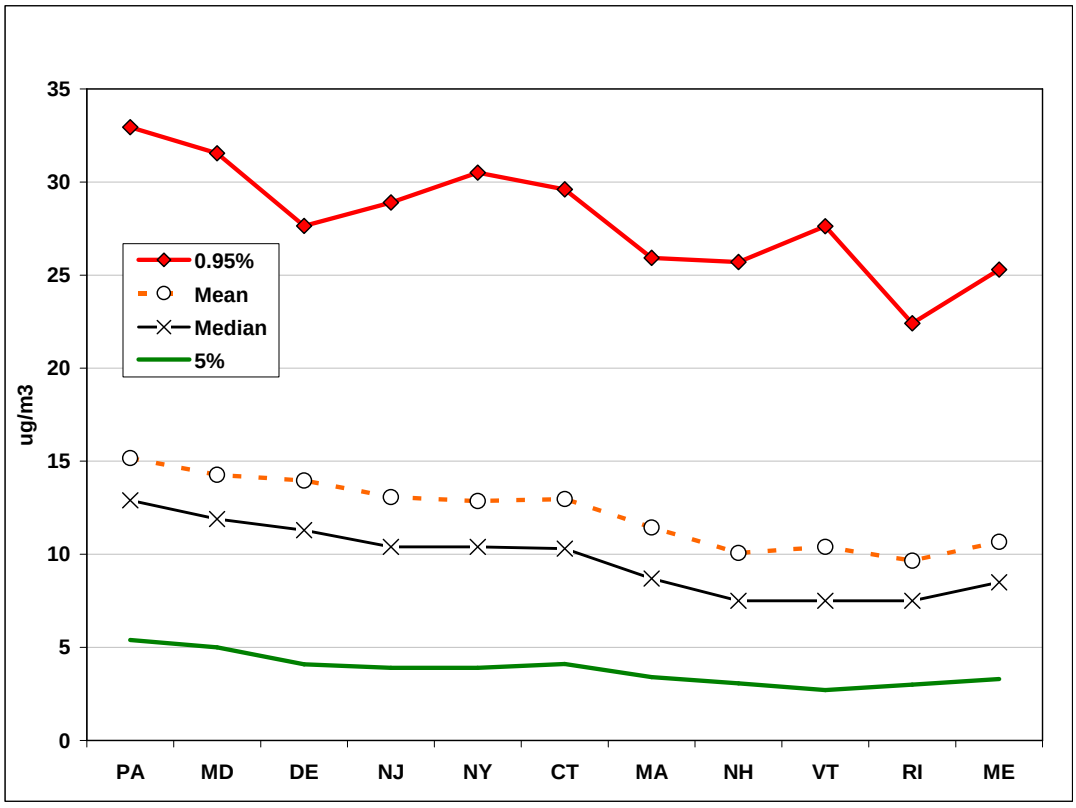

Figure 3-5. 2002 Seasonal average SO4 based on IMPROVE and STN data

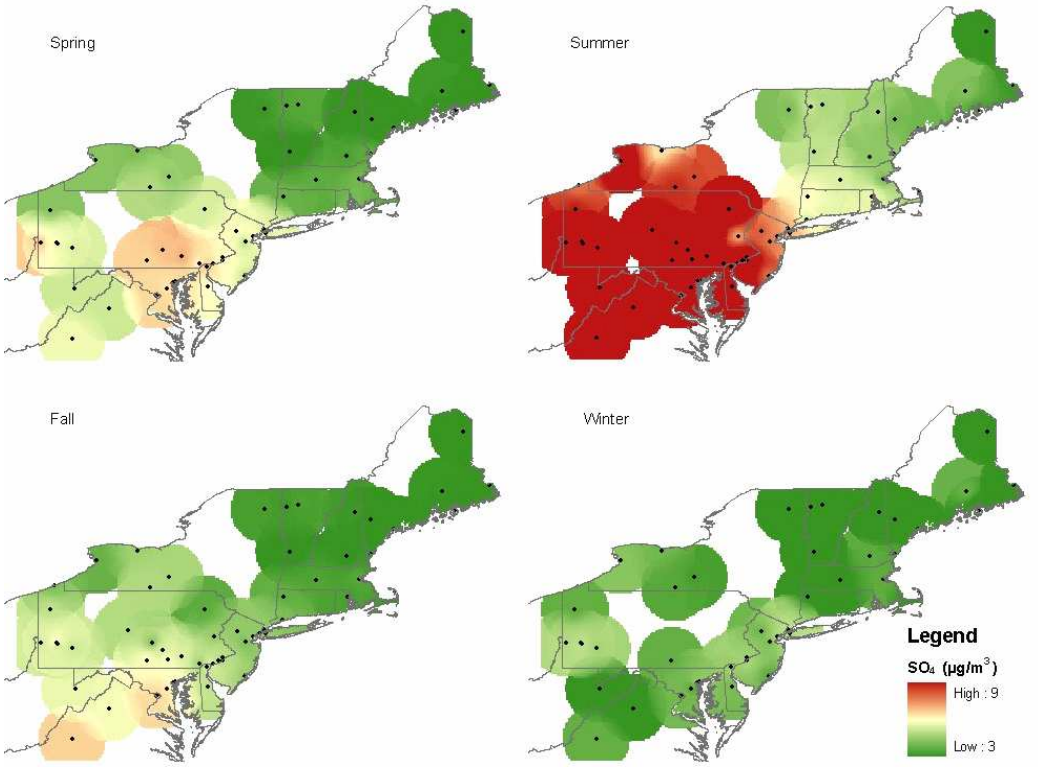

Figure 3-6. 2002 Annual average $PM_{2.5}$, sulfate, nitrate and total carbon for MANE-VU based on IMPROVE and STN data. Mass data are supplemented by the FRM network.

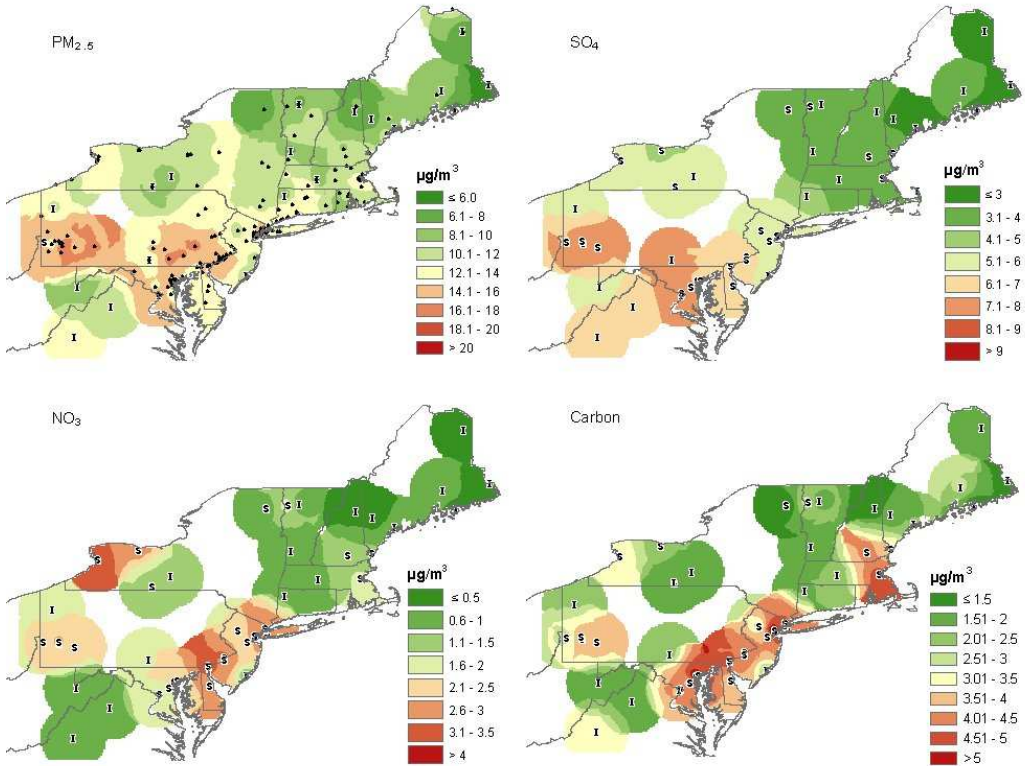

3.2.3. Seasonality

In general, fine particle concentrations in MANE-VU are highest during the warmest (summer) months but also exhibit a secondary peak during the coldest (winter) months. This bimodal seasonal distribution of peak values is readily apparent in Figure 3-7. The figure shows the smoothed 60-day running average of fine particle mass concentrations using continuous monitoring data from two northeastern cities over a period of several years.

Figure 3-7. Moving 60-day average of fine aerosol mass concentrations based on long-term data from two northeastern cities

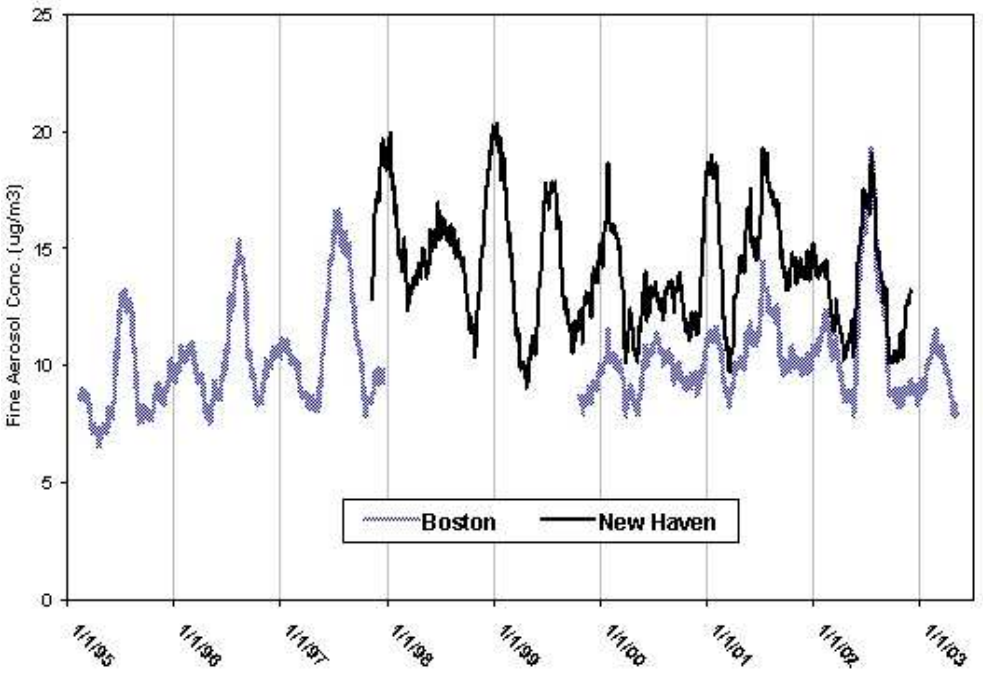

Figure 3-8. 30-day average fine aerosol mass concentrations from eight northeastern cities

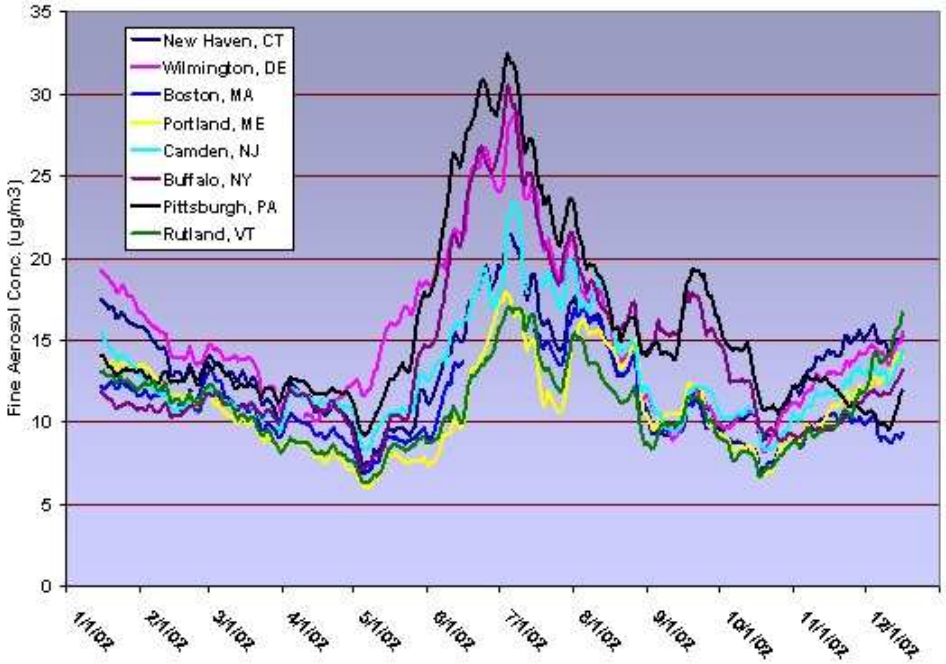

Although the patterns exhibited by these monitoring data include occasional anomalies (as in the summer of 2000), summer peak concentrations in both cities of Figure 3-7 are generally much higher than the surrounding winter peaks. Figure 3-8 also demonstrates this bimodal pattern. Though slightly more difficult to discern in just a single year's worth of data, a "W" pattern does emerge at almost all sites across the region during 2002 with the winter peak somewhat lower than the summer peak at most sites. Urban monitors in Wilmington, Delaware and New Haven, Connecticut have wintertime peak values approaching those of summer.

3.2.4. Seasonal Mechanisms

In the summertime, MANE-VU sites repeatedly experience sulfate events due to transport from regions to the south and west. During such events, rural and urban sites throughout the MANE-VU region record high (i.e., >15 $\mu g/m^3$) daily average $PM_{2.5}$ concentrations. Meteorological conditions during the summer frequently allow for summer "stagnation" events when very low wind speeds and warm temperatures allow pollution levels to build in an air mass as it is slowly transported across the continent. During these events, atmospheric ventilation is poor and local emission sources add to the burden of transported pollution with the result that concentrations throughout the region (both rural and urban) are relatively uniform. Generally there are enough of these events to drive the difference between urban and rural sites down to less than 1 $\mu g/m^3$ during the warm or hot months of the year. As a result, concentrations of fine particles aloft will often be higher than at ground-level during the summertime, especially at rural monitoring sites. Thus, when atmospheric "mixing" occurs during summer[13] mornings (primarily 7 to 11 a.m.), fine particle concentrations at ground-level can actually increase (see Hartford, CT or Camden, NJ in Figure 3-9).

During the wintertime, strong inversions frequently trap local emissions overnight and during the early morning, resulting in elevated urban concentrations. These inversions occur when the earth's surface loses thermal energy by radiating it into the atmosphere (especially on clear nights). The result is a cold, stable layer of air near the ground. At sunrise, local emissions (both mobile and stationary) begin increasing in strength and build-up in the stable ground layer (which may extend only 100 meters or less above-ground). Increasing solar radiation during the period between 10 a.m. and noon typically breaks this cycle by warming the ground layer so that it can rise and mix with air aloft. Because the air aloft during wintertime is typically less polluted than the surface layer, this mixing tends to reduce ground-level particle concentrations (see Figure 3-10). This diurnal cycle generally drives wintertime particle concentrations, although the occasional persistent temperature inversion can have the effect of trapping and concentrating local emissions over a period of several days, thereby producing a significant wintertime pollution episode.

[13] Here we define summer as May, June, July and August.

Figure 3-9. Mean hourly fine aerosol concentrations during the summer season

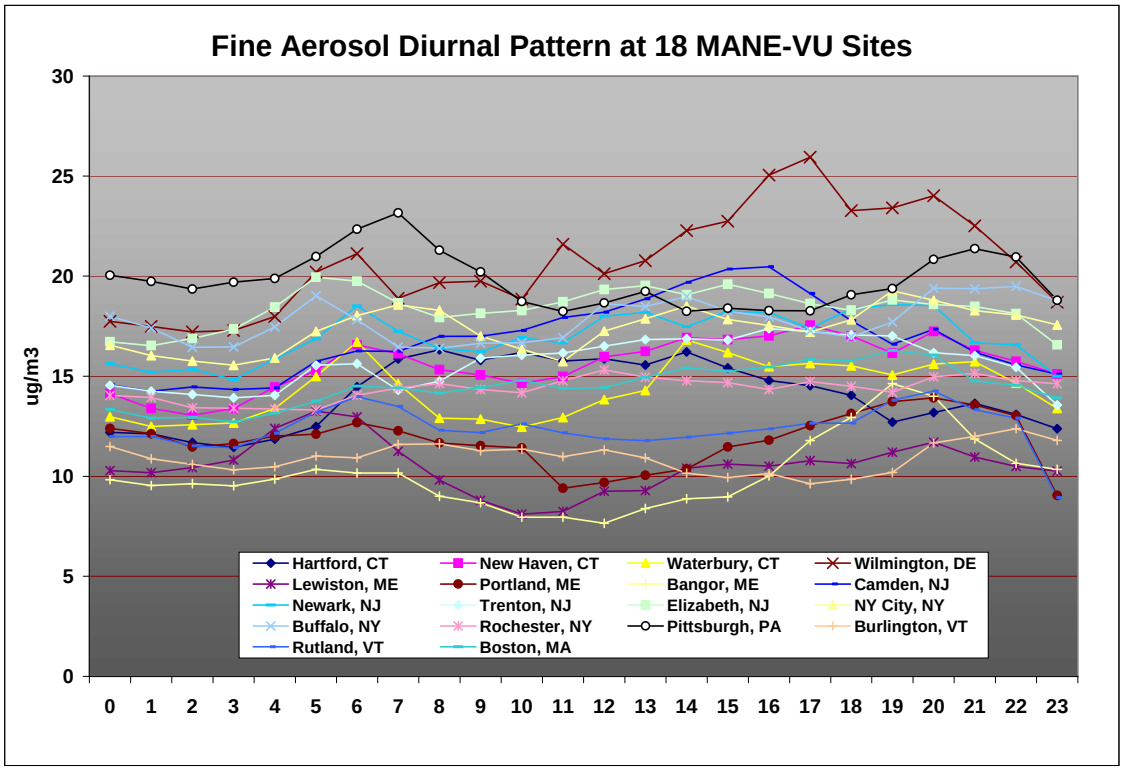

Figure 3-10. Mean hourly fine aerosol concentrations during the winter season

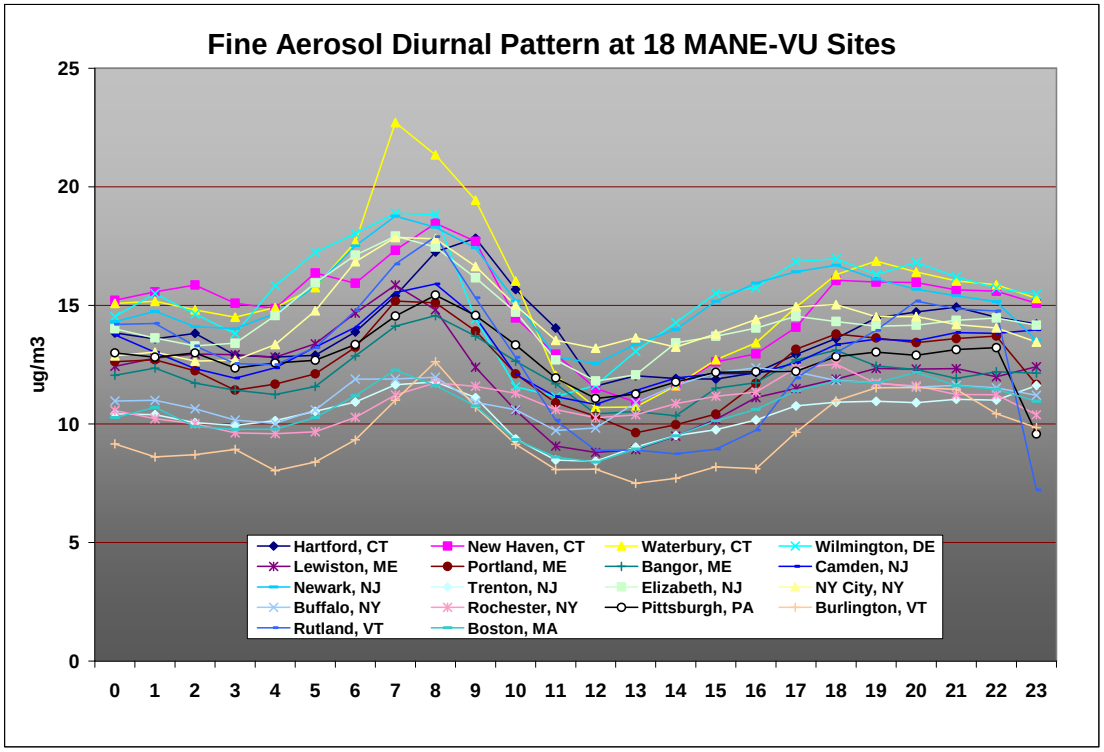

Rural areas experience the same temperature inversions but have relatively fewer local emissions sources so that wintertime concentrations in rural locations tend to be lower than those in nearby urban areas. Medium and long-range fine particle transport events do occur during the winter but to a far lesser extent than in the summertime. In sum, it is the interplay between local and distant sources together with seasonal meteorological conditions that drives the observed 3–4 $\mu g/m^3$ wintertime rural versus urban difference in PM concentrations.

3.3. RAIN data

Routine monitoring networks operated by USEPA, the National Park Service or state monitoring agencies collected much of the monitoring data shown so far. We anticipate that these data will continue to provide crucial information on the nature and extent of visibility impairment across the region. In addition, MANE-VU is also developing a network of enhanced monitoring sites capable of providing continuous data on the concentration, composition, and visibility impacts of fine particles. These data will be critical for understanding the more complex issues associated with organic carbon as well as any tradeoffs between sulfate and nitrate control. This Rural Aerosol Intensive Network (RAIN), which was first deployed in 2004, is therefore likely to play a prominent role in future visibility control programs and in the development of regional haze SIPs due in 2018.

NESCAUM coordinates the RAIN effort as a cooperative effort of the MANE-VU member state air agencies. The network covers the region from western Maryland (near large sulfur sources in the Ohio River Valley) through northwestern Connecticut to Acadia National Park in Maine. The initial network consists of these three rural, moderate elevation (700 to 2,500 feet) sites in a southwest to northeast line, all with detailed PM and visibility related measurements. The network design includes highly time resolved (1-2 hour) aerosol mass, composition, and optical property measurements. These provide enhanced insight into regional aerosol generation and source characterization, which are factors that drive short term visibility, and aerosol model performance and evaluation. In addition to these three sites, as of 2006 the NY-DEC/SUNY-Albany intensive measurement site at Pinnacle State Park (Addison, NY, seven miles southwest of Corning, NY, and seven miles north of the Pennsylvania border) has most of the RAIN parameters and methods other than visibility; efforts are underway to bring that site into the RAIN program (to ensure consistent method operation) and to add visibility measurements.

The RAIN sites use the Sunset Laboratory Model 3 field carbon analyzer and the new Thermo Environmental Model 5020 sulfate analyzer. This is the first use of these methods in routine, ongoing state-run networks. Combined with other more routine measurements such as IMPROVE aerosol, NGN-2 (wet) nephelometers, continuous $PM_{2.5}$, trace SO_2, ozone, meteorology, and automated digital visibility cameras (CAMNET), these methods make up the core RAIN monitoring lineup. Some of the RAIN sites will have additional related measurements, including "true" trace CO, NO_X, dry scattering (NGN-3a nephelometer), and other measurements. An Air and Waste

Management Association conference proceedings paper provides more information on the design of the network and examples of data from the summer of 2004.[14]

A longer term goal of RAIN is to enhance the network with other measurements and sites in future years. A National Weather Service ASOS visibility sensor at a RAIN site would allow the large network of existing ASOS data to be "tethered" to visibility measurements we understand well. Strong aerosol acidity, nitric acid, and ammonia are measurements that would be desirable on either an integrated or real-time basis. There are no continuous nitrate measurements in RAIN at this time because available methods suitable for routine deployment in state networks are not yet sufficiently robust.[15] Lack of continuous nitrate data is not a significant issue for this analysis since nitrate is not (yet) a major visibility factor at these rural sites. We expect that most of the continuous method data from RAIN to be available in real-time to web data resources like VIEWS, FASTNET and AIRNowTech by the end of 2006.

Measurements similar to those in RAIN done towards the west and south borders of the MANE-VU domain (Ohio and Virginia for example) would greatly enhance our understanding of the impact of the large sulfur source region in and around the Ohio River Valley on regional visibility. We encourage agencies and RPOs in those areas to develop intensive sites to complement the RAIN data.

As an initial test of the RAIN network, we examined visibility and related particle information for the third quarter of 2004 to determine how well the data from one (or both) of two recently installed semi-continuous monitors could reproduce the visibility data reported by existing NGN-2a nephelometers. The relevant data came from two monitors of interest: the Thermo Model 5020 (for sulfate) and the Sunset Labs (Model 3) semi-continuous analyzer for elemental and organic carbon. In addition, a Rotronic sensor (Model MP-101A, with active aspiration) measured relative humidity (RH) data on-site in order to supply a correction factor - f(RH) - for estimating the light scattering associated with various fine particle constituents.

Because ammonium sulfate is the major component of haze-producing particulate pollution in the northeastern United States, we examined sulfate data first. The Thermo Model 5020 reports sulfate and the IMPROVE algorithm for calculating visibility parameters assumes that all sulfate is in the form of ammonium sulfate. During high sulfate events in the rural Northeast this is not always the case, although it is still a reasonable first assumption.

The Thermo sulfate method has been shown to consistently under-report sulfate relative to IMPROVE sulfate measurements at the RAIN sites, but not at some other sites. Since the correlation with IMPROVE sulfate is high at all RAIN sites, the hourly RAIN sulfate data can be corrected to be "IMPROVE"-like with reasonable confidence. A RAIN technical memorandum describes this issue in more detail.[16] For the Acadia sulfate data used here, the daily correlation coefficient (R^2) between IMPROVE and

[14] http://www.nescaum.org/documents/allen-awma_haze-rain-paper-oct-2004_proceedings.pdf/
[15] See the EPA method evaluation report at http://www.epa.gov/ttn/amtic/semicontin.html for more information.
[16] "Rural Aerosol Intensive Network (RAIN) Preliminary Data Analysis," available at: http://www.nescaum.org/documents/2006-05-memo8-rain.pdf/

Thermo sulfate is 0.95 (based on third and fourth quarter 2004 data). A correction factor of 1.30 is applied to the Thermo sulfate data based on the linear regression of IMPROVE and Thermo sulfate 24-hour samples for the third and fourth quarters of 2004 data; this correction makes the Thermo sulfate data consistent with the IMPROVE sulfate data.

We need three types of data to relate direct measures of atmospheric light scattering to a re-constructed or calculated estimate of light scattering based on observed sulfate levels: (1) direct measurements of light scattering (via nephelometer); (2) sulfate measurements; and (3) relative humidity measurements. The three RAIN sites in the northeastern United States measure each of these variables. Of these sites, however, only the McFarland Hill site at Acadia National Park in Maine is within a Class I area. Therefore, we selected data from the McFarland Hill site for the preliminary analysis we describe below.

Given the highly non-linear relationship between relative humidity and ammonium sulfate particle size and the limitations of relative humidity (RH) sensor accuracy at very high values of RH, we excluded from this analysis data collected when relative humidity was equal to or greater than 95 percent. Of the 2,208 hourly observations recorded from June 1 through September 30, this relative humidity 'exclusion' removed 525 hours. Data for an additional 92 hours were not available due to missing measurements from either the sulfate monitor or the nephelometer. We excluded a further 35 hours due to flagged nephelometer performance (such flags could be triggered by excess noise or rate-of-change in the signal). This left 1,556 hourly observation pairs for the third quarter, equivalent to a data capture rate of 70 percent - still a substantial sample given the nature of the emerging technology employed at the RAIN sites.

We multiplied sulfate concentrations from the Thermo 5020 by 1.37 to convert them to a mass equivalent for ammonium sulfate (this is the same factor IMPROVE uses). This new variable (SULFATE) is the strongest driver of light extinction in the Northeast because of the extreme size-dependent nature of ammonium sulfate light scattering, which in turn is highly (and very non-linearly) dependent on atmospheric relative humidity. Next, we converted the hourly RH values to a relative humidity function "f(RH)" by using a conversion table adopted by IMPROVE.[17] Then we applied a "dry specific scattering" coefficient of "3"[18] to the hourly SULFATE values. The final equation is shown below:

Reconstructed Sulfate Scattering = 3 * f(RH) * (SULFATE)

When we compared this reconstructed estimate of hourly light scattering to the IMPROVE NGN-2a nephelometer data (via a least-squares linear regression), we obtained an R^2 of 0.888. When two apparent outlier hours are removed (both of which occurred during periods when relative humidity was over 87 percent and changing rapidly) the regression slope is 0.846, the intercept is -5, and R^2 increases to 0.942. This

[17] See: http://vista.cira.colostate.edu/improve/Tools/humidity_correction.htm; this is the original f(RH) table, not the new one.

[18] Described at http://vista.cira.colostate.edu/improve/Tools/ReconBext/reconBext.htm

implies that sulfate alone is responsible for approximately 85 percent of the light scattering (and visibility degradation) for this period of measurement.

Because elemental carbon absorbs light much more strongly than it scatters light, we added only the "light-scattering carbon" (OC) detected by the Sunset Model 3 to this reconstruction. The IMPROVE program uses the following equation to describe the impact of light-scattering carbon:

Reconstructed Carbon Scattering = 4 * f_{org}(RH) * [OMC]

where the dry scattering coefficient of this carbon fraction is set at "4," the relative humidity factor is set at unity (due to the weak hygroscopicity of organic carbon), and OMC represents "organic mass by carbon." The IMPROVE Steering Committee has recently adopted 1.8 as an alternative organic mass multiplier (rather than 1.4) for calculating OMC values for use in reconstructed extinction as described in section 3.1. We have also used 1.8 for the analysis presented below.

Because the RAIN sites collect carbon data over two-hour periods, we averaged the McFarland Hill sulfate (Thermo-5020), scattering (NGN-2) and RH (Rotronic) hourly data into two-hour, whole number blocks in order to bring the data from Sunset Labs into the reconstruction equation. In addition, we subtracted a "filter blank" value for the Sunset OC data of 0.5 $\mu g/m^3$ (empirically derived from user experience of the Model 3) from the OC data prior to their use in the reconstruction calculation (OMC = (Sunset OC – 0.5) x 1.8). See Figure 3-11 for results of these reconstructed estimates of visibility using both sulfate and carbon measurements.

As indicated by Figure 3-11, adding the organic carbon data to the sulfate data significantly improves the agreement between reconstructed estimates of aerosol scattering and direct visibility measurements at the McFarland Hill site. Specifically, it appears that these two components of the ambient aerosol generally explain about 94 percent of the observed scattering at Acadia during the summer, with a very high correlation coefficient even at 2-hour intervals. This is excellent agreement considering that scattering from nitrate and crustal aerosol components is not included in this reconstruction.

These data demonstrate that the highly time-resolved nature of RAIN data is invaluable in examining short-term variations (i.e., on the order of days to weeks) in haze production and transport. The sulfate, carbon and other monitoring capabilities emerging from the RAIN project will provide another valuable tool to state and tribal authorities in seeking to understand the sources of regional haze and to craft effective control strategies. A more detailed analysis of RAIN data is available in a recently released MANE-VU technical memorandum.[19]

[19] "Rural Aerosol Intensive Network (RAIN) Preliminary Data Analysis," available at: http://www.nescaum.org/documents/2006-05-memo8-rain.pdf/

Figure 3-11. 2-Hour Reconstructed scattering at Acadia, Maine using semi-continuous SO_4 and OC data for the third quarter of 2004

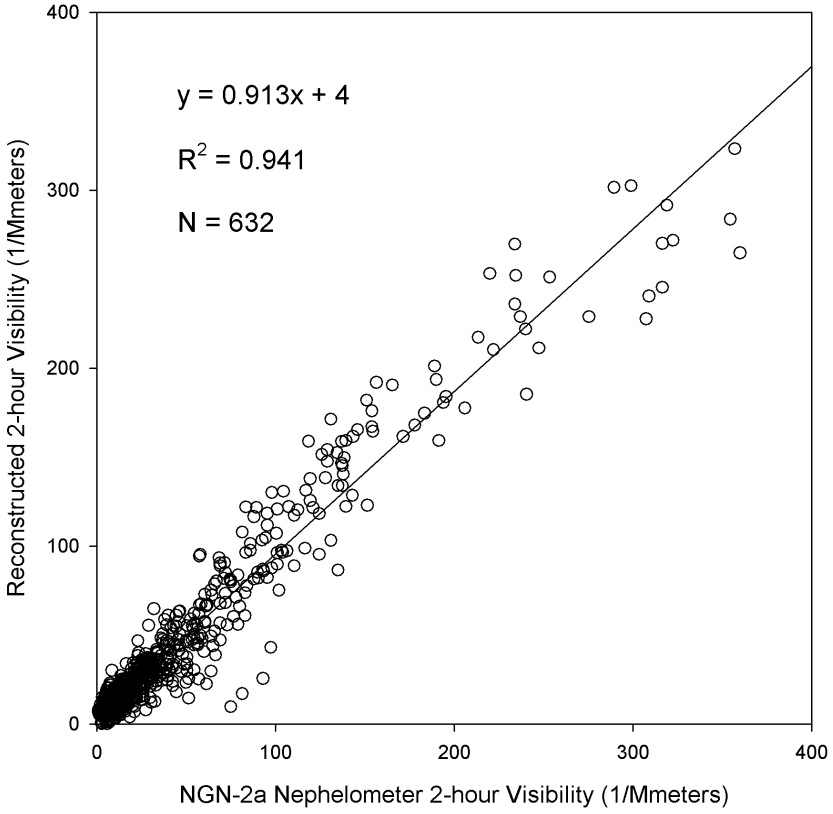

References

NESCAUM, "Natural Background Visibility Conditions: Considerations and Proposed Approach to the Calculation of Natural Background Visibility Conditions at MANE-VU Class I Areas," Northeast States for Coordinated Air Use Management, Boston, MA, June 2004a.

NESCAUM, "2002: A Year in Review," Northeast States for Coordinated Air Use Management, Boston, MA, December, 2004b.

USEPA, "Guidance for Tracking Progress under the Regional Haze Rule," EPA-454/B-03-004 September 2003a.

USEPA, "Guidance for Estimating Natural Visibility Conditions under the Regional Haze Program," EPA-454/B-03-005 September 2003b.

4. HAZE-ASSOCIATED POLLUTANT EMISSIONS

This chapter explores the origin and quantity of haze-forming pollutants emitted in the eastern and the mid-Atlantic United States. It also describes the procedures used to prepare emissions inventory data for use in chemical transport models (Chapter 6 describes in greater detail the models themselves).

The pollutants that affect fine particle formation, and thus contribute to regional haze, are sulfur oxides (SO_X), nitrogen oxides (NO_X), volatile organic compounds (VOC), ammonia (NH_3), and particles with an aerodynamic diameter less than or equal to 10 and 2.5 µm (i.e., primary PM_{10} and $PM_{2.5}$). The emissions dataset illustrated below is the 2002 MANE-VU Version 2 regional haze emissions inventory. The emission inventories include carbon monoxide (CO), but we do not consider that pollutant here as it does not contribute to regional haze. The MANE-VU regional haze emissions inventory version 3.0, released in April 2006, has superseded version 2 for modeling purposes. This inventory update was developed through the Mid-Atlantic Regional Air Management Association (MARAMA) for the MANE-VU RPO. The comparative observations among recent emission inventories presented here (the 1996 USEPA NET and 1999 NEI) would hold true were version 3.0 substituted for version 2.0. [20]

The first section of this chapter describes emission characteristics by pollutant and source type (e.g., point, area, and mobile). The second section describes on-going efforts to process emissions inventory data in support of air quality modeling. The final section provides source apportionment estimates for several MANE-VU Class 1 areas based on 2002 SO_2 inventory data.

4.1. Emissions Inventory Characteristics

4.1.1. Sulfur Dioxide (SO_2)

SO_2 is the primary precursor pollutant for sulfate particles. Sulfate particles commonly account for more than 50 percent of particle-related light extinction at northeastern Class I areas on the clearest days and for as much as or more than 80 percent

[20] EPA's Emission Factor and Inventory Group (EFIG) (USEPA/OAR (Office of Air and Radiation)/OAQPS (Office of Air Quality Planning and Standards)/EMAD (Emissions, Monitoring and Analysis Division) prepares a national database of air emissions information with input from numerous state and local air agencies, from tribes, and from industry. This database contains information on stationary and mobile sources that emit criteria air pollutants and their precursors, as well as hazardous air pollutants (HAPs). The database includes estimates of annual emissions, by source, of air pollutants in each area of the country on an annual basis. The NEI includes emission estimates for all 50 states, the District of Columbia, Puerto Rico, and the Virgin Islands. Emission estimates for individual point or major sources (facilities), as well as county level estimates for area, mobile and other sources, are available currently for years 1985 through 1999 for criteria pollutants, and for years 1996 and 1999 for HAPs. Data from the NEI help support air dispersion modeling, regional strategy development, setting regulation, air toxics risk assessment, and tracking trends in emissions over time. For emission inventories prior to 1999, the National Emission Trends (NET) database maintained criteria pollutant emission estimates and the National Toxics Inventory (NTI) database maintained HAP emission estimates. Beginning with 1999, the NEI began preparing criteria and HAP emissions data in a more integrated fashion to take the place of the NET and the NTI.

on the haziest days. Hence, SO_2 emissions are an obvious target of opportunity for reducing regional haze in the eastern United States. Combustion of coal and, to a substantially lesser extent, of certain petroleum products accounts for most anthropogenic SO_2 emissions. In fact, in 1998 a single source category — coal-burning power plants — was responsible for two-thirds of total SO_2 emissions nationwide (NESCAUM, 2001a).

Figure 4-1 shows SO_2 emissions trends in the MANE-VU states extracted from the NEI for the years 1996, 1999, and the 2002 MANE-VU inventory (USEPA, 2005; MARAMA, 2004). Most of the states (with the exception of Maryland) show declines in year 2002 annual SO_2 emissions as compared to 1996 emissions. Some of the states show an increase in 1999 followed by a decline in 2002 and others show consistent declines throughout the entire period. The upward trend in emissions after 1996 probably reflects electricity demand growth during the late 1990s combined with the availability of banked emissions allowances from initial over-compliance with control requirements in Phase 1 of the USEPA Acid Rain Program. This led to relatively low market prices for allowances later in the decade, which encouraged utilities to purchase allowances rather than implement new controls as electricity output expanded. The observed decline in the 2002 SO_2 emissions inventory reflects implementation of the second phase of the USEPA Acid Rain Program, which in 2000 further reduced allowable emissions and extended emissions limits to more power plants. Figure 4-2 shows the percent contribution from different source categories to overall, annual 2002 SO_2 emissions in the MANE-VU states. The chart shows that point sources dominate SO_2 emissions, which primarily consist of stationary combustion sources for generating electricity, industrial energy, and heat. Smaller stationary combustion sources called “area sources” (primarily commercial and residential heating) are another important source category in the MANE-VU states. By contrast, on-road and non-road mobile sources make only a relatively small contribution to overall SO_2 emissions in the region (NESCAUM, 2001a).

4.1.2. Volatile Organic Compounds (VOC)

Existing emission inventories generally refer to “volatile organic compounds” (VOCs) for hydrocarbons whose volatility in the atmosphere makes them particularly important from the standpoint of ozone formation. From a regional haze perspective, we are concerned less with the volatile organic gases emitted directly to the atmosphere and more with the secondary organic aerosol (SOA) that the VOCs form after condensation and oxidation processes. Thus the VOC inventory category is of interest primarily from the organic carbon perspective of $PM_{2.5}$. After sulfate, organic carbon generally accounts for the next largest share of fine particle mass and particle-related light extinction at northeastern Class I sites. The term organic carbon encompasses a large number and variety of chemical compounds that may come directly from emission sources as a part of primary PM or may form in the atmosphere as secondary pollutants. The organic carbon present at Class I sites almost certainly includes a mix of species, including pollutants originating from anthropogenic (i.e., manmade) sources as well as biogenic hydrocarbons emitted by vegetation. Recent efforts to reduce manmade organic carbon emissions have been undertaken primarily to address summertime ozone formation in urban centers. Future efforts to further reduce organic carbon emissions may be driven by programs that address fine particles and visibility.

Figure 4-1. State Level Sulfur Dioxide Emissions

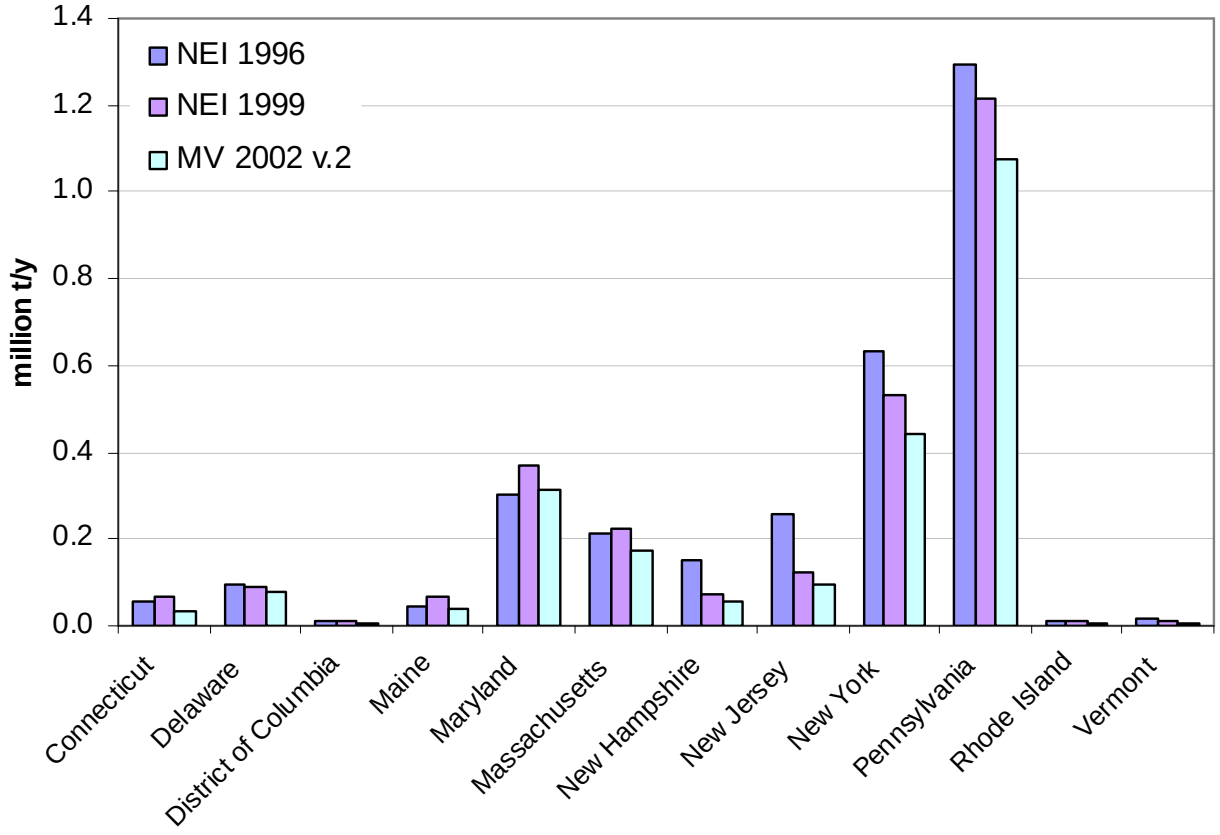

Figure 4-2. SO_2 (Bar graph: Percentage fraction of four source categories, Circle: Annual emissions amount in 10^6 tons per year)

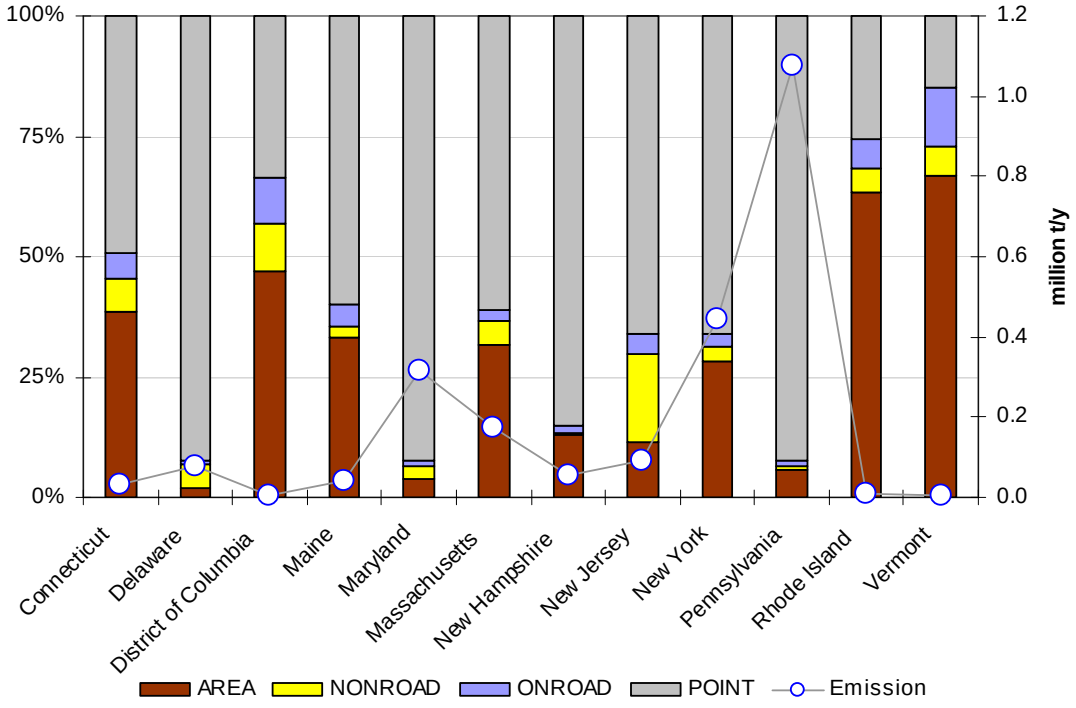

Understanding the transport dynamics and source regions for organic carbon in northeastern Class I areas is likely to be more complex than for sulfate. This is partly because of the large number and variety of OC species, the fact that their transport characteristics vary widely, and the fact that a given species may undergo numerous complex chemical reactions in the atmosphere. Thus, the organic carbon contribution to visibility impairment at most Class I sites in the East is likely to include manmade pollution transported from a distance, manmade pollution from nearby sources, and biogenic emissions, especially terpenes from coniferous forests.

As shown in Figure 4-3, the VOC inventory is dominated by mobile and area sources. On-road mobile sources of VOCs include exhaust emissions from gasoline passenger vehicles and diesel-powered heavy-duty vehicles as well as evaporative emissions from transportation fuels. VOC emissions may also originate from a variety of area sources (including solvents, architectural coatings, and dry cleaners) as well as from some point sources (e.g., industrial facilities and petroleum refineries).

Biogenic VOCs may play an important role within the rural settings typical of Class I sites. The oxidation of hydrocarbon molecules containing seven or more carbon atoms is generally the most significant pathway for the formation of light-scattering organic aerosol particles (Odum et al., 1997). Smaller reactive hydrocarbons that may contribute significantly to urban smog (ozone) are less likely to play a role in organic aerosol formation, though we note that high ozone levels can have an indirect effect on visibility by promoting the oxidation of other available hydrocarbons, including biogenic

Figure 4-3. VOC (Bar graph: Percentage fraction of four source categories, Circle: Annual emissions amount in 10^6 tons per year)

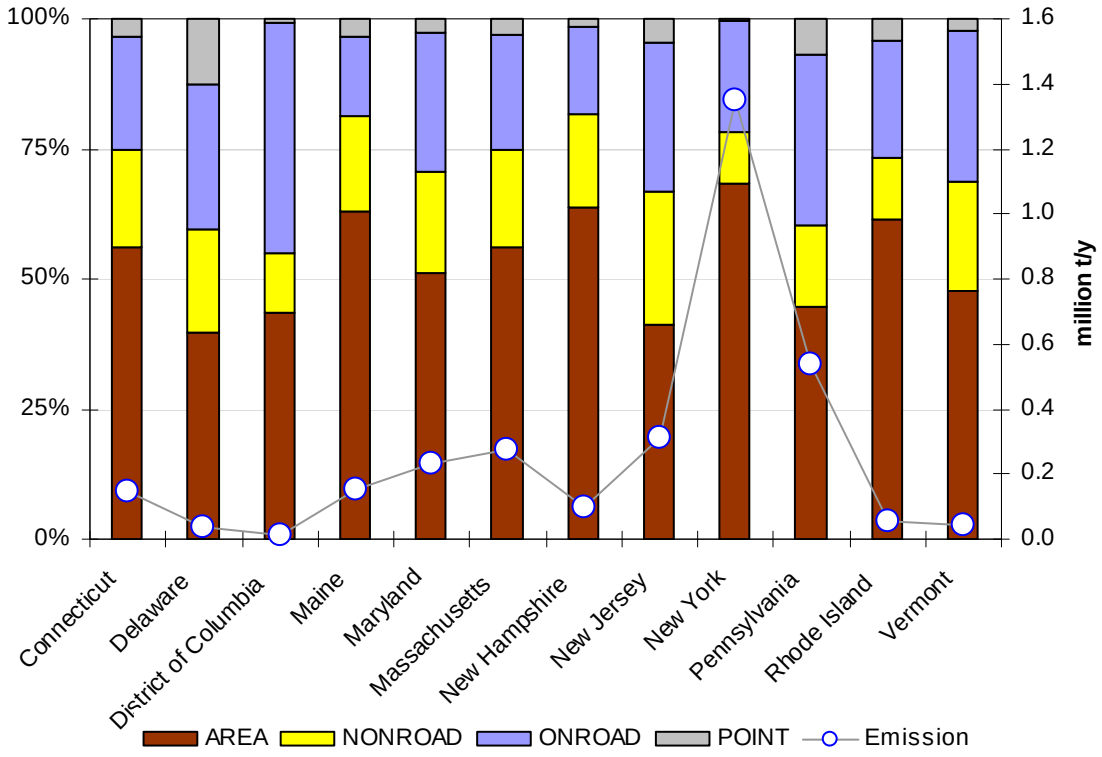

emissions (NESCAUM, January 2001). In short, we need further work to characterize the organic carbon contribution to regional haze in the Northeast and Mid-Atlantic states and to develop emissions inventories that will be of greater value for visibility planning purposes.

4.1.3. Oxides of Nitrogen (NO_X)

NO_X emissions contribute directly to visibility impairment in the eastern U.S. by forming light-scattering nitrate particles. Nitrate generally accounts for a substantially smaller fraction of fine particle mass and related light extinction than sulfate and organic carbon at northeastern Class I sites. Notably, nitrate may play a more important role at urban sites and in the wintertime. In addition, NO_X may have an indirect effect on summertime visibility by virtue of its role in the formation of ozone, which in turn promotes the formation of secondary organic aerosols (NESCAUM 2001a).

Figure 4-4 shows NO_X emissions in the MANE-VU region at the state level. Since 1980, nationwide emissions of NO_X from all sources have shown little change. In fact, emissions increased by 2 percent between 1989 and 1998 (USEPA, 2000a). This increase is most likely due to industrial sources and the transportation sector, as power plant combustion sources have implemented modest emissions reductions during the same time period. Most states in the MANE-VU region experienced declining NO_X emissions from 1996 through 2002, except Massachusetts, Maryland, New York, and Rhode Island, which show an increase in NO_X emissions in 1999 before declining to levels below 1996 emissions in 2002.

Power plants and mobile sources generally dominate state and national NO_X emissions inventories. Nationally, power plants account for more than one-quarter of all NO_X emissions, amounting to over six million tons. The electric sector plays an even larger role, however, in parts of the industrial Midwest where high NO_X emissions have a particularly significant power plant contribution. By contrast, mobile sources dominate the NO_X inventories for more urbanized Mid-Atlantic and New England states to a far greater extent, as shown in Figure 4-5. In these states, on-road mobile sources — a category that mainly includes highway vehicles — represent the most significant NO_X source category. Emissions from non-road (i.e., off-highway) mobile sources, primarily diesel-fired engines, also represent a substantial fraction of the inventory. While there are fewer uncertainties associated with available NO_X estimates than in the case of other key haze-related pollutants — including primary fine particle and ammonia emissions — further efforts could improve current inventories in a number of areas (NESCAUM, 2001a).

In particular, better information on the contribution of area and non-highway mobile sources may be of most interest in the context of regional haze planning. First, available emission estimation methodologies are weaker for these types of sources than for the large stationary combustion sources. Moreover, because SO_2 and NO_X emissions must mix with ammonia to participate in secondary particle formation, emissions that occur over large areas at the surface may be more efficient in secondary fine particulate formation than concentrated emissions from isolated tall stacks (Duyzer, 1994).

Figure 4-4. State Level Nitrogen Oxides Emissions

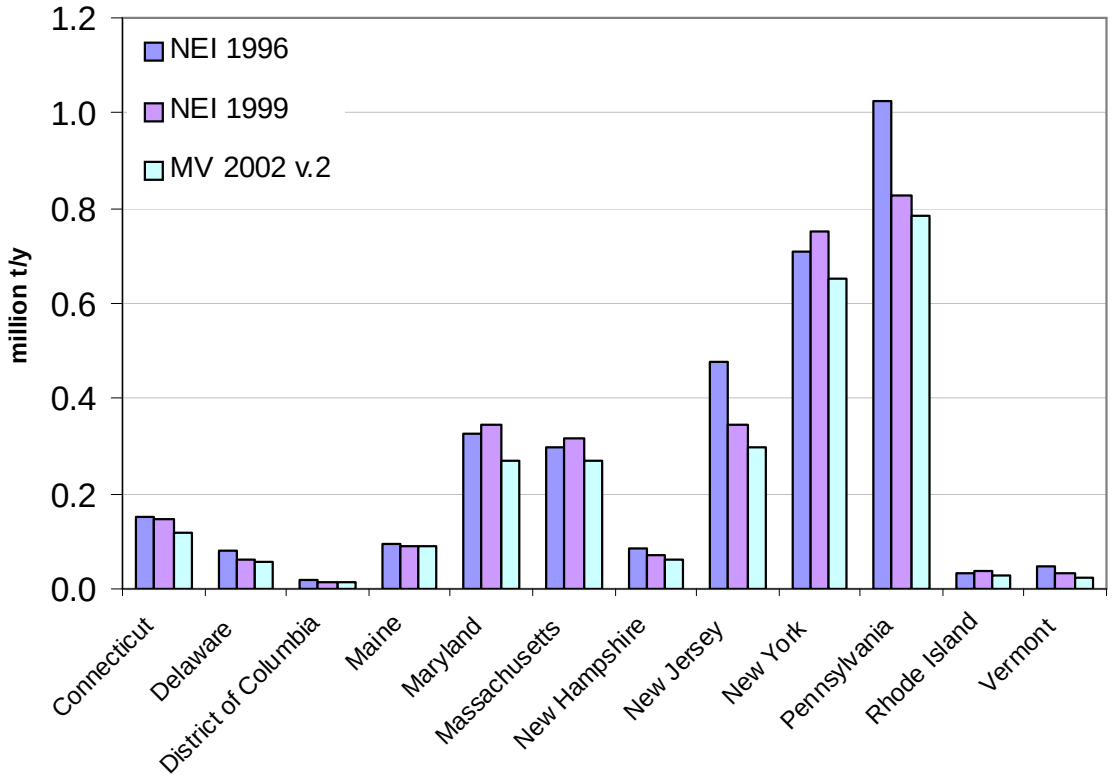

Figure 4-5. NO_X (Bar graph: Percentage fraction of four source categories, Circle: Annual emissions amount in 10^6 tons per year)

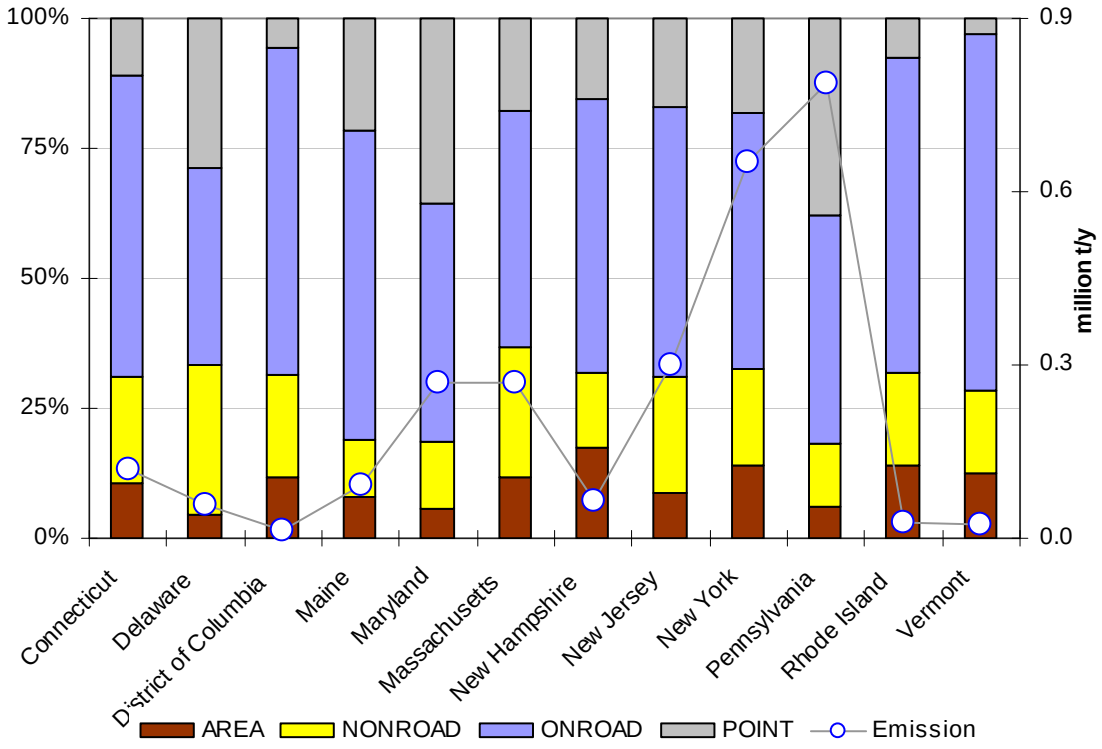

4.1.4. Primary Particulate Matter (PM_{10} and $PM_{2.5}$)

Directly-emitted or "primary" particles (as distinct from secondary particles that form in the atmosphere through chemical reactions involving precursor pollutants like SO_2 and NO_X) can also contribute to regional haze. For regulatory purposes, we make a distinction between particles with an aerodynamic diameter less than or equal to 10 micrometers and smaller particles with an aerodynamic diameter less than or equal to 2.5 micrometers (i.e., primary PM_{10} and $PM_{2.5}$, respectively).

Figure 4-6 and Figure 4-7 show PM_{10} and $PM_{2.5}$ emissions for the MANE-VU states for the years 1996, 1999, and 2002. Note that for PM_{10} the inventory values are drawn from the 2002 NEI. Most states show a steady decline in annual PM_{10} emissions over this time period. By contrast, emission trends for primary $PM_{2.5}$ are more variable.

Crustal sources are significant contributors of primary PM emissions. This category includes fugitive dust emissions from construction activities, paved and unpaved roads, and agricultural tilling. Typically, monitors estimate PM_{10} emissions from these types of sources by measuring the horizontal flux of particulate mass at a fixed downwind sampling location within perhaps 10 meters of a road or field. Comparisons between estimated emission rates for fine particles using these types of measurement techniques and observed concentrations of crustal matter in the ambient air at downwind receptor sites suggest that physical or chemical processes remove a significant fraction of crustal material relatively quickly. As a result, it rarely entrains into layers of the atmosphere where it can transport to downwind receptor locations. Because of this discrepancy between estimated emissions and observed ambient concentrations, modelers typically reduce estimates of total $PM_{2.5}$ emissions from all crustal sources by applying a factor of 0.15 to 0.25 before including in modeling analyses.

From a regional haze perspective, crustal material generally does not play a major role. On the 20 percent best-visibility days during the baseline period (2000-2004), it accounted for six to eleven percent of particle-related light extinction at MANE-VU Class 1 sites. On the 20 percent worst-visibility days, however, crustal material generally plays a much smaller role relative to other haze-forming pollutants, ranging from two to three percent. Moreover, the crustal fraction includes material of natural origin (such as soil or sea salt) that is not targeted under the Haze Rule. Of course, the crustal fraction can be influenced by certain human activities, such as construction, agricultural practices, and road maintenance (including wintertime salting) — thus, to the extent that these types of activities are found to affect visibility at northeastern Class I sites, control measures targeted at crustal material may prove beneficial.

Experience from the western United States, where the crustal component has generally played a more significant role in driving overall particulate levels, may be helpful to the extent that it is relevant in the eastern context. In addition, a few areas in the Northeast, such as New Haven, Connecticut and Presque Isle, Maine, have some experience with the control of dust and road-salt as a result of regulatory obligations stemming from their past non-attainment status with respect to the NAAQS for PM_{10}.

Figure 4-6. State Level Primary PM_{10} Emissions

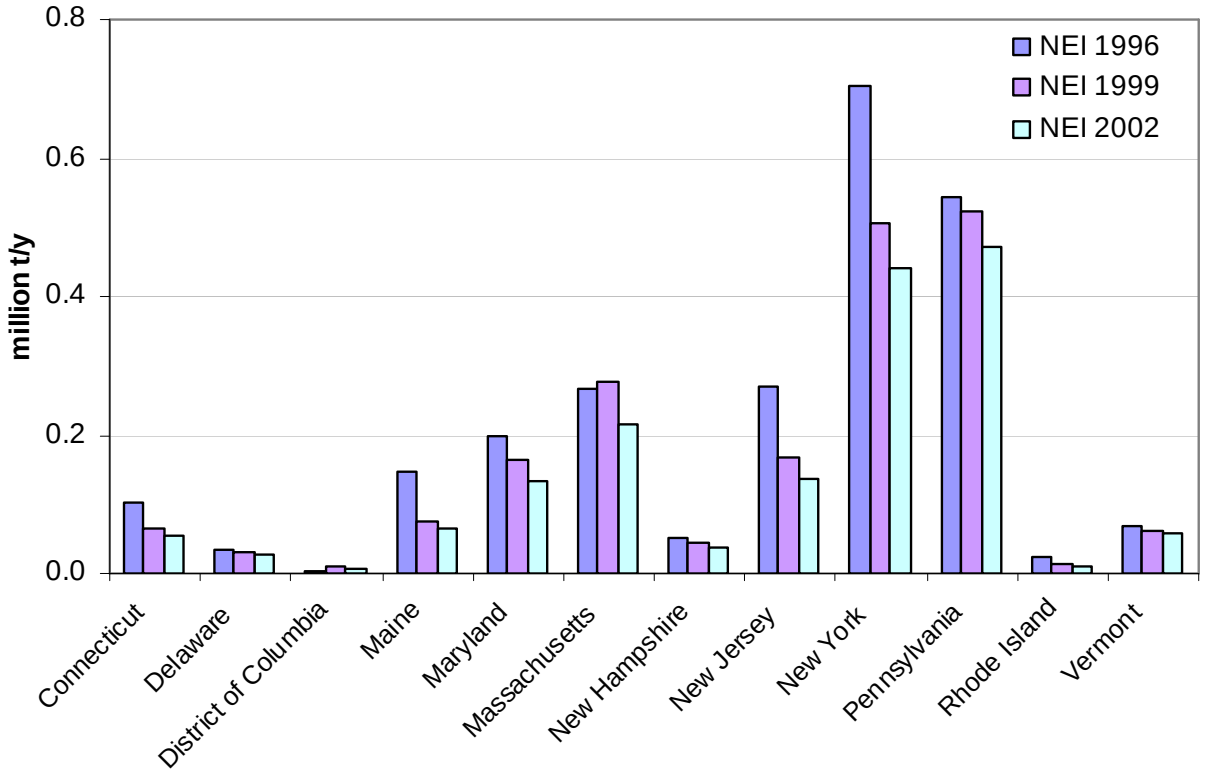

Figure 4-7. State Level Primary $PM_{2.5}$ Emissions

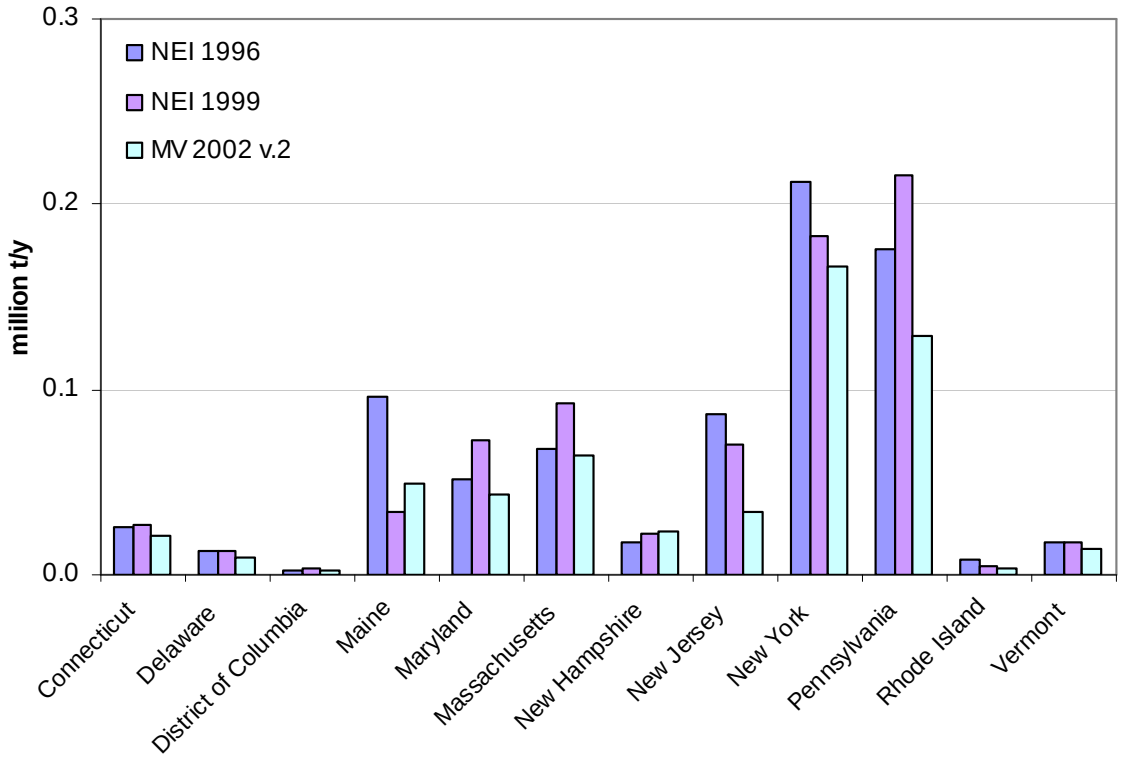

Current emissions inventories for the entire MANE-VU area indicate residential wood combustion represents 25 percent of primary fine particulate emissions in the region. This implies that rural sources can play an important role in addition to the contribution from the region's many highly populated urban areas. An important consideration in this regard is that residential wood combustion occurs primarily in the winter months, while managed or prescribed burning activities occur largely in other seasons. The latter category includes agricultural field-burning activities, prescribed burning of forested areas and other burning activities such as construction waste burning. Limiting burning to times when favorable meteorological conditions can efficiently disperse resulting emissions can manage many of these types of sources.

Figure 4-8 and Figure 4-9 show that area and mobile sources dominate primary PM emissions. (The NEI inventory categorizes residential wood combustion and some other combustion sources as area sources.) The relative contribution of point sources is larger in the primary $PM_{2.5}$ inventory than in the primary PM_{10} inventory since the crustal component (which consists mainly of larger or "coarse-mode" particles) contributes mostly to overall PM_{10} levels. At the same time, pollution control equipment commonly installed at large point sources is usually more efficient at capturing coarse-mode particles.

4.1.5. Ammonia Emissions (NH_3)

Knowledge of ammonia emission sources will be necessary in developing effective regional haze reduction strategies because of the importance of ammonium sulfate and ammonium nitrate in determining overall fine particle mass and light scattering. According to 1998 estimates, livestock agriculture and fertilizer use accounted for approximately 86 percent of all ammonia emissions to the atmosphere (USEPA, 2000b). We need, however, better ammonia inventory data for the photochemical models used to simulate fine particle formation and transport in the eastern United States. Because the USEPA does not regulate ammonia as a criteria pollutant or as a criteria pollutant precursor, these data do not presently exist at the same level of detail or certainty as for NO_X and SO_2.

Ammonium ion (formed from ammonia emissions to the atmosphere) is an important constituent of airborne particulate matter, typically accounting for 10–20 percent of total fine particle mass. Reductions in ammonium ion concentrations can be extremely beneficial because a more-than-proportional reduction in fine particle mass can result. Ansari and Pandis (1998) showed that a one $\mu g/m^3$ reduction in ammonium ion could result in up to a four $\mu g/m^3$ reduction in fine particulate matter. Decision makers, however, must weigh the benefits of ammonia reduction against the significant role it plays in neutralizing acidic aerosol.[21]

[21] SO_2 reacts in the atmosphere to form sulfuric acid (H_2SO_4). Ammonia can partially or fully neutralize this strong acid to form ammonium bisulfate or ammonium sulfate. If planners focus future control strategies on ammonia and do not achieve corresponding SO_2 reductions, fine particles formed in the atmosphere will be substantially more acidic than those presently observed.

Figure 4-8. Primary PM_{10} (Bar graph: Percentage fraction of four source categories, Circle: Annual emissions amount in 10^6 tons per year)

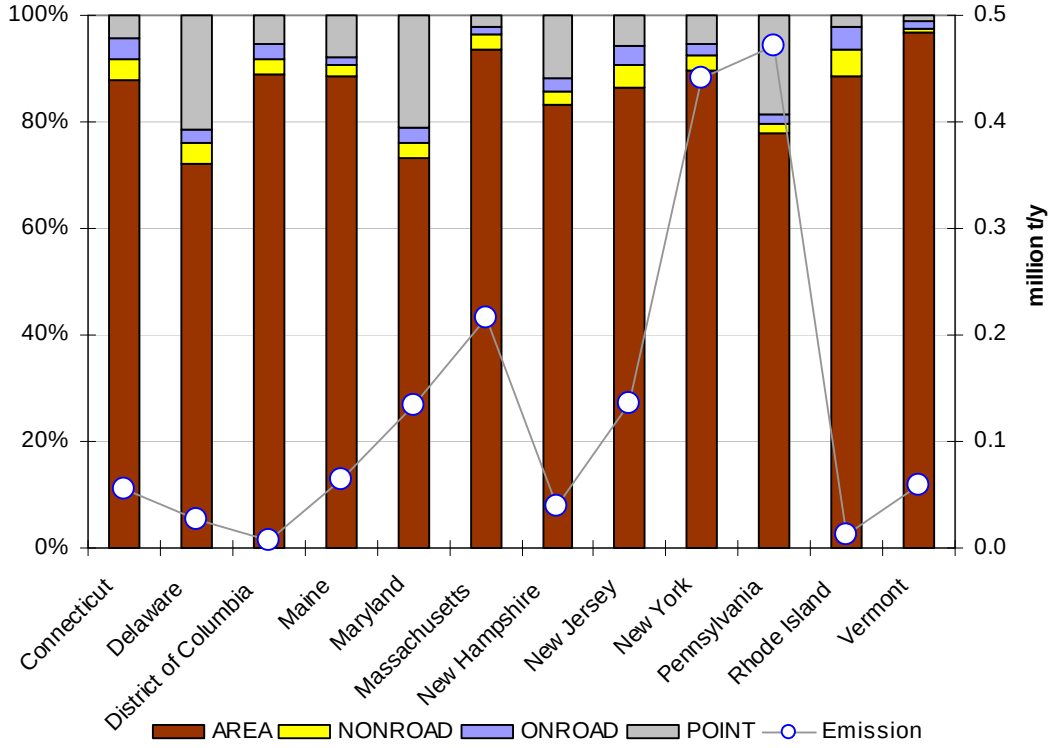

Figure 4-9. Primary $PM_{2.5}$ (Bar graph: Percentage fraction of four source categories, Circle: Annual emissions amount in 106 tons per year)

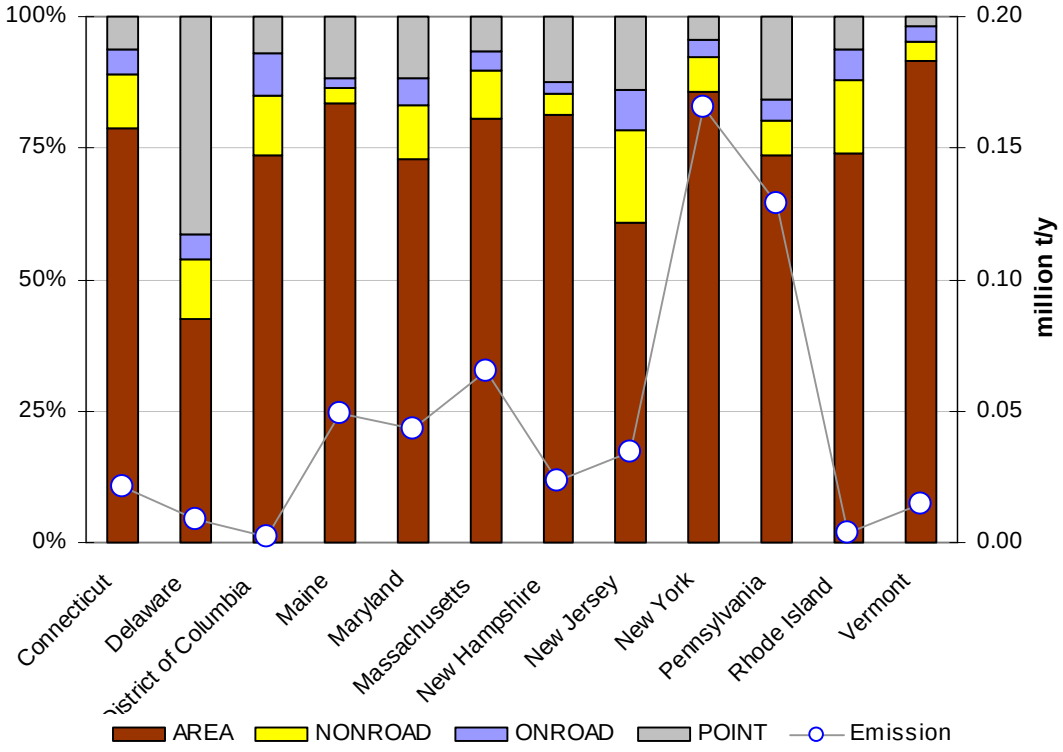

To address the need for improved ammonia inventories, MARAMA, NESCAUM and USEPA funded researchers at Carnegie Mellon University (CMU) in Pittsburgh to develop a regional ammonia inventory (Davidson et al., 1999). This study focused on three issues with respect to current emissions estimates: (1) a wide range of ammonia emission factor values, (2) inadequate temporal and spatial resolution of ammonia emissions estimates, and (3) a lack of standardized ammonia source categories.

The CMU project established an inventory framework with source categories, emissions factors, and activity data that are readily accessible to the user. With this framework, users can obtain data in a variety of formats[22] and can make updates easily, allowing additional ammonia sources to be added or emissions factors to be replaced as better information becomes available (Strader et al., 2000; NESCAUM, 2001b).

Figure 4-10 shows that estimated ammonia emissions were fairly stable in the 1996, 1999, and 2002 NEI for MANE-VU states, with some increases observed for Massachusetts, New Jersey and New York. Area and on-road mobile sources dominate the ammonia inventory, according to Figure 4-11. Specifically, emissions from agricultural sources and livestock production account for the largest share of estimated ammonia emissions in the MANE-VU region, except in the District of Columbia. The two remaining sources with a significant emissions contribution are wastewater treatment systems and gasoline exhaust from highway vehicles.

Figure 4-10. State Level Ammonia Emissions

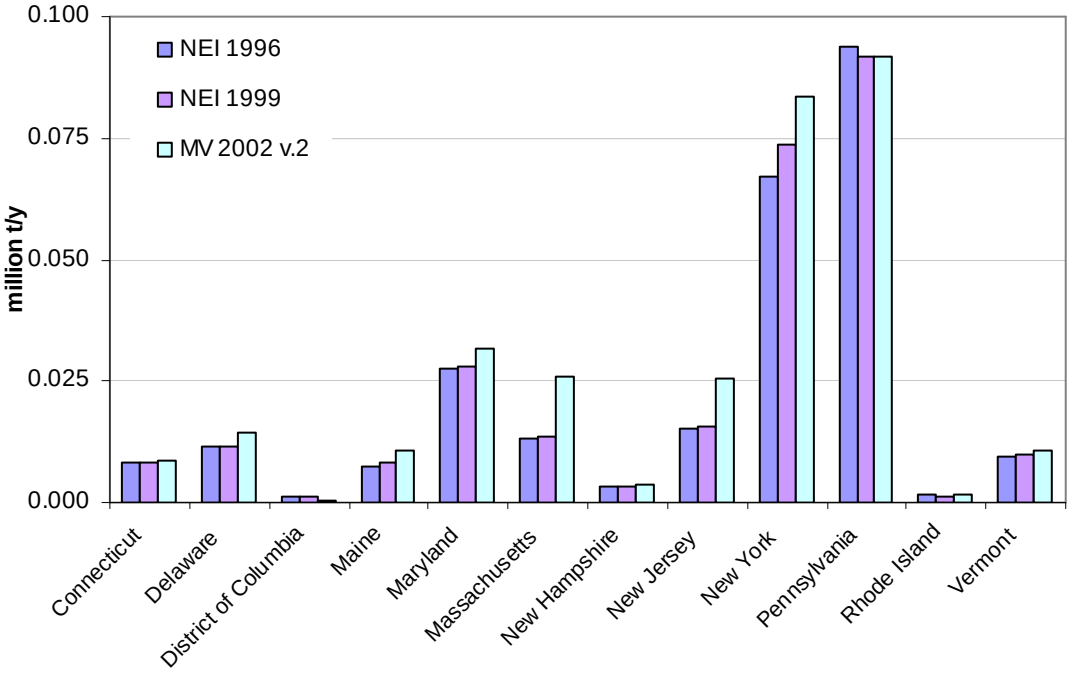

[22] For example, the user will have the flexibility to choose the temporal resolution of the output emissions data or to spatially attribute emissions based on land-use data.

Figure 4-11. NH_3 (Bar graph: Percentage fraction of four source categories, Circle: Annual emissions amount in 10^6 tons per year)

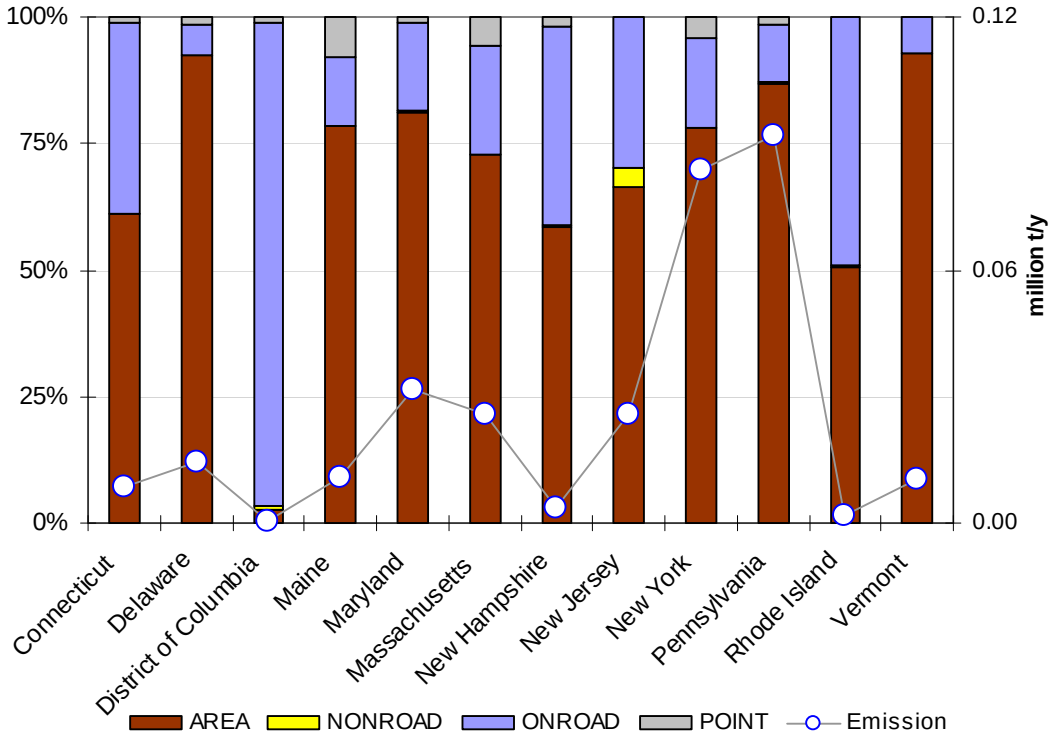

4.2. Contribution Assessments Based on Emissions Inventories

Two data analysis methods have been developed that directly combine emission inventory data with meteorological data in order to provide first-order contributions to observed sulfate from individual states. The first approach, known as "Q/d," evaluates the state contribution as a proportion of the ratio of the total SO_2 emissions from that state and the distance from the state to the receptor. States and sources are assigned wind sectors to account for prevailing wind patterns in establishing contributions. The second approach, known as "Emissions times Upwind Probability," evaluates the state contribution through the use of ensemble back trajectories (See Appendix A for a more detailed description of trajectory methods). The back trajectory-derived residence times of air parcels have been mapped onto a grid to create a "residence time probability field," which is then multiplied by an SO_2 emissions field to obtain estimated source contributions. The results of the two approaches are compared for receptor sites in and around the MANE-VU region.

4.2.1. Sulfur Dioxide Emissions Divided by Distance

Aggregated over long periods of time and large geographic areas, the total atmospheric sulfate contribution from a specific source, state, or region should be approximately proportionate to its SO_2 emissions. For specific receptor locations, like a Class 1 visibility area, relative impacts decrease with increasing distance from the source. Impacts diminish over distance as pollutants are dispersed in the atmosphere and removed through deposition. For non-reactive primary pollutant emissions, the

relationship between atmospheric concentrations and distance (d) can be approximated as a function of $1/d^2$. For secondary pollutants like sulfate, reductions in ambient concentrations that occur as a result of dispersion and deposition mechanisms are partially offset by the formation of secondary aerosol such that an increasing fraction of the remaining downwind sulfur is converted to aerosol sulfate. In these cases, the effects of distance are better characterized by the function 1/d. During regional sulfate episodes when sulfur conversion rates are enhanced by the presence of gas and aqueous-phase oxidants, pollutant concentrations decline even less rapidly with distance as accelerated aerosol formation rates work to both generate more sulfate and reduce the remaining sulfur available for deposition (deposition rates are roughly an order of magnitude slower for sulfate than for SO_2).

One simple technique for deducing the relative impact of emissions from specific point sources on a specific receptor site involves calculating the ratio of annual emissions (Q) to source-receptor distance (d).[23] This empirical relationship is reasonable based on simple dispersion assumptions. Results from SO_2 modeling using the CALPUFF (California Puff) model (EarthTech, 2004) further bolster its validity by showing a strong relationship between emissions and distance. In fact, this extremely simple method of estimating impact can be significantly improved to account for some aspects of meteorology by scaling results according to the extremely linear relationships between CALPUFF and Q/d values within specific wind sectors.

The geographic domain of the sources included in the Q/d study consisted of U.S. states in the CENRAP, MANE-VU, VISTAS, and MIDWEST RPO regions. Canadian provinces in the lower eastern region were also included. The categories of SO_2 emission sources included in this analysis were area sources (e.g., residential boilers and heaters), non-road mobile sources (e.g., tractors and construction vehicles), and point sources (e.g., industrial smokestacks and power generation facilities).[24] Results were calculated for seven receptors including: Acadia National Park, Brigantine Wilderness in the Forsythe Wildlife Preserve, Dolly Sods Wilderness, Lye Brook Wilderness, Moosehorn Wilderness, Presidential Range-Dry River Wilderness, and Shenandoah National Park.

The empirical formula that relates emission source strength and estimated impact can be expressed through the equation $I=C_i*Q/d$. In this equation, the strength of an emission source, Q, is linearly related to the impact, I, that it will have on a receptor located a distance, d, away. The effect of meteorological prevailing winds can be factored into this approach by establishing the constant, C_i, as a function of the sectors relative to the receptor site. This relationship can be established by comparing Q/d values to modeled impacts, which are also dependent on prevailing wind patterns at the site of impact. By establishing a different constant for each sector, based on prior modeling results – in this case, CALPUFF results – we are in effect "scaling" Q/d results

[23] We calculated distances using the Haversine formula, which uses spherical geometry to calculate the distance between two points on the surface of a sphere. Because the Earth is not an exact sphere, use of this formula introduces a small amount of error — on the order of 0.5% — in the distance calculations for any two locations on the Earth's surface (see http://mathforum.org/library/drmath for further details).

[24] On-road mobile sources contribute about 2% of the SO_2 inventory nationally (See Figure 4-2 for regional breakdown) and were not considered significant enough to include in this analysis, which does not provide results to that level of precision.

by CALPUFF-calculated source impacts. The absolute impacts produced are then dependent on the CALPUFF results, however the relative contributions of each source within a wind sector is established completely independent of the CALPUFF calculation, yielding a quasi-independent method of apportionment to add to our weight-of-evidence approach.

To determine the appropriate constant for each wind sector relative to a given receptor, a linear regression analysis was performed on 778 sources in the eastern U.S. with emissions data available from the continuous emissions monitoring system (CEMS) for 2002. The Q/d values were calculated for these sources and compared with their modeled source impacts from the CALPUFF model (see Phase I modeling discussed in Appendix D). The sites were grouped by angle into "wind sectors" such that each wind sector had a best-fit line with as high a correlation coefficient (R^2) value as possible. Most sectors had an R^2 above or near 0.90. The slopes of the resulting best-fit lines were used as the constants in the above equation.[25]

To calculate the impact that each state had on a given receptor, the area and non-road SO_2 emission sources were summed across the entire state, and the distance to the receptor site for those emission sources was calculated based on that state's geographic center, adjusted for population density.[26] In this way, the area and non-road emissions were treated as a single point source located at the population-weighted center of each state. These impacts were then added to the impact of the point sources that were calculated individually. The sum of area, non-road, and point source impacts for each state was used to compare the contributions relative to other states in the eastern U.S. and parts of Canada.

The principal contributors to the MANE-VU receptors, according to this method, include the midwestern states of Indiana and Ohio, as well as Pennsylvania and New York. This is due not only to the large emissions from these states, but also to the predominantly westerly winds that carry Midwest pollution eastward (the Midwest was located in the wind sector with the highest C_i-value, five times that of the lowest Ci-value). Table 4-1 shows the relative contribution of eastern states and Canadian provinces on several receptor sites in the region. Figure 4-12 and Figure 4-13 show the corresponding Q/d rankings across a set of northern and southern Class I areas in or near MANE-VU.

---

[25] The analysis resulted in best-fit lines that did not always go through the origin. By forcing the regression lines through the origin, we ensure that a source with zero emissions would correspond to zero impact at the receptor. After having forced the best-fit lines through the origin, R^2 values remained greater than 0.77 and changed less than 0.01 from the original regression. The changes to the slope were considered insignificant, with an average change of 4%, ranging from -11% to 16%; the extremes occurred for plots with relatively few points and on the low end of R-squared correlations. Some angle ranges were not associated with a wind sector because of insufficient data for that angle range. For example, there was a lack of data for Lye Brook Wilderness receptor in the 0-144^o angle range. This angle sector and similar sectors lacking adequate data were assigned the lowest C_i-value amongst the other wind sectors of the same receptor site. The impact of this decision should be small given the relatively few sources in these directions and their tendency to be downwind of the receptor.

[26] Calculations using county-level emissions and distance to county centroid to receptor were compared to the approach used here. This added complexity, however, did not substantially change the predicted impacts nor the relative rankings among states.

Table 4-1. 2002 SO_2 CALPUFF-scaled Emissions over Distance Impact ($\mu g/m^3$)

STATE	ACADIA	LYE BROOK	BRIGANTINE	SHENANDOAH	EMISSIONS
Pennsylvania	0.19	0.30	0.38	0.43	1,090,562
Ohio	0.19	0.23	0.27	0.46	1,273,755
West Virginia	0.08	0.09	0.16	0.32	573,136
Maryland	0.05	0.06	0.24	0.21	292,970
New York	0.12	0.15	0.15	0.13	341,493
Indiana	0.11	0.11	0.14	0.18	914,039
North Carolina	0.07	0.06	0.14	0.26	510,452
Virginia	0.06	0.04	0.14	0.17	309,709
Georgia	0.07	0.07	0.11	0.14	605,040
Kentucky	0.06	0.06	0.11	0.14	521,583
Michigan	0.08	0.08	0.06	0.10	432,166
Illinois	0.07	0.07	0.07	0.10	642,264
Tennessee	0.04	0.04	0.07	0.09	423,705
New Jersey	0.02	0.02	0.14	0.07	64,437
Alabama	0.05	0.05	0.07	0.08	548,054
Texas	0.04	0.04	0.05	0.06	849,831
Florida	0.04	0.03	0.06	0.07	537,327
Massachusetts	0.08	0.02	0.03	0.05	123,754
South Carolina	0.04	0.02	0.05	0.07	262,867
Delaware	0.02	0.02	0.10	0.04	83,549
Missouri	0.04	0.04	0.05	0.05	361,911
Wisconsin	0.03	0.03	0.03	0.04	263,040
Maine	0.05	<0.01	<0.01	0.01	39,423
Kansas	0.01	0.01	0.01	0.01	136,104
New Hampshire	0.03	<0.01	0.01	0.01	53,772
Minnesota	0.01	0.01	0.01	0.01	124,151
Mississippi	0.01	0.01	0.01	0.02	126,456
Iowa	0.01	0.01	0.01	0.01	230,676
Connecticut	0.01	0.01	0.01	0.01	41,093
Oklahoma	0.01	0.01	0.01	0.01	139,327
Louisiana	0.01	0.01	0.01	0.02	346,170
Arkansas	<0.01	<0.01	0.01	0.01	140,096
Nebraska	0.01	<0.01	<0.01	0.01	46,074
Rhode Island	<0.01	<0.01	<0.01	<0.01	2,531
Vermont	<0.01	<0.01	<0.01	<0.01	1,575
Dist. of Columbia	<0.01	<0.01	<0.01	<0.01	1,715
Ontario	0.01	0.24	0.12	0.15	5,010
New Brunswick	0.15	0.01	0.02	0.02	1,261
Quebec	0.09	0.02	0.03	0.05	6,567
Nova Scotia	0.08	0.01	0.02	0.02	7,566
Newfoundland	0.01	<0.01	<0.01	0.01	15,287
Prince Edward Is.	<0.01	<0.01	<0.01	<0.01	10,157

Figure 4-12. Ranked state percent sulfate contributions to Northeast Class I receptors based on emissions divided by distance (Q/d) results

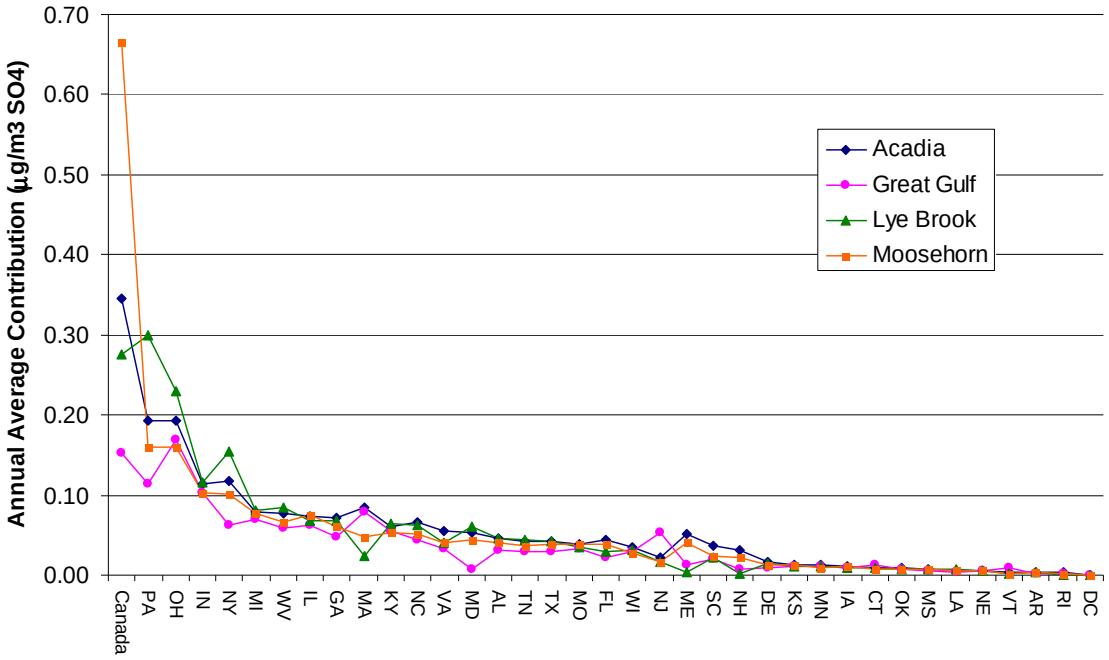

Figure 4-13. Ranked state percent sulfate contributions to Mid-Atlantic Class I receptors based on emissions divided by distance (Q/d) results

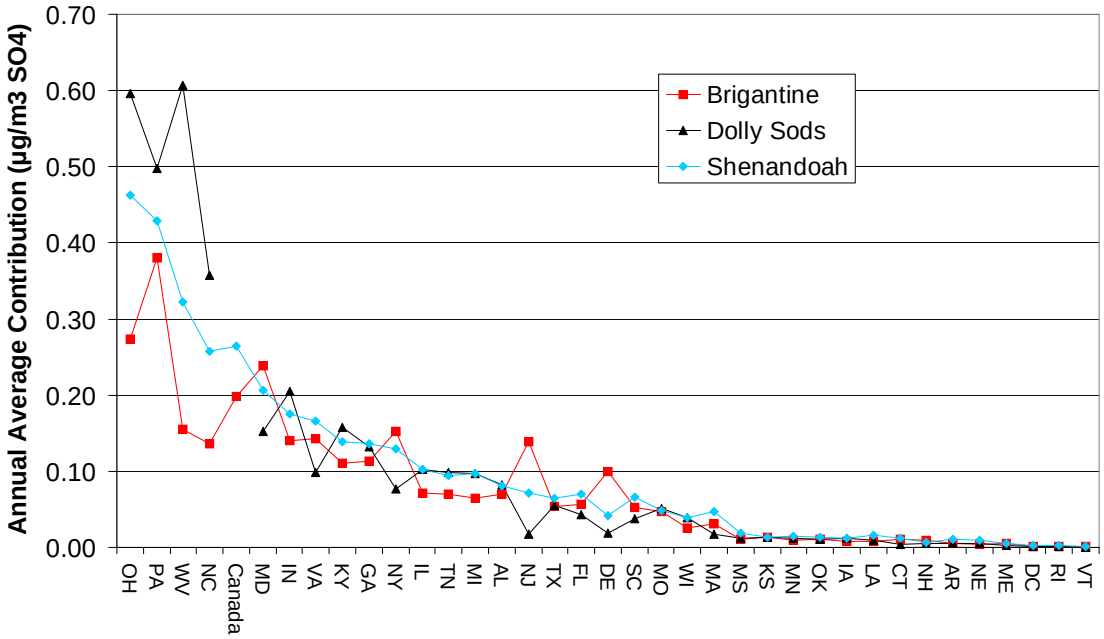

It is difficult to draw firm conclusions from what is essentially an empirical relationship between emission source strength, distance and observed impacts at receptor sites, but the addition of the CALPUFF-derived scale factors to this approach yields important insights as to the abilities of fairly simple screening techniques to accurately predict potential contributions to downwind receptors. This is borne out by the high degree of correspondence between the relative contributions of regions as identified by this and other techniques shown in Chapter 8.

4.2.2. Emissions times Upwind Probability

The Emissions times Upwind Probability method of assessing contribution to pollution involves multiplying the back-trajectory calculated residence time probability for a grid cell with the total emissions – over the same time period – from that grid cell. The product is an emissions-weighted probability field that can be integrated within state boundaries to calculate relative probabilities of each state contributing to pollution transport.

A back trajectory is the path that a parcel of air is calculated to have taken prior to its arrival at a given receptor (See Chapter 5). The back trajectories used in this study were calculated by the HYSPLIT system (Draxler, 1997 and 1998). Five years of back trajectories, calculated eight times per day results in 14,600 back trajectories. The back trajectories are 72-hours in length and have calculated endpoints, or locations, at hourly intervals that specify the air mass path. The endpoints from all trajectories are mapped into a matrix of residence times spent in individual grid cells over the five year period. The resulting sum expresses the likelihood that air spent time in a particular quarter degree longitude by quarter degree latitude grid cell over a domain between 25^o and 57^o latitude and -110^o to -50^o longitude. These residence times are then multiplied by the MANE-VU base year SO_2 emission inventory that has been allocated to a 12 km horizontal grid based on a Lambert Conformal projection.[27] The resulting product matrix contains the SO_2-weighted residence times that are then numerically integrated within the boundaries of each state to define a "contribution" for each state. This provides a relative ranking of contribution by state that can be used to compare with other methods of attribution.[28]

The area of analysis included states from Maine to Mississippi. Several states lie on the periphery of our available SO_2 emissions field and were used in the study despite an incomplete inventory of SO_2 emissions for the far edges of each state; these included

[27] Since the latitude-longitude projection of the residence time grid is different than the Lambert conformal projection of the emissions grid, there is not a one-to-one mapping. We therefore interpolated each residence time grid cell to increase the spatial resolution to $1/20^o$ latitude by $1/20^o$ longitude. Each residence time cell was then associated with the nearest SO_2 emission cell to ensure that each SO_2 emission component of the inventory was associated with the approximate residence time that was spent in nearest proximity to the emissions region. A distance of one-quarter degree between associated grid cells was used as a cutoff for the analysis. In other words, the product of a particular SO_2 cell and residence time cell would not be used if the geographical distance between them was greater than one-quarter degree (latitude or longitude).

[28] Note that the absolute units are expressed as nmole/hr, which represent a fractional contribution of a grid cell's emission rate that is likely to influence a downwind receptor. The physical meaning of this contribution is not clear, so this has been used in a relative sense only.

Missouri, Arkansas, Mississippi, Alabama, and Georgia.[29] Canada has significant SO_2 emissions in the domain of the SO_2 grid, hence contributions have been calculated for portions of Ontario, Quebec and New Brunswick that were within the SO_2 emission grid. Table 4-2 provides a ranking of state contributions and Figure 4-14 and Figure 4-15 show the ranked contribution for two groupings of Class I sites in or near MANE-VU.

Table 4-2. 2002 SO_2 Upwind Probability (percent contribution)

	ACADIA	LYEBROOK	BRIGANTINE	SHENANDOAH
West Virginia	0.06	0.07	0.09	0.19
Ohio	0.09	0.11	0.10	0.12
Pennsylvania	0.09	0.13	0.13	0.07
Kentucky	0.04	0.05	0.06	0.09
Indiana	0.05	0.05	0.05	0.06
New York	0.07	0.11	0.04	0.02
Virginia	0.03	0.02	0.06	0.06
North Carolina	0.02	0.01	0.05	0.07
Illinois	0.06	0.05	0.04	0.04
Georgia	0.02	0.02	0.04	0.05
Michigan	0.04	0.04	0.02	0.02
Tennessee	0.02	0.01	0.02	0.04
Maryland	0.02	0.02	0.04	0.03
New Jersey	0.02	0.02	0.07	0.01
Alabama	0.01	0.01	0.02	0.02
South Carolina	0.01	0.01	0.02	0.02
Wisconsin	0.02	0.02	0.01	0.01
Missouri	0.01	0.01	0.01	0.01
Delaware	<0.01	0.01	0.02	<0.01
Massachusetts	0.02	0.01	<0.01	<0.01
New Hampshire	0.02	0.01	<0.01	<0.01
Minnesota	0.01	0.01	<0.01	<0.01
Connecticut	0.01	0.01	<0.01	<0.01
Maine	0.02	<0.01	<0.01	<0.01
Iowa	0.01	<0.01	<0.01	<0.01
Dist. of Columbia	<0.01	<0.01	<0.01	<0.01
Arkansas	<0.01	<0.01	<0.01	<0.01
Mississippi	<0.01	<0.01	<0.01	<0.01
Vermont	<0.01	<0.01	<0.01	<0.01
Louisiana	<0.01	<0.01	<0.01	<0.01
Rhode Island	<0.01	<0.01	<0.01	<0.01
Texas	<0.01	<0.01	<0.01	<0.01
Canada	0.23	0.20	0.08	0.05

[29] These states still had significant areas that were not covered by the SO_2 grid. Thus only a fraction of these states' emissions were included in the total state contribution. The following are estimates of the area *not* covered by the SO_2 grid: MO-20%, AR-10%, MS-25%, AL-20%, GA-5%.

Figure 4-14. Ranked state percent sulfate contributions to Northeast Class I receptors based on emissions times upwind probability (E x UP) results

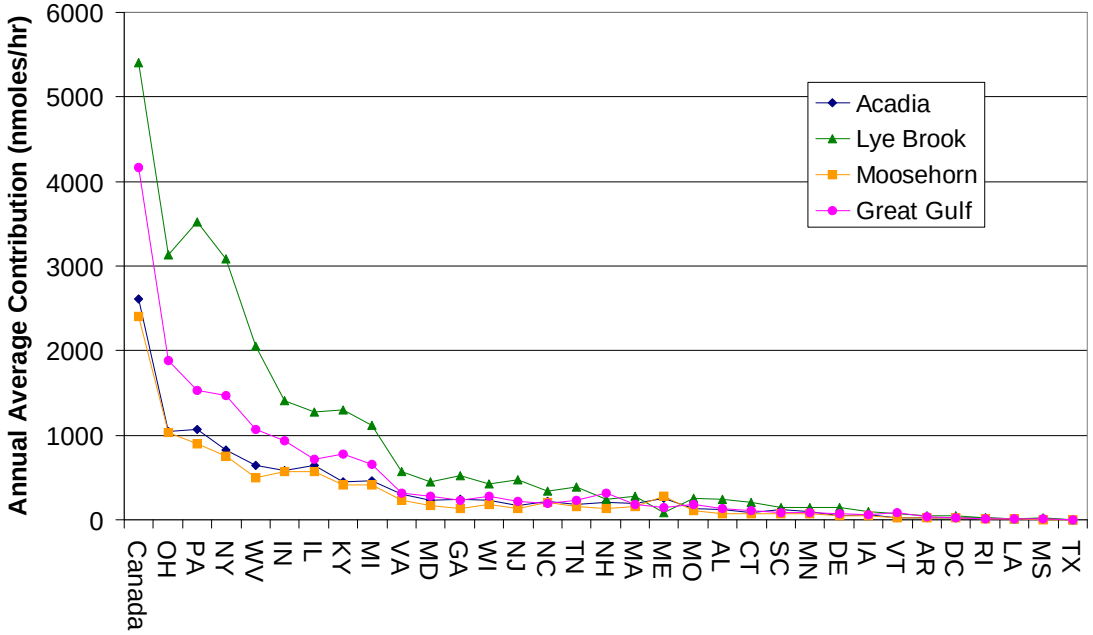

Figure 4-15. Ranked state percent sulfate contributions to Mid-Atlantic Class I receptors based on emissions times upwind probability (E x UP) results

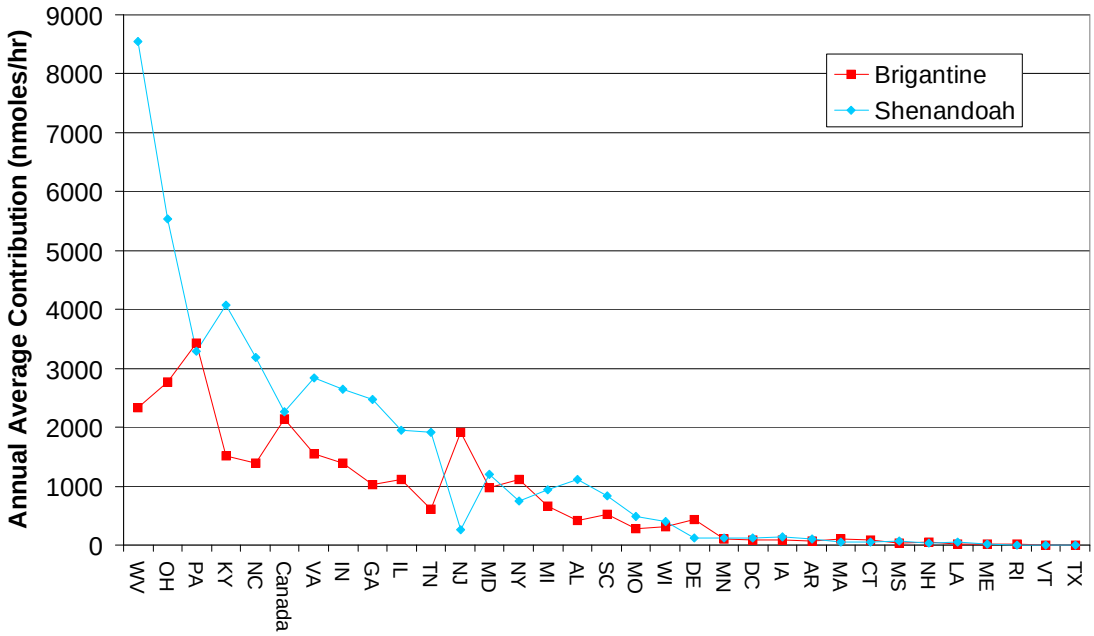

References

Ansari, A. S., and Pandis, S.N., "Response of inorganic PM to precursor concentrations," *Environ. Sci. Technol.*, 32, 2706-2714, 1998.

Davidson, C., Strader, R., Pandis, S., and Robinson, A., *Preliminary Proposal to MARAMA and NESCAUM: Development of an Ammonia Emissions Inventory for the Mid-Atlantic States and New England*. Carnegie Mellon University, Pittsburgh, PA. 7-Jan. 1999.

Draxler, R.D. and Hess, G.D., "Description of the HYSPLIT-4 Modeling System," *NOAA Technical Memorandum ERL, ARL-224*, Air Resources Laboratory, Silver Springs, Maryland, 24 pgs., 1997.

Draxler, R.D. and Hess, G.D., "An Overview of the HYSPLIT-4 Modeling System for Trajectories, Dispersion, and Deposition," *Australian Meteorological Magazine*, 1998, 47, 295-308.

Duyzer, J., "Dry Deposition of Ammonia and Ammonium Aerosols over Heathland," *J. Geophys. Res.*, 99(D9):18,757 – 18,763, 1994.

EarthTech, 2004, http://src.com/calpuff/calpuff1.htm

MARAMA 2004, http://www.marama.org/visibility/2002%20NEI/index.html

NESCAUM, "Regional Haze and Visibility in the Northeast and Mid-Atlantic States," January 2001a.

NESCAUM, "Development of an Improved Ammonia Emissions Inventory for the United States," December 2001b.

NESCAUM, "2002: A Year in Review," December, 2004.

Odum, J.R., Jungkamp, T.P.W., Griffin, R.J., Flagan, R.C., and Seinfeld, J.H., "The Atmospheric Aerosol-forming Potential of Whole Gasoline Vapor," *Science*, 276, 96-99, 1997.

Strader, R., Anderson, N., and Davidson, C., *Development of an Ammonia Inventory for the Mid-Atlantic States and New England, Progress Report, October 18, 2000*, available online: http://marama.org/rt_center/MARAMAprogress10-18-00.pdf, 2000.

USEPA, *National Air Quality and Emission Trends Report, 1998*, EPA 454/R-00-003, available online: http://www.epa.gov/oar/aqtrnd98/, 2000a.

USEPA, *National Air Pollutant Trends, 1900 – 1998*, EPA 454/R-00-002, available online: http://www.epa.gov/ttn/chief/trends/trends98/trends98.pdf, 2000b.

USEPA 2005, http://www.epa.gov/ttn/chief/eiinformation.html.

5. DATA ANALYSIS TECHNIQUES

Trajectory analyses have historically been used to trace the path of polluted air masses prior to their arrival at a given receptor site. Such analyses, by linking downwind measurements of ambient air quality with specific geographic areas upwind, can be very helpful in exploring the relative contribution of transported emissions from potential source regions on high and low pollution days. As with all of the tools and modeling techniques discussed in this report, trajectory analysis is not without some uncertainties and limitations. One such limitation is the fact that these analyses are typically unable to distinguish emission contributions from one point along the length of the trajectory from a different point along the path. In addition, the accuracy of any individual back trajectory calculation for a single observation or episode may be compromised by inherent limitations in the underlying Lagrangian trajectory models, which tend to become less accurate as the calculation progresses further back in time. Fortunately, a variety of techniques are available to mitigate these uncertainties and enhance confidence in the results obtained using trajectory analysis. These include techniques for triangulating results across multiple sites, ensemble techniques that combine the results of large numbers of back trajectories, clustering algorithms that group similar trajectories based on their spatial characteristics, and techniques for combining trajectory analyses with source apportionment models. All of these strategies can be useful in improving and refining traditional trajectory analyses.

This chapter describes the results of back trajectory analyses that have been conducted to date for key pollutant species observed at MANE-VU and nearby receptor sites. In addition, we explore novel techniques for improving the accuracy of individual trajectories by grouping meteorologically similar back-trajectories into trajectory "clusters" and examining the relationship between the transport pathways defined by these clusters and downwind air quality observations. We then turn to source apportionment models which can be used to group available monitoring data for various components of $PM_{2.5}$ in logical combinations that best explain the variation in observed species concentrations in terms of specific "source profiles." These source profiles are used to distinguish the emissions from common pollution sources (e.g., mobile sources, coal combustion). The information obtained through source apportionment analysis can then be used in combination with back trajectory analysis to link specific geographic source regions with downwind air quality conditions and to establish the relative contribution of different source regions to visibility impacts at the receptor site.

This chapter provides further description of several trajectory analysis techniques, before proceeding to a review of the insights gained to date by applying these techniques to analyze source regions for particulate pollution in the MANE-VU region. Preliminary results and interpretation are presented and used to support and bolster the basic conceptual model of regional haze outlined in Chapter 2.

5.1. Trajectory Analysis

The Hybrid Single Particle Lagrangian Integrated Trajectory (HYSPLIT) model (Draxler, 1997 and 1998) was used to calculate back trajectories for 13 sites in the northeastern United States. Most of these sites are located in Class I areas that are

subject to the Haze Rule, but several others are located in areas where potential nonattainment with the $PM_{2.5}$ NAAQS warrant analysis. Back trajectories were calculated eight times per day for starting heights of 200, 500, and 1,000 meters above ground level using meteorological wind fields for the five-year period from 2000 through 2004. Meteorological data from the National Oceanic and Atmospheric Administration (NOAA) Air Resources Laboratory (ARL) archives were used. These include wind fields from the Eta Data Assimilation System (EDAS), which cover North America with an 80 km spatial resolution and are based on 3-hourly variational analyses (Rolph, 2003). For the analyses presented here, we exclusively used the 500 meter EDAS trajectories from the baseline period (2000-2004).

Each trajectory was matched with corresponding monitoring data collected as close in time as possible to the "start" time of the back trajectory calculation. The analysis included ambient measurements for $PM_{2.5}$ and ozone (O_3), as well as all particulate matter constituents that are routinely measured as part of the IMPROVE program.

The resulting database of air quality monitoring results and associated back trajectories was used to develop several statistical measures of the probability or likelihood that a given upwind source region is associated with good or poor air quality at the receptor sites analyzed. Appendix A provides a detailed description of the metrics that were developed for this purpose and how they were calculated using both traditional trajectory analysis and cluster analysis techniques. This appendix also provides site-specific results.

5.1.1. Incremental Probability

The incremental probability (IP) field represents a measure of the likelihood that a given source region contributes more than "average" to high concentrations of a particular pollutant at a downwind receptor site (see Appendix A for a more complete definition). This technique can also be used to identify locations that are *less* likely to contribute to poor air quality at a given receptor site, thus allowing for more robust conclusions to be drawn about likely source regions for individual fine particle constituents.

Calculating IP fields for a subset of back trajectories within a complete sample can help further illuminate the different roles of different source regions. For example, it is interesting to note distinct differences between the IP field for back trajectories corresponding to the 10 percent highest observed sulfate values in the Northeast (three sites are shown that bracket the MANE-VU region's Class I sites) and the IP field for trajectories corresponding to the lowest sulfate values in the Northeast (specifically, sulfate values in the lowest 10^{th} percentile). Figure 5-1 and Figure 5-2 illustrate the IP fields for each set of observations, respectively.

In Figure 5-1 and Figure 5-2, note that the red color indicates areas with greater probability of contributing to transport on the selected days. These show that the very highest observed sulfate values across the region are strongly associated with transport from a source region that encompasses the Ohio River Valley, western Pennsylvania, and

the urban East Coast corridor. On the days with the lowest measured sulfate, transport is associated with northwesterly winds from Canada and weather patterns off the Atlantic.

Figure 5-1. Incremental Probability (Top 10% Sulfate) at Acadia, Brigantine and Lye Brook 2000-2004

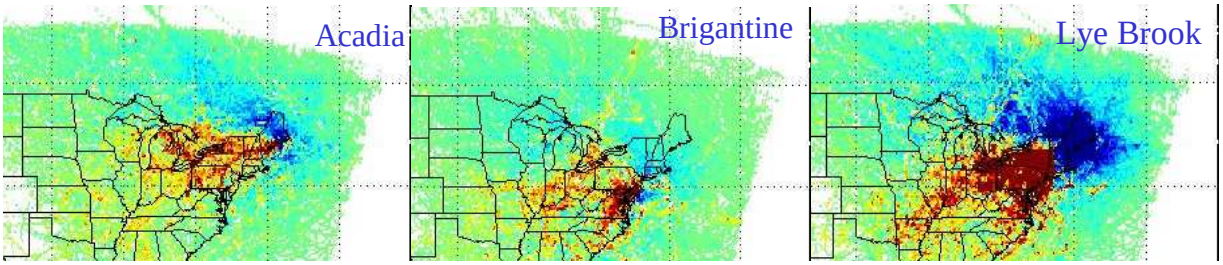

Figure 5-2. Incremental Probability (Bottom 10% Sulfate) at Acadia, Brigantine and Lye Brook 2000-2004

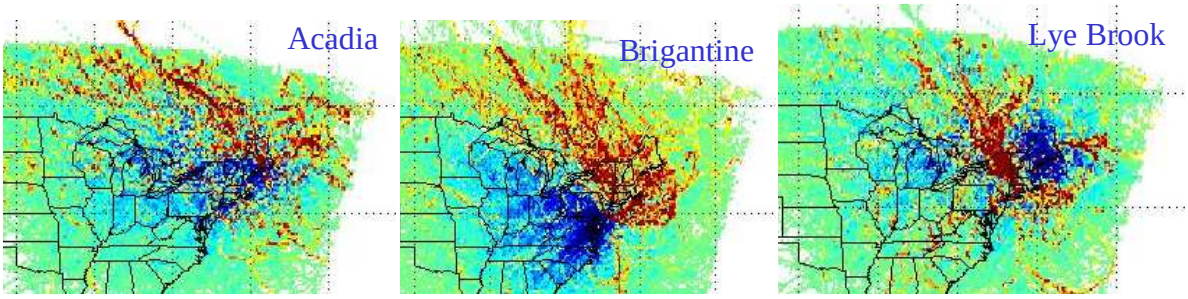

5.1.2. Clustered Back-Trajectories

Each of the IP fields shown in Figure 5-1 or Figure 5-2 incorporate results from over 14,000 back trajectories over the five-year period analyzed. In cases like these, where IP fields are calculated from a very large set of data points, the error in the calculation of any individual trajectory — which can be as high as 30 percent or more of the total transport distance involved in a given trajectory — is not likely to affect the overall result. Assuming that such errors are randomly distributed (i.e., no systematic bias exists in the calculations used by the trajectory model to calculate wind speed or direction), the use of large numbers of individual trajectories will effectively ensure that the random errors cancel out. To further minimize the effect of any errors with respect to individual trajectories, it is also possible to cluster large numbers of back trajectories according to their three-dimensional similarity (see Appendix A for a detailed description of several methodologies used). Figure 5-3 shows residence-time probability fields for clusters of similar back trajectories grouped according to their proximity to unique meteorological pathways. This metric yields probabilistic representations of the meteorological pathways which were most likely to be associated with the highest observed sulfate concentrations at the receptor site. Such probabilistic representations reduce the reliance on any one back trajectory and ensure that the general pattern used to associate a transport pathway with a downwind receptor site is more likely to be accurate.

Figure 5-3. Proximity based cluster with the highest associated sulfate value for three sites in the MANE-VU region, Acadia (sulf=3.19 μg/m^3), Brigantine (sulf=6.79 μg/m^3), and Lye Brook (sulf=3.92 μg/m^3)

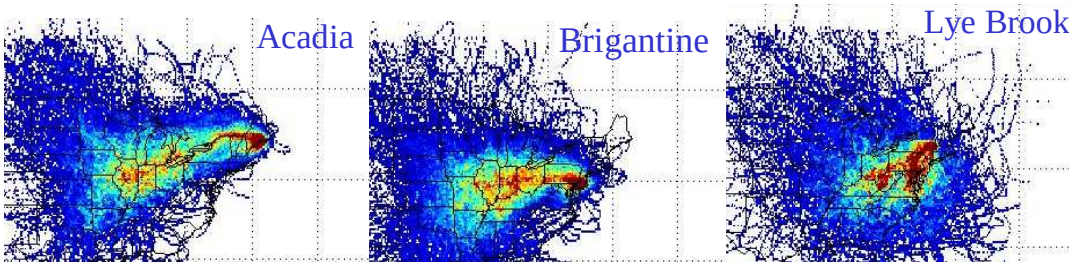

5.1.3. Cluster-Weighted Probability

The clusters derived above can be used individually or combined in an "ensemble cluster" approach similar to how individual trajectories are combined to develop the IP metric. This second method for associating transport patterns with downwind pollution measurements involves using all clusters generated by the clustering algorithms described in the preceding section (and in detail in Appendix A) and weighting them by their average observed sulfate value. Simply averaging the residence-time probability of all clusters would yield the "everyday" probabilities that are used in calculating IP fields. Instead, weighting each cluster *before* the averaging process serves to highlight transport patterns that are associated with high sulfate levels at the receptor site, while downplaying patterns that are associated with low values. Figure 5-4 shows the resulting cluster-weighted probability (CWP) field. Results are similar to those obtained using the incremental probability metric described previously, but they now include all clusters, not just the high-day values.

A noteworthy feature of the clustering process is that while it reduces uncertainty about prevailing transport patterns, it is not helpful in taking advantage of weather variations to identify specific source regions. Thus, results for a particular site should be interpreted as showing that observed air quality conditions have an increased probability of being associated with the transport of a specific pollutant, as opposed to being associated with a particular source region for a given pollutant. Put another way, it is difficult to make an association with a specific point along the pathway defined by a cluster. As with the IP approach described earlier, however, multi-site averaging can address this ambiguity by making it possible to triangulate on regions that are associated with the transport of pollution to multiple sites in different locations, as shown in Figure 5-4.

Both trajectory-based approaches (i.e., IP and CWP) have also been applied to Class I receptor sites in the nearby VISTAS region, which includes the Dolly Sods and Otter Creek Wilderness Areas in West Virginia as well as Shenandoah National Park and the James River Face Wilderness Area in Virginia. Results for the VISTAS Class I sites are presented at the conclusion of Appendix A.

Figure 5-4. Cluster Weighted Probability at Acadia, Brigantine and Lye Brook 2000-2004

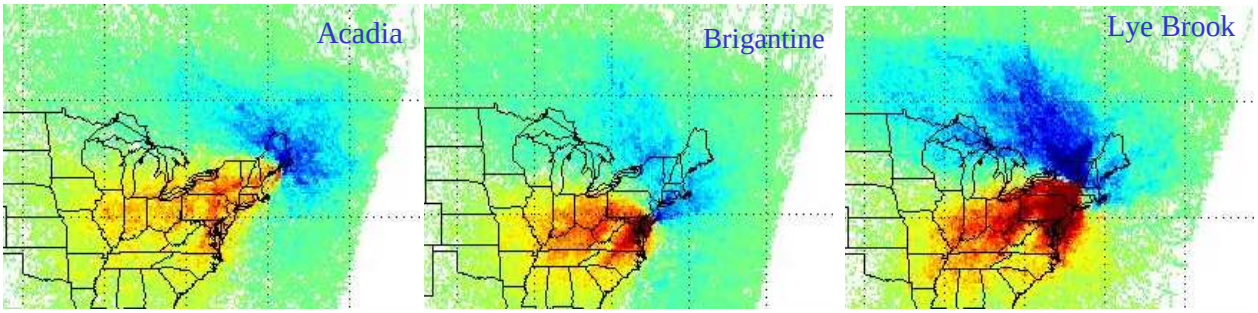

5.2. Source Apportionment Models and Ensemble Trajectory Analysis of Source Apportionment Results

Previous sections of this chapter have discussed a category of receptor-based assessment techniques known more generally as ensemble trajectory analysis. The latter category includes residence time analysis (RTA) as well as potential source contribution function (PSCF) and cluster analysis (see also Appendix A). In this section we turn to multivariate mathematical models for analyzing source contributions, such as chemical mass balance (CMB) models, principal component analysis (PCA), positive matrix factorization (PMF), and UNMIX.

Receptor-based models begin with ambient air quality measurements at one or more receptor locations and work "backward" to identify logical combinations of pollutant species that best fit a "source profile." Sources matching that profile are assumed to have contributed to the ambient pollutant concentrations historically observed at the receptor locations. These models are typically driven by variations in PM constituent concentrations across multiple observations at one or more sites. An advantage of PCA, PMF, and UNMIX is that source profiles do not need to be known in advance; however, this does mean that the results must be subjectively interpreted to identify and distinguish likely sources.

Because of these complexities and because the multivariate models typically rely entirely on measurements of PM constituents without regard to meteorology, it can be extremely useful to consider results obtained through the ensemble trajectory techniques (which rely on meteorology only) when interpreting or evaluating the outputs from a multivariate modeling exercise.

Appendix B provides details of numerous source apportionment and associated ensemble back trajectory analyses. These details cover results obtained for many of the most significant components of fine particulate mass and resulting light extinction. Here we focus on the "secondary sulfate" or "coal" source profile that was identified at nearly every site in the eastern United States. Secondary sulfate typically accounts for 30–60 percent of overall fine particle mass and 60–80 percent of visibility impairment on the haziest days in the Northeast.

Figure 5-5 shows results from one of the broadest studies conducted to date of sulfate sources and characteristics at nine eastern IMPROVE sites. The bars on the left

show the fraction of total sulfate measured at each site that is contributed by the "sulfate/coal" source profile as determined by the source apportionment models. The bars on the right show the fraction of each "sulfate/coal" source profile that is composed of sulfate. Figure 5-5 suggests that: (1) large sources contribute 70–90 percent of the total sulfate measured at these sites, and (2) that the contribution from these large sources consists of 50–90 percent sulfate.

Figure 5-5. Sulfate characteristics of "secondary sulfate" (coal) sources identified at eastern sites

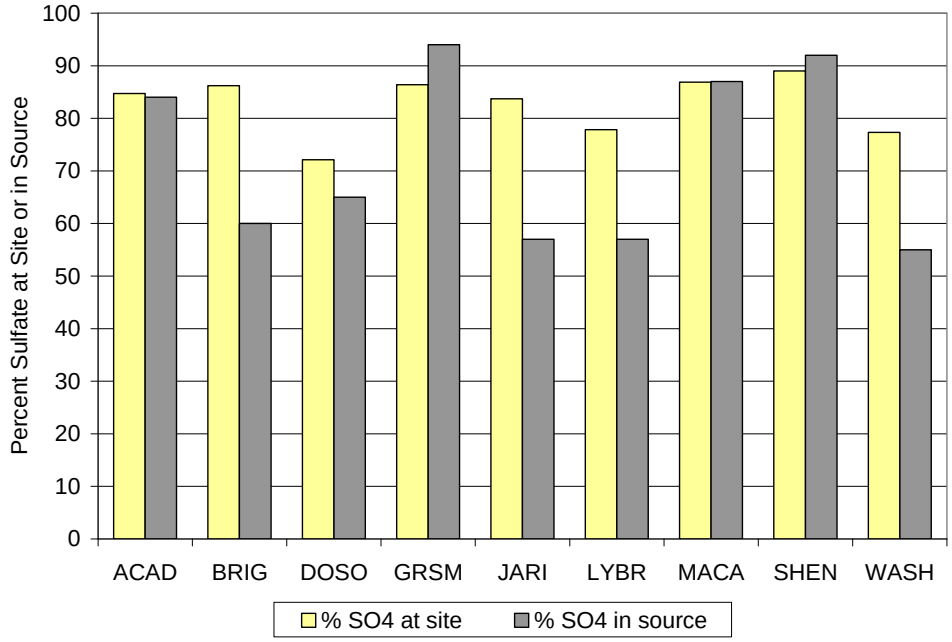

When large sulfate sources are associated with upwind states or regions through the use of back trajectories (Figure 5-6), it becomes clear that many Class I and urban sites in MANE-VU and adjoining areas are influenced by a common source region. These findings suggest that reductions in coal-related SO_2 emissions would have substantial benefits in terms of improved visibility and reduced PM concentrations over a large part of the eastern United States and eastern Canada.

This conclusion is further reinforced by comparing regions with significant emissions that match the "source profiles" generated by available mathematical modeling tools to regions identified through trajectory analysis as having a high probability of being upwind on days with high sulfate levels and high reconstructed extinction values. As shown in Figure 5-6, the degree of correspondence between these regions is substantial. This indicates that the "secondary sulfate/coal combustion" source profile prominent at several eastern sites is strongly linked to regions associated with the highest 10 percent of recorded sulfate and reconstructed extinction values. It is noteworthy that the upwind regions identified in Figure 5-7 are derived from measurements spanning the entire IMPROVE network, suggesting that the source region for "secondary sulfate/coal combustion," which is a dominant contributor to visibility impairment in parts of the eastern United States, is also a major contributor to observed sulfate and extinction outside the MANE-VU region.

Figure 5-6. Incremental Probabilities for "Secondary Sulfate" (Coal) Sources in Eastern U.S.

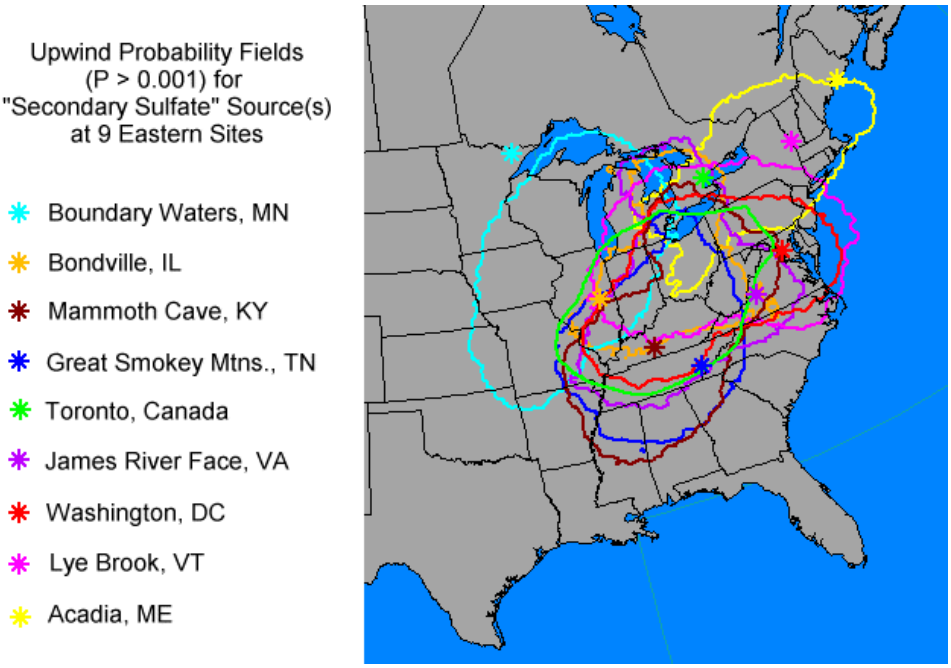

5.3. Trajectory Model Evaluation and Future Work

The geographical correspondence exhibited in Figure 5-7 extends to the multi-site average IP fields calculated for the MANE-VU region and shown previously in Figure 5-1. It also extends to the multi-site average IP field calculated using the ATAD model and shown in Figure B-30 in Appendix B. Essentially, both figures are versions of the same thing, but they do exhibit some subtle differences. These differences are highlighted in Figure 5-8 which compares the results of ATAD and HYSPLIT IP calculations for the top 10 percent of sulfate, selenium, and nickel observations at Lye Brook, Vermont. Sulfate is a secondary pollutant that tends to peak in the summer, whereas nickel and selenium are primary pollutants that typically peak in the wintertime. Ni and Se serve as excellent markers for residual oil and coal combustion respectively. The figure indicates strong agreement between the two models in terms of

Figure 5-7. Comparison of probability fields for observed sulfate, "sulfate" source profiles for seven eastern sites and reconstructed deciviews

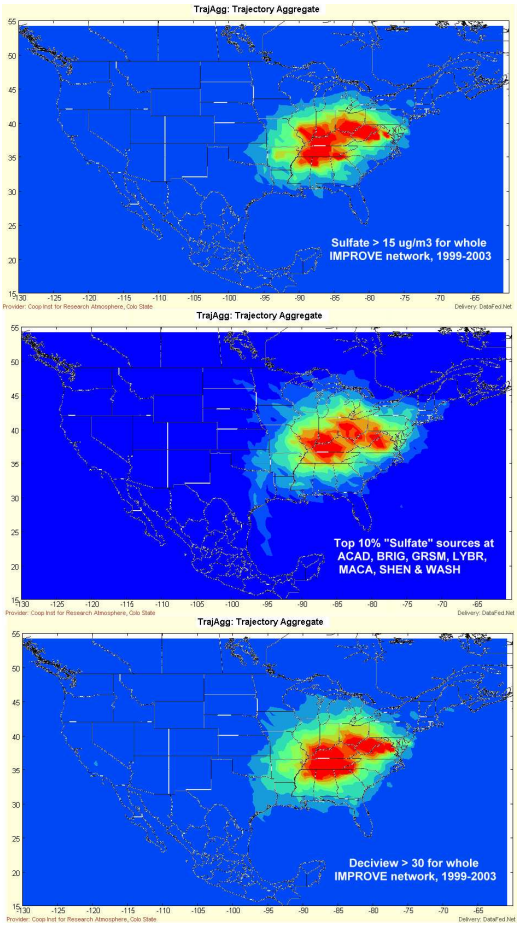

the IP fields they calculate for nickel, suggesting that — during wintertime — primary pollutants are tracked well by both techniques. There is less agreement between the IP fields for sulfate, suggesting either a southerly bias to the HYSPLIT calculations for this secondary pollutant, or a westerly bias to the ATAD results.

Seasonal differences in the meteorology that affects Lye Brook and other East Coast sites during the summer versus during the winter may help to explain these model discrepancies. Some of the largest absolute differences between the ATAD and HYSPLIT estimates occur for the highest sulfate days. While there are many differences between the models, one key difference is in their trajectory start heights. The HYSPLIT trajectories all start at 500 meters above ground level while the ATAD model first estimates a "transport layer depth" (TLD) and then initiates the trajectory (while constraining subsequent trajectory endpoints) at a point roughly half way between ground level and the TLD. During summer, when the largest sulfate events occur, the resulting ATAD start heights are roughly twice as high as the 500 m HYSPLIT start heights (see Figure 5-9). Hence the ATAD calculations tend to extend over a greater distance to the west, while the summer HYSPLIT trajectories may be more reflective of flows that are nearer the surface and more frequently east of the Appalachian Mountains. Both flow regimes are important. In fact, Blumenthal et al. (1997) have observed that the highest ozone concentrations in the Northeast (which often coincide with episodes of high sulfate concentrations) tend to occur when surface flows up the Northeast urban corridor combine with synoptic flows over the Appalachian Mountains from the west, a pattern that is often accompanied by lower level nocturnal jets along the Northeast corridor and through gaps in the Appalachians.

Figure 5-8. Comparison of IP contours generated by ATAD and HYSPLIT (both EDAS and FNL) for sulfate, nickel and selenium at Lye Brook

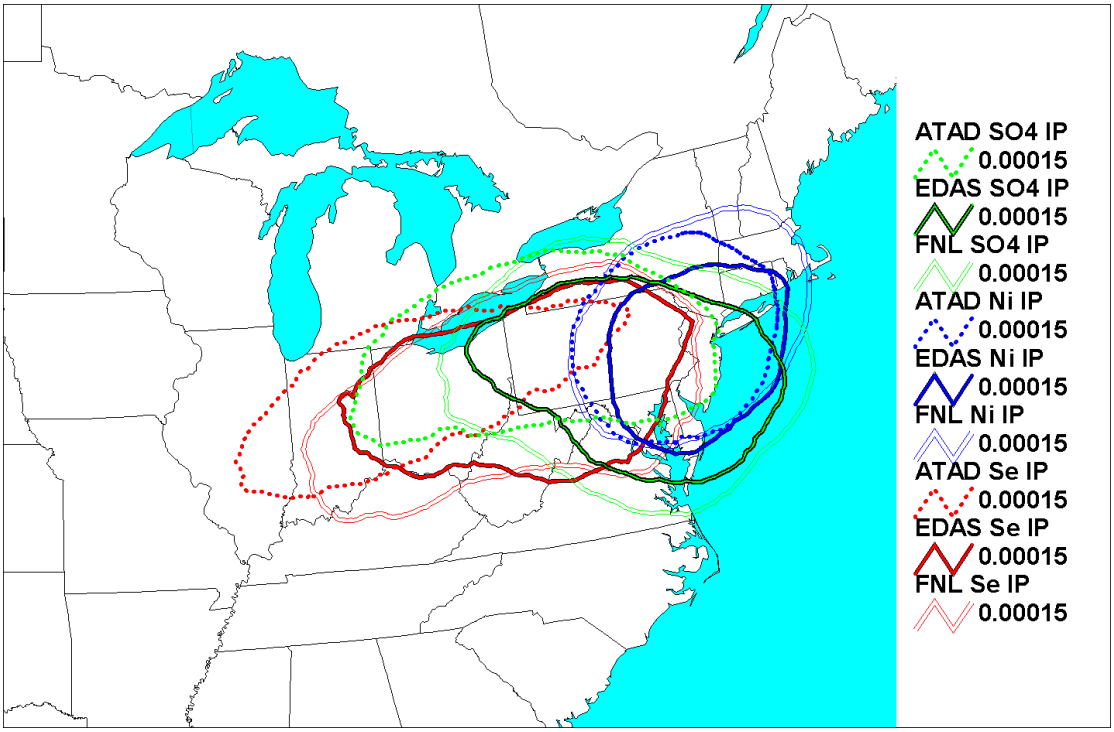

An extensive evaluation of the performance of HYSPLIT, ATAD, and Capita Monte Carlo trajectory models using a variety of different meteorological drivers, ensemble trajectory techniques, and performance tracers was recently conducted as part of the Big Bend Regional Aerosol and Visibility Observational (BRAVO) study (Pitchford et al., 2004). No one model consistently out-performed the others at that site, hence results from these and more sophisticated photochemical grid models (REMSAD and CMAQ) were merged to produce a best-estimate, "consensus" apportionment of sulfate in the BRAVO study.

MANE-VU is using all available trajectory models, trajectory-related metrics, and improved understanding of transport phenomena to further explore and support the development of emission control strategies for reducing regional haze.

Figure 5-9. ATAD Transport Layer Depth (TLD) by month. Color indicates the length of time prior to arriving at the receptor.

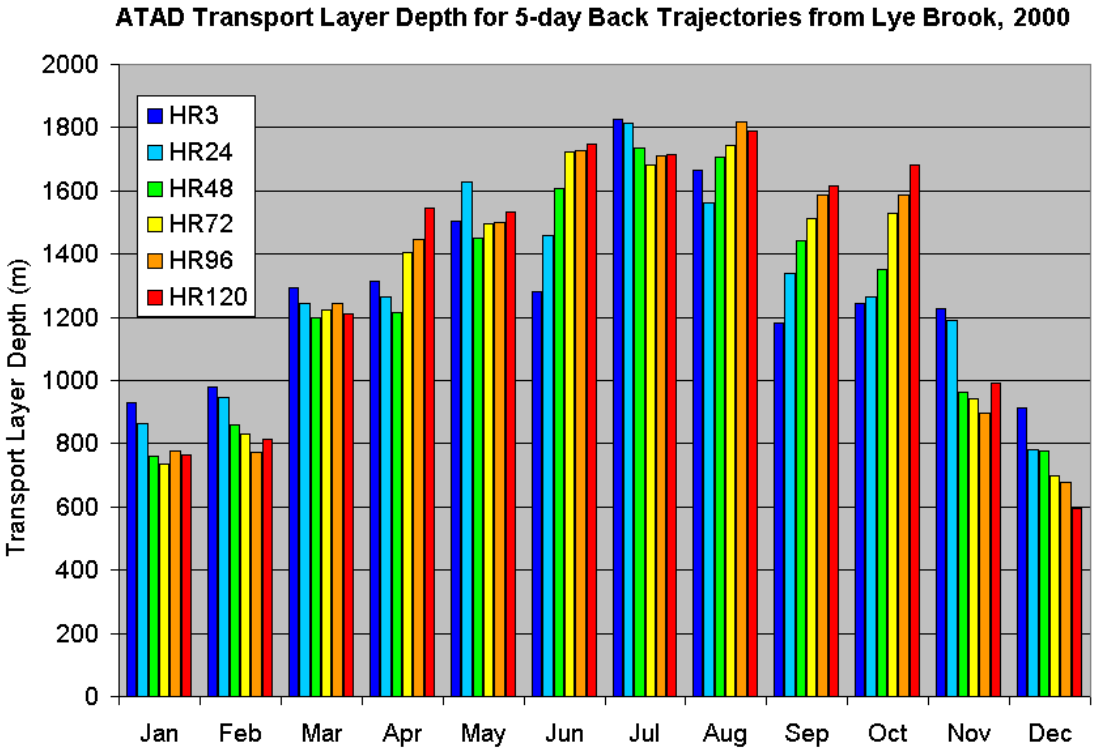

References

Blumenthal, D.L., Lurmann, F.W., Kumar, N., Ray, S.E, Korc, M.E., Londergan, R., Moore, G., Transport and mixing phenomena related to ozone exceedances in the Northeast U.S. Working Draft No. 1.1 prepared for Ozone Transport Assessment Group Air Quality Analysis Workgroup by Sonoma Technology, Inc., Santa Rosa, CA and Earth Tech, Concord, MA, STI-996133-1710-WD1.1, February 1997.

Draxler, R.D. and Hess, G.D., "Description of the HYSPLIT-4 Modeling System," *NOAA Technical Memorandum ERL, ARL-224*, Air Resources Laboratory, Silver Springs, Maryland, 24 pgs., 1997.

Draxler, R.D. and Hess, G.D., "An Overview of the HYSPLIT-4 Modelling System for Trajectories, Dispersion, and Deposition," *Australian Meteorological Magazine*, 47, 295-308, 1998.

Pitchford, M.L., Schichtel, B.A., Gebhart, K.A., Barna, M.G., Malm, W.C., Tombach, I.H., and Knipping, E.M., "Causes of Haze at Big Bend National Park – Results of the BRAVO Study and More" Regional and Global Perspectives on Haze: Causes, Consequences and Controversies – Visibility Specialty Conference, Air & Waste Management Association, Asheville, NC October 25-29, 2004.

Rolph, G.D., Real-time Environmental Applications and Display sYstem (READY) Website (http://www.arl.noaa.gov/ready/hysplit4.html). NOAA Air Resources Laboratory, Silver Spring, MD., 2003.

6. CHEMICAL TRANSPORT MODELS

Eulerian or "grid" models have traditionally served as the workhorse of air quality planning programs. These tools strive to be comprehensive in accounting for emissions, meteorological dynamics, chemical production, transformation, and destruction as well as wet and dry deposition and microphysical processes. With this degree of sophistication comes attendant uncertainty. Many of the more complex processes (e.g., cloud processes and boundary layer dynamics) are handled through parameterizations that attempt to approximate the real atmosphere at an appropriate level of detail. Chemical transport models for ozone and fine particles have improved markedly over the past several years as various groups have developed competing models and as the different strengths and weaknesses of these models help to shed light on various aspects of the underlying science.

Two regional-scale air quality models have been evaluated and used by NESCAUM to perform air quality simulations. These are the Community Multi-scale Air Quality modeling system (CMAQ)[30] and the Regional Modeling System for Aerosols and Deposition (REMSAD).[31] Appendix C provides detailed descriptions of these models and of their use by NESCAUM, together with performance evaluations and preliminary results. A brief overview of the two modeling platforms in terms of their relevance to future SIP work is provided here, along with highlights of the findings.

6.1. Chemical Transport Model (CTM) platforms – Overview

Both REMSAD and CMAQ are being used with a 12 km grid[32] in the eastern U.S. domain (see Figure 6-1(b)). Air quality is modeled on 22 vertical layers with hourly temporal resolution for the entire calendar year 2002. REMSAD has simplified chemistry but allows for emissions tracking of sulfate, nitrate, and mercury through a tagging feature that calculates the contribution of specific sources to ambient concentrations, visibility impacts, and wet or dry deposition. REMSAD has shown good performance when reproducing annual or seasonal statistics for sulfate and mercury chemistry, while CMAQ has shown good performance for multiple species. A new release of CMAQ (version 4.5) may improve performance for sulfate, nitrate and organics over what Appendix C presents and will be used with the quality-assured meteorology and emission inventory inputs described below for final SIP submissions in 2007 or 2008.

Meteorological inputs have been developed by the University of Maryland (UMD) using the Fifth-Generation Pennsylvania State University/National Center for Atmospheric Research (NCAR) Mesoscale Model (MM5) system.[33] A modified Blackadar boundary layer scheme is used as well as physics options including explicit representations of cloud physics with simple ice microphysics (no mixed-phase processes) and the Kain-Fritsch cumulus parameterization.

---

[30] See Byun and Ching, 1999.
[31] See ICF/SAI, 2002.
[32] 12 km grid describes a 12 by 12 km grid cell
[33] http://www.mmm.ucar.edu/mm5/

The New York Department of Environmental Conservation and NESCAUM are processing emissions inputs using the Sparse Matrix Operator Kernel Emissions (SMOKE) Modeling System. To model biogenic emissions, SMOKE uses the Biogenic Emission Inventory System, version 2.3 (BEIS2) and version 3.09 and 3.12 (BEIS3). SMOKE has also been integrated with the MOBILE6 model for on-road emissions. MANE-VU has developed a quality-assured 2002 emissions inventory which is being merged with the regional inventories for other RPOs in order to provide a comprehensive emissions inventory for the entire Northeast domain shown in Figure 6-1(b).

A dynamic 3-dimensional boundary condition feeds ambient concentration fields in at the domain boundaries which are representative of actual concentrations during 2002. This dynamic boundary condition was developed by applying the output of a global model run (Park et al., 2004) with 4 degree longitude by 5 degree latitude horizontal resolution at the boundaries of the 36 km grid domain shown in Figure 6-1(a). The results of this annual simulation are then applied at the boundary of our 12km grid domain, ensuring acceptable representation of the general trends and sulfate patterns that were present during the simulation period.

Figure 6-1. Modeling domains used in NESCAUM air quality modeling studies. (a) Domain 1: 36 km National US grid domain with location of 12 km grid domain highlighted; (b) Domain 2: 12km Northeast US grid domain. The gridlines are shown at 180 km intervals (5 x 5 36 km cells or 15 x 15 12 km cells).

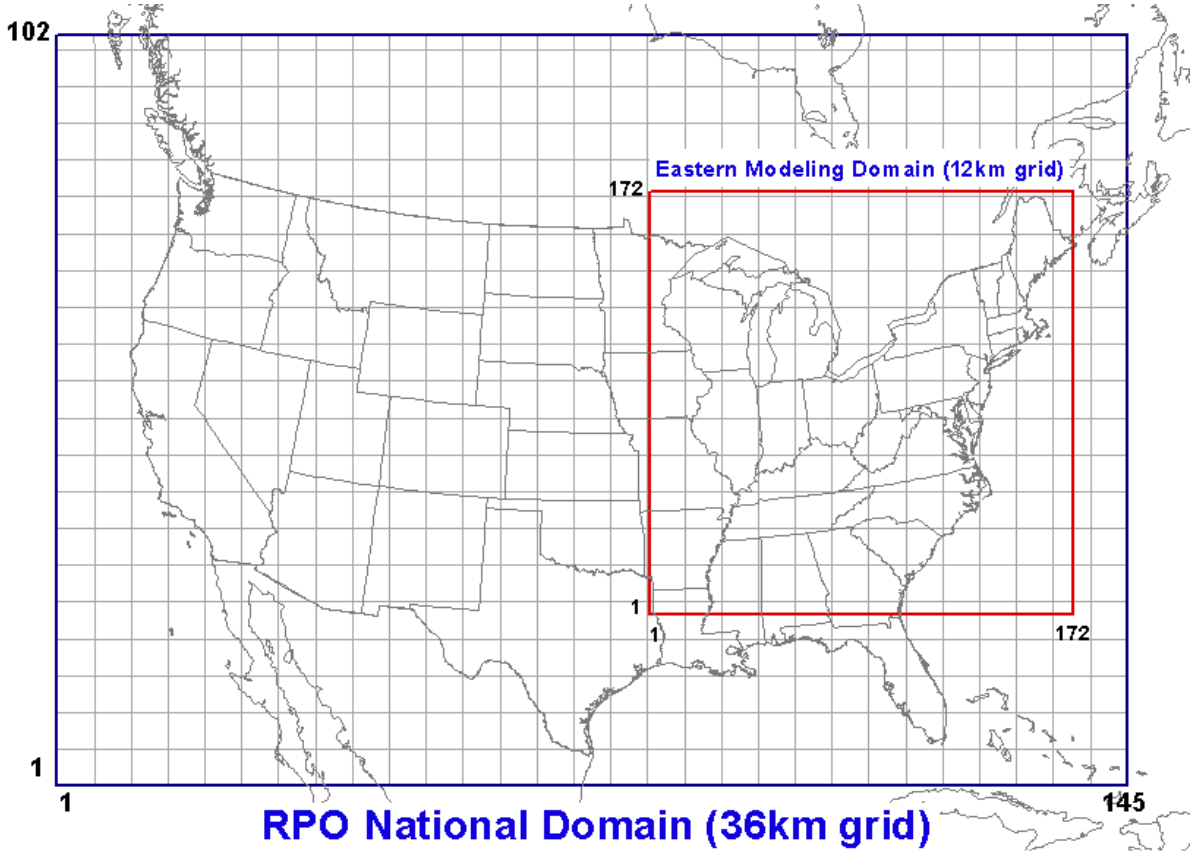

6.2. Preliminary Results

CMAQ has been run for a complete set of baseline simulations including 2002, 2009 and 2018. These preliminary runs are described in greater detail in Appendix C, but include inventory and meteorological drivers which will be updated for final SIP submissions. Nonetheless, these preliminary results suggest that implementation of existing regulations (including USEPA's Clean Air Interstate Rule, or CAIR) will continue to yield significant improvements in visibility over the next decade, primarily as a result of regional sulfate reductions (See Figure 6-2 a and b below for visibility improvement and see Figure C-27 in Appendix C for sulfate mass reductions). Despite these potential improvements, not all MANE-VU Class I areas are anticipated to achieve uniform progress goals as described by current USEPA guidance.[34] Brigantine Wilderness Area in New Jersey is projected to fall about a half deciview short of the uniform rate under existing emission reduction plans.

A significant difference between the CMAQ and the REMSAD results presented here is that NESCAUM has taken the additional step of reprocessing the SO_2 emission sources from each state such that these model inputs are formatted to take advantage of

Figure 6-2(a) and (b): CMAQ Integrated SIP Modeling Platform simulation results for 2002, 2009 and 2018 relative to Uniform Progress Goals calculated according to current USEPA guidance for (a) Northeast Class I sites in MANE-VU and (b) Mid-Atlantic Class I sites in or near MANE-VU.

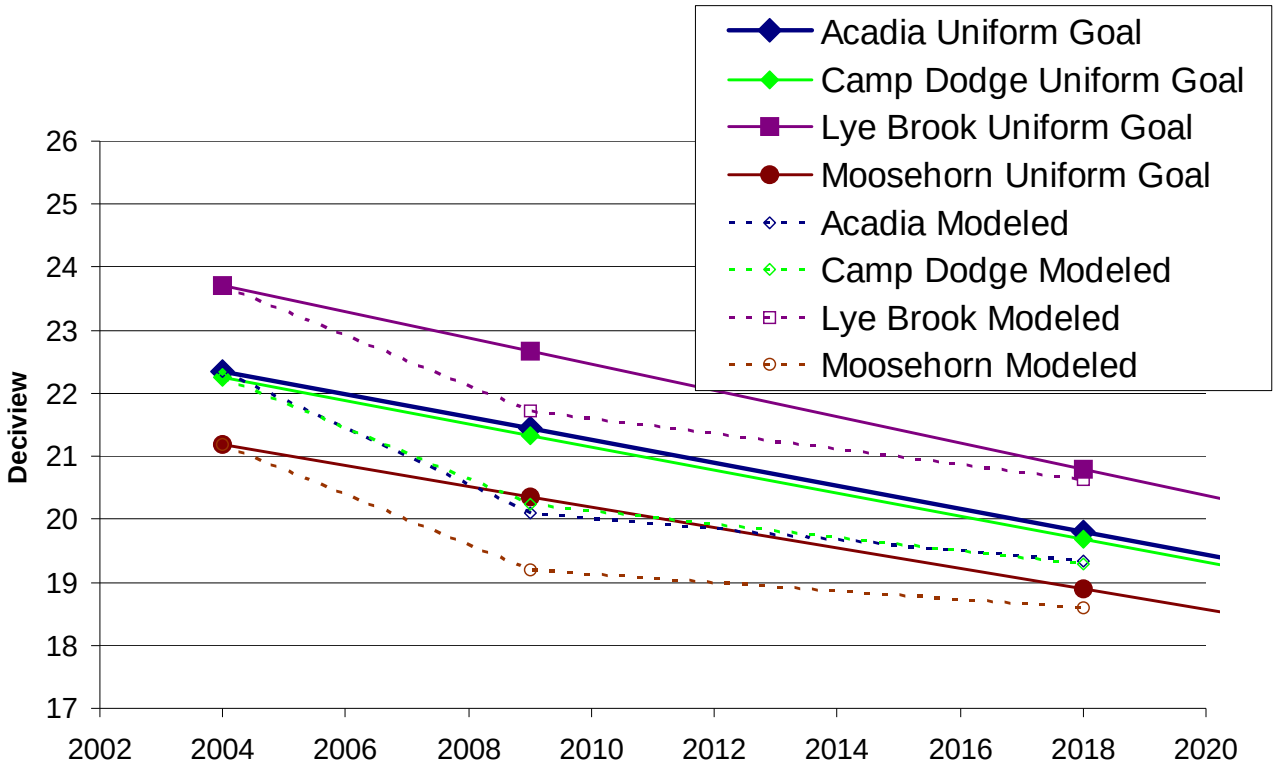

[34] We note that uniform progress goals do not necessarily dictate visibility levels required by statute, but do represent a point of comparison for states when establishing *reasonable* progress goals toward our national visibility goal of no anthropogenic visibility impairment by 2064.

Figure 6-2(b).

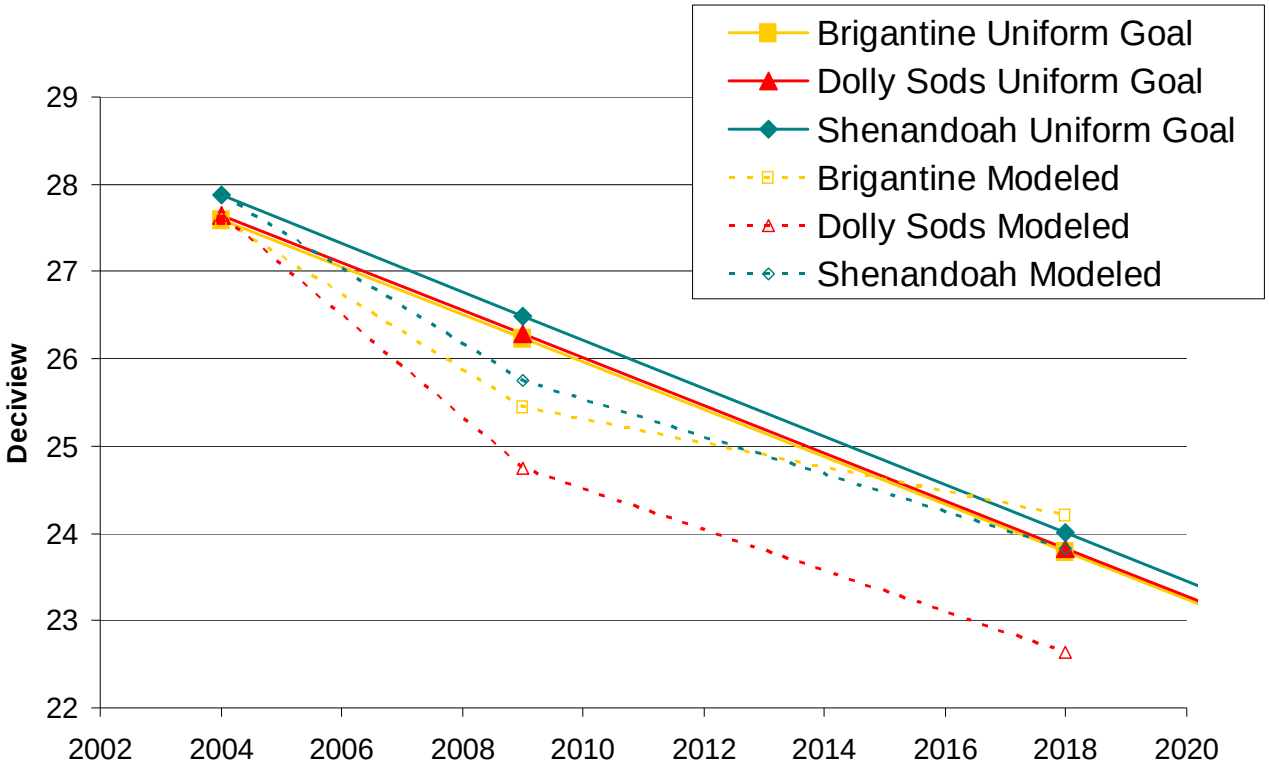

REMSAD's tagging capabilities. Thus, all SO_2 emissions included in the model for the eastern half of the country, Canada and the boundary conditions have been tagged according to state of origin. This allows for a rough estimation of the total contribution from elevated point sources in each state to simulated sulfate concentrations at eastern receptor sites. The tagging scheme employed for this analysis is illustrated in Figure 6-3. Using identical emission and meteorological inputs to those prepared for the Integrated SIP (CMAQ) platform, REMSAD was used to simulate the annual average impact of each state's SO_2 emission sources on the sulfate fraction of $PM_{2.5}$ over the northeastern United States.

Results of these tagged runs indicate that elevated point sources in Pennsylvania, Ohio, and New York contribute significantly, on an annual basis, to sulfate concentrations at all MANE-VU sites. Northern sites (e.g., Acadia) are more influenced by sources in upper midwestern states (e.g., Wisconsin and Michigan) whereas southern sites like Brigantine are more influenced by sources in more southerly states such as West Virginia, Maryland, and Virginia. Shenandoah, a VISTAS Class I site appears to be most strongly influenced by sources in Ohio, Pennsylvania, and West Virginia, followed by other nearby Southeast and Midwest states. Figure 6-4 through Figure 6-7 present these results showing the breakout of sulfate by individual tag. Note that the large "other" fraction of sulfate includes all sources outside the analysis domain, which includes some portions of the VISTAS and CENRAP RPO, Northern and Western Canada in addition to all other (i.e., inter-continental) sources of SO_2. Figure 6-8 shows similar results summarized by RPO for the 20% worst days.

Figure 6-3. REMSAD modeling tagging schemes.
(black: group 1, red: group 2, and blue: group 3)

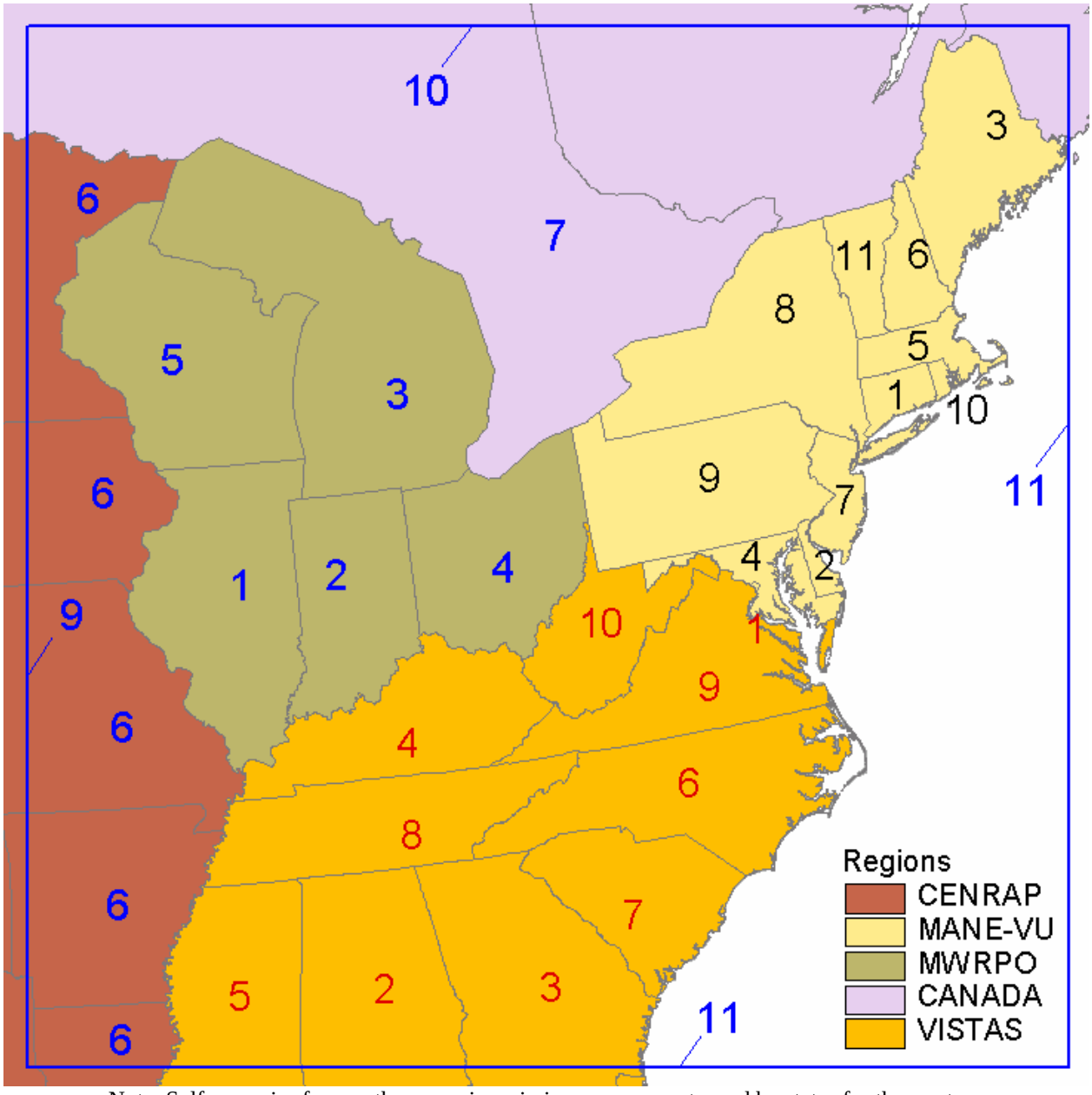

Note: Sulfur species from anthropogenic emission sources are tagged by states for three sets of tags. Tag group 3 also includes boundary conditions. The color of the numbers represents tag groups (black: group 1, red: group 2, and blue: group 3)

Figure 6-4. 2002 Eastern states' contribution to annual PM sulfate in Acadia, ME

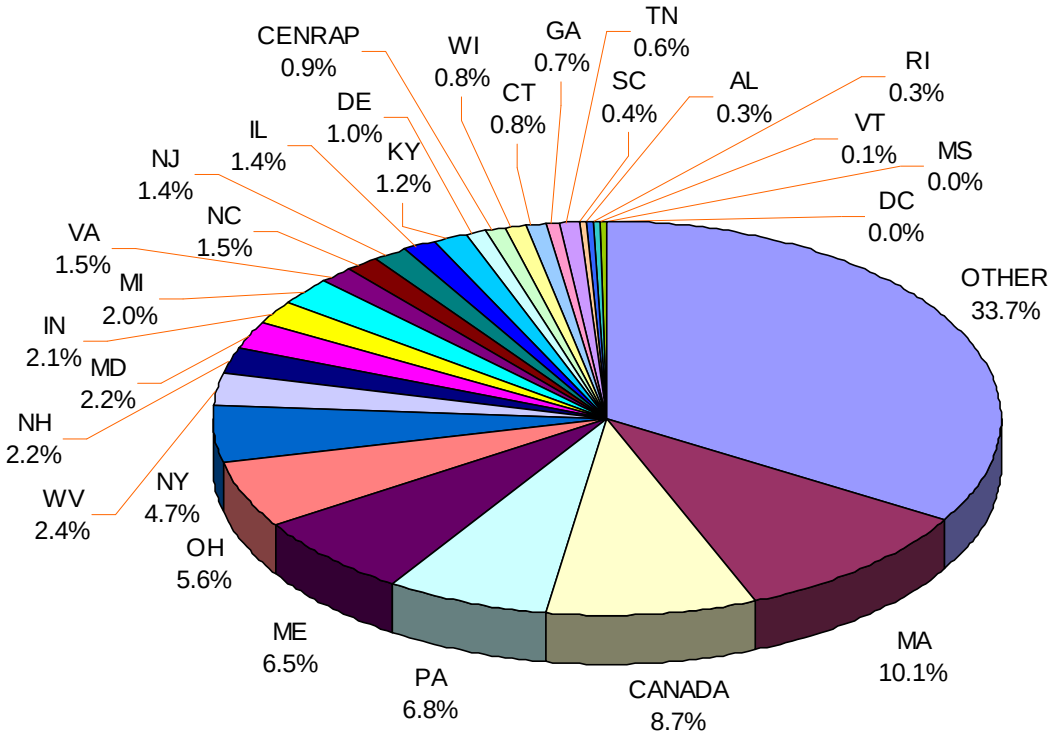

Figure 6-5. 2002 Eastern states' contribution to annual PM sulfate in Brigantine, NJ

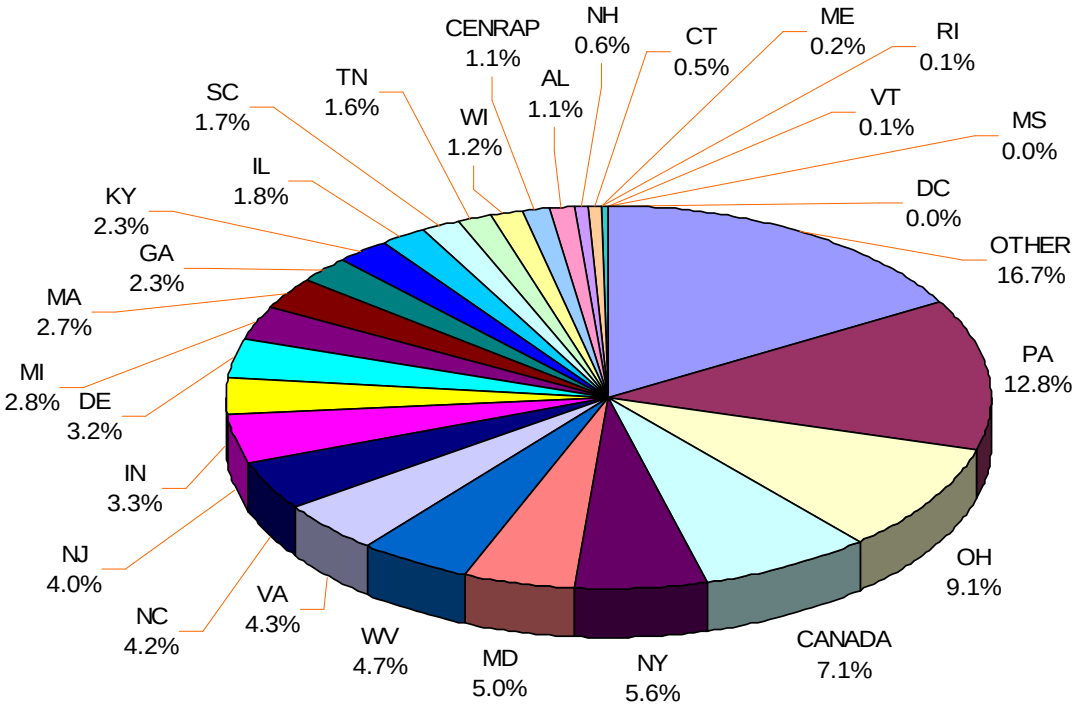

Figure 6-6. 2002 Eastern states' contribution to annual PM sulfate in Lye Brook, VT

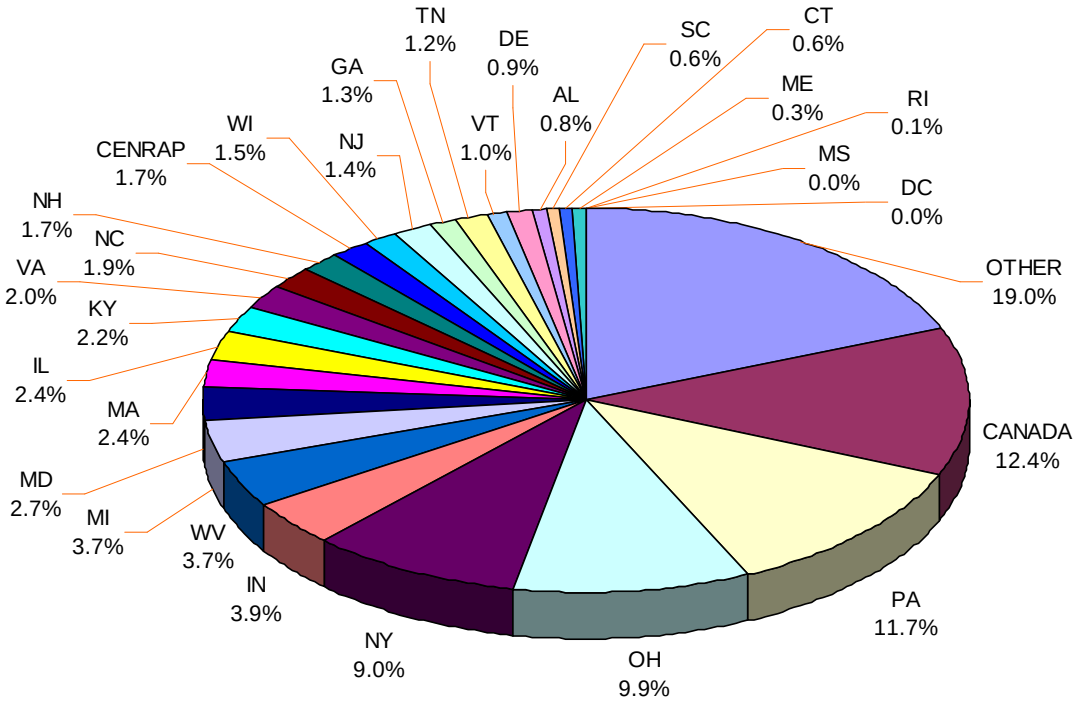

Figure 6-7. 2002 Eastern states' contribution to annual PM sulfate in Shenandoah, VA

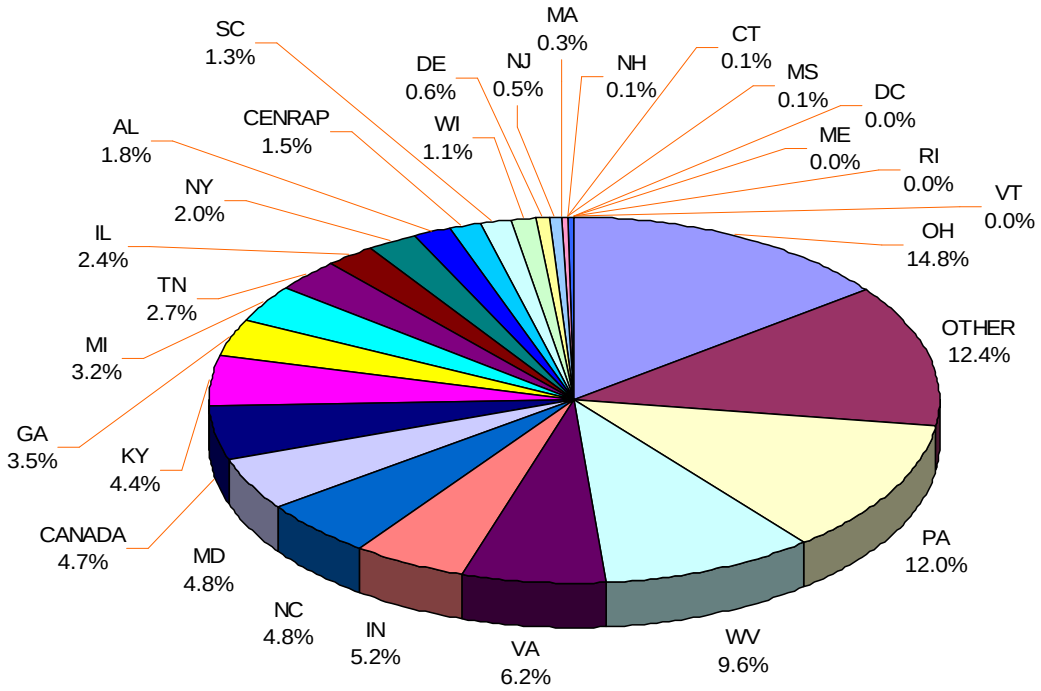

Figure 6-8. Comparison of Sulfate Extinctions on 20% Worst Visibility Days

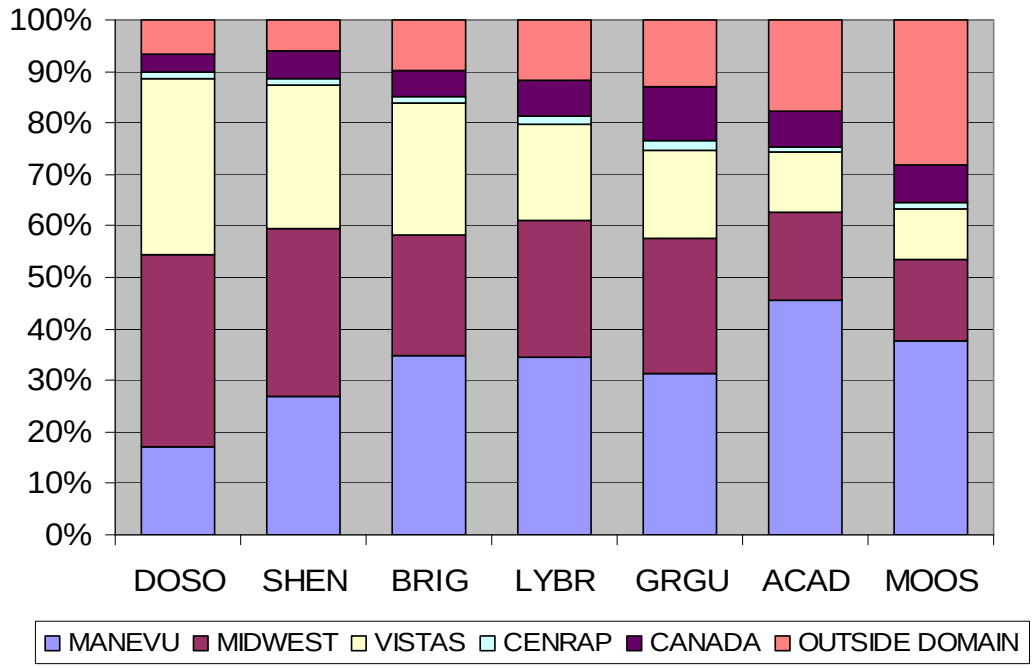

References

Byun, D.W., and Ching, J.K.S., *Science Algorithms of the EPA Models-3 Community Multiscale Air Quality (CMAQ) Modeling System*, EPA/600/R-99/030, March 1999.

Park, R. J., Jacob, D. J., Field, B. D., Yantosca, R. M., and Chin, M., *Natural and transboundary pollution influences on sulfate-nitrate-ammonium aerosols in the United States: implications for policy* , J. Geophys. Res., D15204, 10.1029/2003JD004473, 2004.

SAI, *User's Guide to the Regional Modeling System for Aerosols and Deposition (REMSAD), Version 7*, ICF Consulting/SAI, San Francisco, CA, 2002.

7. LAGRANGIAN DISPERSION MODELS

Dispersion models are commonly used to study the impacts of pollutant plumes or specific point source emissions on surrounding areas. The scale of these models has traditionally been limited to a few hundred kilometers because of a perceived lack of ability to accurately reproduce horizontal dispersion beyond these distances. Recent advances in the CALPUFF system (USEPA, 2006) — including enhancements to its horizontal diffusion and dispersion algorithms as well as the addition of chemical transformation parameterizations — have resulted in improved performance over much greater distances. In fact, the most recent proposed guidance for implementing the BART (Best Available Retrofit Technology) requirements of the Regional Haze Rule provide for the use of CALPUFF to analyze dispersion over distances exceeding 200 km as long as a detailed modeling protocol is included for approval by the appropriate reviewing authority (40 CFR Part 51, pg. 25194, May 5, 2004).

Appendix D provides specific information related to two CALPUFF platforms that have been developed for a large domain (see Figure 7-1) by the Vermont Department of Environmental Conservation (VT DEC) Air Pollution Control Branch and by the State of Maryland's Department of the Environment (MDE) and Department of Natural Resources (MDNR) with contract assistance provided by Environmental Resources Management (ERM). Appendix D contains detailed descriptions of the two platforms; the processing and evaluation of both MM5- and National Weather Service (NWS)-based meteorological data; the processing and evaluation of CEMS (Continuous Emissions Monitoring System)- and 2002 RPO-based emissions data; performance evaluations of

Figure 7-1. CALPUFF modeling domain utilized by MANE-VU

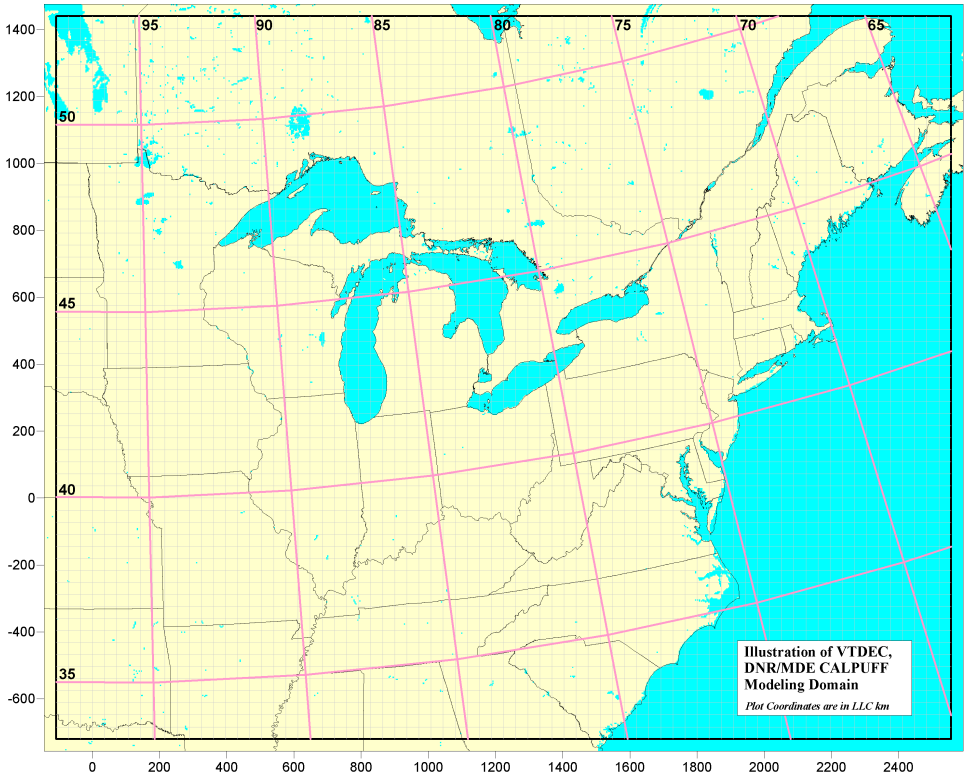

the overall modeling system; preliminary results of modeling to determine annual average and maximum 24-hour impact by individual unit and by state; and discussion of the future application of these platforms to the BART program. This chapter provides an overview of the two modeling platforms, a summary of initial results, and a brief analysis of the differences between the two platforms.

While CALPUFF will certainly play a role in helping MANE-VU assess potential visibility impacts for BART-eligible sources, the development of twin CALPUFF platforms utilizing both MM5-based and NWS-based meteorological drivers further expands the suite of analytical tools available for assessing contributions — at both the facility and state level — to downwind visibility impairment in the MANE-VU region.

7.1. Platform Overview

The VT DEC developed meteorological inputs for CALPUFF using observation-based inputs (i.e., rawinsonde and surface measurements) from the NWS and by applying CALMET. VT DEC also developed hourly emissions and exhaust flow data from the Acid Rain Program's CEMS data files for 869 large electric generating units (EGUs). These emissions data were utilized as inputs to CALPUFF, along with emissions data for four additional source sectors: non-EGU point sources, mobile (on-road), mobile (off-road), and general area sources. The emission inputs for these source sectors were derived from the 2002 RPO inventories.

The MDNR and MDE developed meteorological inputs for CALPUFF using MM5 data developed by the University of Maryland for the MANE-VU and Ozone Transport Commission SIP modeling work. The Maryland agencies utilized the CEMS data files developed by VT DEC, and independently developed emissions and source parameters for the other four source sectors based on the same inter-RPO 2002 inventories.

Both platforms were used to model the entire calendar year 2002. These simulations have been configured to provide estimates for both individual source impacts and cumulative state impacts and to allow for inter-platform comparisons. The modeling domain has been designed to be consistent with the other modeling systems described in this report (e.g., REMSAD, CMAQ), so that conclusions regarding the most significant sources of sulfate-related visibility impacts in MANE-VU can be compared. Consistency across a broad range of approaches will add credibility to the conclusions reached in the overall contribution assessment.

7.2. CALPUFF Modeling Results for Individual Sources

To explore differences between the two CALPUFF modeling platforms, each was used to create a ranked list of the 100 emissions sources that contribute most to ambient sulfate levels at each of several eastern Class I sites. Of the 100 top sources identified for the Brigantine Wilderness Area, 70 sources appeared on the lists generated by both platforms. At Acadia, Lye Brook, and Shenandoah, there was even more agreement between the model results, with both platforms identifying 78, 76, and 85 out of 100 of the same top sources for each of these sites, respectively. Figure 7-2 shows the correlation between estimated annual average impacts for the sources that were identified by both platforms as among the top 100 sulfate contributors. While the

NWS/rawindsonde-based meteorology consistently produced slightly lower estimates of impact than the MM5-based platform, the correlations are relatively robust, ranging from 0.89 at Brigantine to 0.93 at Lye Brook.

Overall, the CALPUFF modeling results to date demonstrate reasonably good comparability between the two platforms (as illustrated by Figure 7-2 and Table 7-1), but they also suggest a consistent pattern of under prediction for one platform relative to the other.

7.3. CALPUFF Modeling Results Overview

Table 7-1 provides further comparisons of the results of CALPUFF modeling utilizing the two different platforms described earlier in this chapter: VT DEC (NWS/rawinsonde-based meteorology) and Maryland (MM5-based meteorology).[35] The table summarizes annual average sulfate concentrations by source category for each of the two platforms relative to observed concentrations.

Table 7-1. CALPUFF Overall Modeling Summary

	Annual Average SO_4 Ion Concentration ($\mu g/m^3$)								
	NWS/Rawinsonde-based Meteorology				**MM5-based Meteorology**				**Observed**
	CEMS EGU	**Non-CEMS Point**	**Area/Mobile**	**Total**	**CEMS EGU**	**Non-CEMS Point**	**Area/Mobile**	**Total**	
Shenandoah	2.271	0.412	0.106	2.789	2.98	0.46	0.22	3.66	4.61
Brigantine	1.847	0.421	0.257	2.526	2.6	0.51	0.38	3.48	4.06
Acadia	0.965	0.385	0.218	1.569	1.42	0.42	0.28	2.13	1.86
Lye Brook	1.178	0.342	0.178	1.698	1.65	0.36	0.25	2.26	2.17

Generally, the NWS/rawinsonde platform predicts lower sulfate ion concentrations than the MM5 platform. On an annual average basis, the concentrations predicted using the MM5 platform are much closer to observed values than the concentrations predicted using the NWS/rawindsonde platform.

7.4. CALPUFF Results for Ranked State Sulfate Contributions

This section focuses on the ranked contribution of emissions from individual states to overall sulfate levels at specific receptor sites (additional results are summarized in a number of different ways in Appendix D). The rankings were calculated by summing impacts from EGUs included in the 2002 data base for each state. State contributions are then sorted by total annual impact. Predicted annual average sulfate ion concentrations from other source sectors were added to these data in Table 7-2(a-d) for both platforms. As in previous chapters, estimated contributions to receptor impact by state (using the results presented in Table 7-2) are depicted graphically in Figure 7-3 and Figure 7-4 for the observation-based and MM5-based platforms, respectively. States are ranked along the horizontal axis by averaging the individual results calculated for each state using the two CALPUFF platforms.

[35] The Maryland Department of the Environment is contributing toward this work through the Maryland Department of Natural Resources and their contractor ERM, Inc. who have developed the MM5-based meteorology and CALPUFF platform.

Figure 7-2. Correlation between MM5-based source contributions (Maryland/ERM) and NWS/rawindsonde-based source contributions (VT DEC) for common EGUs modeled at four receptor sites in or near MANE-VU

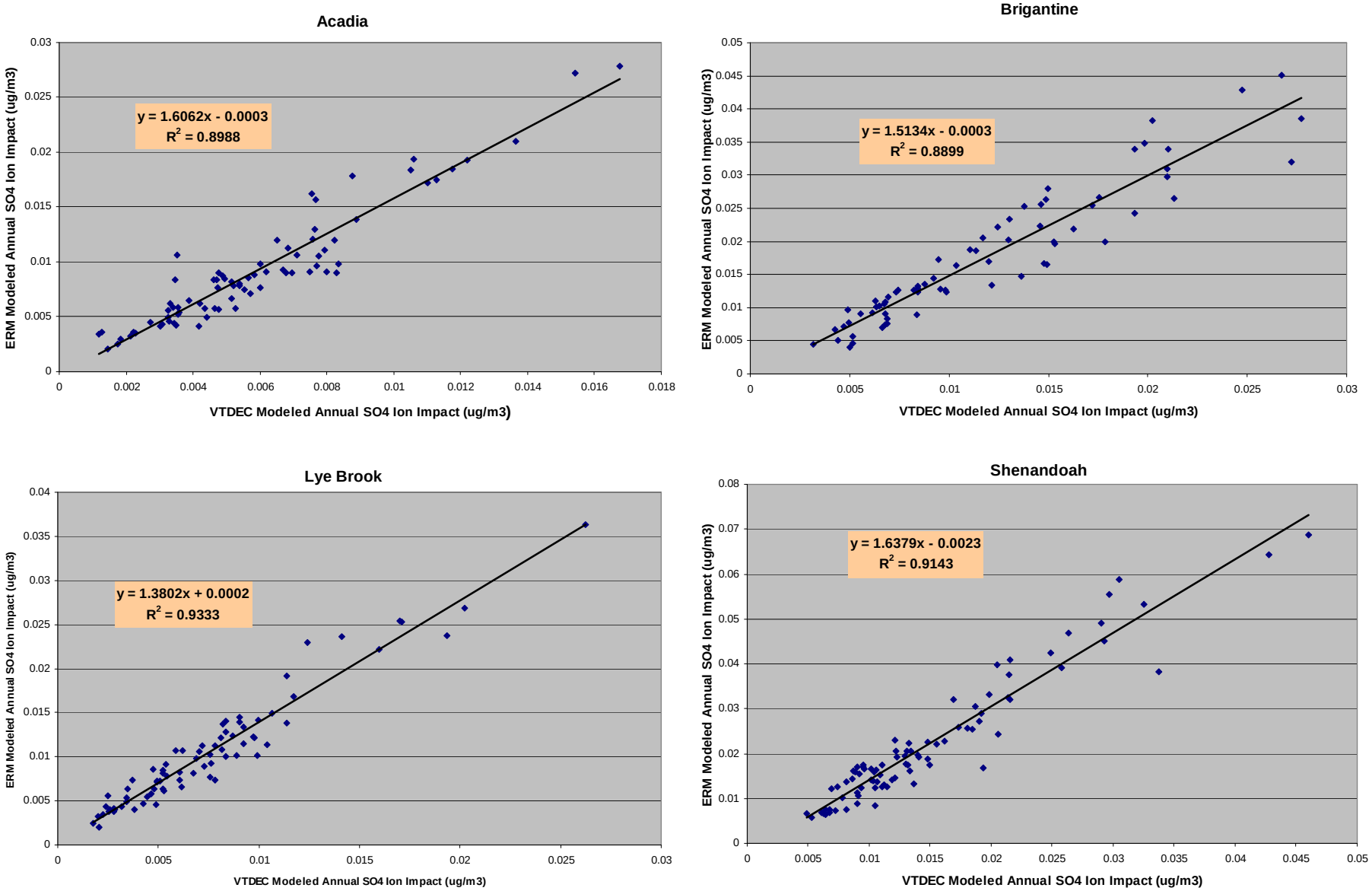

Table 7-2a. Sulfate Ion Impacts by State (Annual Average)
Acadia National Park

	NWS-based Meteorology (VT DEC) µg/m^3				MM5-based Meteorology (MDE/MDNR) µg/m^3			
STATE	**CEM PT**	**Non-CEM PT**	**Area/ Mobile**	**TOTAL PT**	**CEM PT**	**Non-CEM PT**	**Area/ Mobile**	**TOTAL**
AL(a)	0.0086	0.0013	0.0003	0.0102	0.0139	0.0009	0.0011	0.0159
AR(a)	0.0039	0	0	0.0039	0.0054	0.0020	0.0010	0.0083
CT	0.0041	0.0012	0.0085	0.0138	0.0074	0.0011	0.0072	0.0156
DC	0.0001	0.0001	0.0002	0.0004	6.9E-05	0.0001	0.0003	0.0005
DE	0.0087	0.002	0.0008	0.0115	0.0093	0.0109	0.0018	0.0219
GA(a)	0.0142	0.0008	0.0005	0.0155	0.0259	0.0009	0.0019	0.0287
IA	0.0097	0.0122	0.0001	0.0219	0.0149	0.0120	0.0030	0.0299
IL	0.0342	0.0157	0.0004	0.0504	0.0486	0.0172	0.0034	0.0693
IN	0.0758	0.0103	0.001	0.087	0.1089	0.0119	0.0099	0.1307
KS(a)	0.0081	0	0	0.0081	0.0137	0.0012	0.0010	0.0159
KY	0.0411	0.0054	0.0023	0.0487	0.0632	0.0038	0.0069	0.0740
MA	0.0653	0.0127	0.0579	0.136	0.0860	0.1544	0.0773	0.3176
MD	0.0398	0.0019	0.0034	0.0451	0.0780	0.0062	0.0040	0.0882
ME	0.0032	0.0243	0.0294	0.057	0.0030	0.0356	0.0236	0.0622
MI	0.0611	0.0083	0.0031	0.0726	0.0656	0.0095	0.0093	0.0844
MN	0.0089	0.0043	0.0005	0.0137	0.0107	0.0022	0.0023	0.0151
MO	0.014	0	0	0.014	0.0215	0.0115	0.0041	0.0371
MS(a)	0	0.0002	0.0002	0.0003	0	0.0002	0.0002	0.0004
NC	0.0342	0.0081	0.0014	0.0437	0.0554	0.0057	0.0019	0.0630
ND(a)					0	0.0009	0.0012	0.0021
NE(a)	0.0017	0	0	0.0017	0.0028	0	0.0009	0.0037
NH	0.0386	0.0022	0.0071	0.0479	0.0666	0.0020	0.0065	0.0750
NJ	0.013	0.0025	0.0076	0.0232	0.0187	0.0033	0.0133	0.0354
NY	0.0577	0.0118	0.0505	0.12	0.0736	0.0363	0.0578	0.1677
OH	0.1402	0.0081	0.0013	0.1496	0.2248	0.0457	0.0055	0.2759
OK(a)	0.0059	0	0	0.0059	0.0071	0.0015	0.0006	0.0092
PA	0.1383	0.0196	0.0126	0.1706	0.2354	0.0214	0.0156	0.2725
RI	0	0	0.0074	0.0074	5.9E-06	0.0007	0.0043	0.0050
SC	0.0092	0.003	0.001	0.0132	0.0134	0.0036	0.0012	0.0182
SD(a)	0.0009	0	0	0.0009	0.0012	2.8E-05	0.0009	0.0022
TN	0.0192	0.0045	0.0024	0.0261	0.0286	0.0076	0.0031	0.0393
TX(a)	0	0	0	0	1.1E-05	0	2.3E-05	3.5E-05
VA	0.0319	0.0082	0.0007	0.0407	0.0389	0.0081	0.0029	0.0499
VT	0	0.0004	0.0169	0.0173	4.0E-06	0.0004	0.0026	0.0030
WI	0.0152	0.0196	0.0005	0.0353	0.0254	0.0085	0.0019	0.0358
WV	0.0583	0.0053	0.0006	0.0642	0.0865	0.0086	0.0016	0.0966
Canada(b)	0	0.1914	0	0.1914				
Totals	**0.96511**	**0.3854**	**0.21832**	**1.5688**	**1.45**	**0.44**	**0.28**	**2.17**

Notes:

(a) Only sources in that portion of the state within the RPO modeling domain were modeled.

(b) 52 Canadian point sources > 250 tons/yr SO_2 emissions during 2002 (from Canadian NPRI).

Table 7-2b. Sulfate Ion Impacts by State (Annual Average) Brigantine Wilderness Area

	NWS-based Meteorology (VT DEC) µg/m^3				MM5-based Meteorology (MDE/MDNR) µg/m^3			
STATE	**CEM PT**	**Non-CEM PT**	**Area/ Mobile**	**TOTAL PT**	**CEM PT**	**Non-CEM PT**	**Area/ Mobile**	**TOTAL**
AL(a)	0.0317	0.0055	0.0011	0.0383	0.0304	0.0017	0.0020	0.0341
AR(a)	0.0047	0	0	0.0047	0.0088	0.0032	0.0017	0.0137
CT	0.0041	0.0013	0.0099	0.0153	0.0044	0.0009	0.0063	0.0116
DC	0.0009	0.0004	0.0008	0.0021	0.0012	0.0005	0.0013	0.0030
DE	0.0395	0.0111	0.0073	0.0579	0.0524	0.0549	0.0138	0.1211
GA(a)	0.0576	0.0044	0.0030	0.0649	0.0672	0.0024	0.0057	0.0753
IA	0.0156	0.0176	0.0001	0.0333	0.0152	0.0137	0.0032	0.0321
IL	0.0521	0.0192	0.0005	0.0719	0.0535	0.0190	0.0043	0.0768
IN	0.1165	0.0125	0.0011	0.1302	0.1632	0.0162	0.0128	0.1921
KS(a)	0.0113	0	0	0.0113	0.0107	0.0009	0.0008	0.0124
KY	0.0846	0.0098	0.0039	0.0982	0.1285	0.0076	0.0135	0.1496
MA	0.0240	0.0049	0.0191	0.0480	0.0234	0.0406	0.0168	0.0808
MD	0.1351	0.0073	0.0165	0.1589	0.2191	0.0228	0.0210	0.2630
ME	0.0004	0.0017	0.0016	0.0037	0.0002	0.0017	0.0011	0.0030
MI	0.0579	0.0077	0.0028	0.0685	0.0810	0.0110	0.0120	0.1040
MN	0.0120	0.0056	0.0007	0.0183	0.0114	0.0025	0.0027	0.0166
MO	0.0179	0	0	0.0179	0.0202	0.0108	0.0036	0.0346
MS(a)	0	0.0006	0.0003	0.0009	0	0.0006	0.0005	0.0012
NC	0.1414	0.0360	0.0060	0.1835	0.1609	0.0160	0.0054	0.1823
ND(a)					0	0.0011	0.0015	0.0026
NE(a)	0.0031	0	0	0.0031	0.0025	0	0.0009	0.0035
NH	0.0064	0.0004	0.0012	0.0080	0.0100	0.0003	0.0010	0.0113
NJ	0.0426	0.0081	0.0518	0.1024	0.0625	0.0124	0.0805	0.1553
NY	0.0658	0.0120	0.0719	0.1497	0.0810	0.0307	0.0779	0.1896
OH	0.2611	0.0130	0.0017	0.2757	0.4297	0.0836	0.0088	0.5221
OK(a)	0.0068	0	0	0.0068	0.0077	0.0014	0.0007	0.0098
PA	0.2538	0.0460	0.0339	0.3336	0.4407	0.0553	0.0461	0.5421
RI	0	0	0.0042	0.0042	2.1E-06	0.0003	0.0016	0.0019
SC	0.0362	0.0139	0.0042	0.0542	0.0341	0.0101	0.0032	0.0475
SD(a)	0.0011	0	0	0.0011	0.0012	3.4E-05	0.0012	0.0024
TN	0.0477	0.0138	0.0049	0.0664	0.0630	0.0188	0.0061	0.0879
TX(a)	0	0	0	0	2.5E-07	0	2.9E-05	3.0E-05
VA	0.1442	0.0447	0.0035	0.1924	0.1577	0.0331	0.0119	0.2027
VT	0	0.0002	0.0033	0.0035	1.5E-06	0.0001	0.0006	0.0008
WI	0.0216	0.0312	0.0007	0.0535	0.0315	0.0106	0.0026	0.0447
WV	0.1499	0.0118	0.0016	0.1633	0.2340	0.0202	0.0046	0.2588
Canada(b)	0	0.0807	0	0.0807				
Totals	**1.84732**	**0.42121**	**0.25746**	**2.526**	**2.61**	**0.51**	**0.38**	**3.49**

Notes:

(a) Only sources in that portion of the state within the RPO modeling domain were modeled.

(b) 52 Canadian point sources > 250 tons/yr SO_2 emissions during 2002 (from Canadian NPRI).

Table 7-2c. Sulfate Ion Impacts by State (Annual Average)
Lye Brook Wilderness Area

	NWS-based Meteorology (VT DEC) µg/m^3				MM5-based Meteorology (MDE/MDNR) µg/m^3			
STATE	**CEM PT**	**Non-CEM PT**	**Area/ Mobile**	**TOTAL PT**	**CEM PT**	**Non-CEM PT**	**Area/ Mobile**	**TOTAL**
AL(a)	0.0151	0.0023	0.0005	0.0179	0.0209	0.0013	0.0015	0.0238
AR(a)	0.0053	0	0	0.0053	0.0072	0.0029	0.0015	0.0116
CT	0.0015	0.0004	0.0038	0.0057	0.0024	0.0006	0.0045	0.0075
DC	0.0001	0.0002	0.0003	0.0005	7.9E-05	0.0002	0.0004	0.0006
DE	0.0045	0.0017	0.0007	0.0068	0.0076	0.0123	0.0020	0.0219
GA(a)	0.0270	0.0016	0.0011	0.0296	0.0351	0.0012	0.0029	0.0392
IA	0.0151	0.0175	0.0001	0.0326	0.0184	0.0158	0.0041	0.0383
IL	0.0473	0.0173	0.0005	0.0651	0.0550	0.0208	0.0047	0.0805
IN	0.1039	0.0120	0.0011	0.1170	0.1369	0.0148	0.0128	0.1645
KS(a)	0.0115	0	0	0.0115	0.0167	0.0016	0.0013	0.0195
KY	0.0647	0.0075	0.0031	0.0753	0.0820	0.0047	0.0099	0.0967
MA	0.0106	0.0040	0.0125	0.0270	0.0161	0.0291	0.0203	0.0655
MD	0.0452	0.0025	0.0040	0.0518	0.0686	0.0088	0.0052	0.0826
ME	0.0001	0.0020	0.0017	0.0038	0.0003	0.0024	0.0018	0.0044
MI	0.0841	0.0113	0.0041	0.0995	0.0798	0.0121	0.0120	0.1039
MN	0.0130	0.0062	0.0007	0.0200	0.0147	0.0031	0.0035	0.0213
MO	0.0191	0	0	0.0191	0.0253	0.0140	0.0052	0.0445
MS(a)	0	0.0004	0.0002	0.0006	0	0.0006	0.0004	0.0011
NC	0.0424	0.0088	0.0016	0.0528	0.0680	0.0058	0.0022	0.0760
ND(a)					0	0.0014	0.0020	0.0035
NE(a)	0.0027	0	0	0.0027	0.0032	0	0.0012	0.0044
NH	0.0072	0.0007	0.0020	0.0098	0.0137	0.0008	0.0023	0.0167
NJ	0.0071	0.0017	0.0051	0.0139	0.0128	0.0029	0.0115	0.0272
NY	0.0637	0.0289	0.0586	0.1511	0.0985	0.0613	0.0842	0.2440
OH	0.2108	0.0112	0.0016	0.2237	0.2963	0.0649	0.0078	0.3690
OK(a)	0.0086	0	0	0.0086	0.0097	0.0020	0.0009	0.0127
PA	0.1918	0.0255	0.0169	0.2342	0.3050	0.0288	0.0219	0.3558
RI	0	0	0.0013	0.0013	1.4E-06	0.0002	0.0010	0.0012
SC	0.0088	0.0037	0.0013	0.0138	0.0133	0.0040	0.0014	0.0187
SD(a)	0.0014	0	0	0.0014	0.0017	4.3E-05	0.0014	0.0031
TN	0.0281	0.0065	0.0032	0.0378	0.0407	0.0098	0.0042	0.0546
TX(a)	0	0	0	0	8.4E-06	0	3.2E-05	4.0E-05
VA	0.0295	0.0088	0.0008	0.0391	0.0454	0.0104	0.0037	0.0596
VT	0	0.0006	0.0499	0.0505	4.0E-06	0.0017	0.0083	0.0100
WI	0.0229	0.0293	0.0007	0.0529	0.0351	0.0116	0.0028	0.0495
WV	0.0852	0.0079	0.0009	0.0939	0.1232	0.0121	0.0023	0.1375
Canada(b)	0	0.1211	0	0.1211				
Totals	**1.1780**	**0.3416**	**0.1781**	**1.6977**	**1.65**	**0.36**	**0.25**	**2.27**

Notes:

(a) Only sources in that portion of the state within the RPO modeling domain were modeled.

(b) 52 Canadian point sources > 250 tons/yr SO_2 emissions during 2002 (from Canadian NPRI).

Table 7-2d. Sulfate Ion Impacts by State (Annual Average) Shenandoah National Park

	NWS-based Meteorology (VT DEC) µg/m^3				MM5-based Meteorology (MDE/MDNR) µg/m^3			
STATE	**CEM PT**	**Non-CEM PT**	**Area/ Mobile**	**TOTAL PT**	**CEM PT**	**Non-CEM PT**	**Area/ Mobile**	**TOTAL**
AL(a)	0.0521	0.0084	0.0018	0.0623	0.0504	0.0029	0.0034	0.0567
AR(a)	0.0074	0	0	0.0074	0.0087	0.0035	0.0019	0.0141
CT	0.0005	0.0002	0.0011	0.0018	0.0007	0.0001	0.0009	0.0017
DC	0.0004	0.0004	0.0008	0.0016	8.1E-05	0.0003	0.0009	0.0013
DE	0.0101	0.0029	0.0011	0.0141	0.0086	0.0136	0.0021	0.0243
GA(a)	0.0879	0.0056	0.0040	0.0975	0.0963	0.0032	0.0079	0.1073
IA	0.0192	0.0181	0.0001	0.0374	0.0152	0.0130	0.0036	0.0318
IL	0.0646	0.0222	0.0006	0.0874	0.0561	0.0189	0.0045	0.0794
IN	0.1782	0.0156	0.0015	0.1952	0.1907	0.0181	0.0155	0.2243
KS(a)	0.0137	0	0	0.0137	0.0091	0.0007	0.0006	0.0104
KY	0.1273	0.0135	0.0057	0.1465	0.1741	0.0106	0.0184	0.2031
MA	0.0036	0.0005	0.0020	0.0060	0.0029	0.0047	0.0023	0.0098
MD	0.1045	0.0116	0.0118	0.1280	0.1365	0.0373	0.0109	0.1847
ME	0	0.0004	0.0003	0.0007	2.8E-05	0.0003	0.0002	0.0006
MI	0.0830	0.0082	0.0036	0.0948	0.0860	0.0100	0.0125	0.1085
MN	0.0148	0.0055	0.0007	0.0210	0.0109	0.0023	0.0028	0.0160
MO	0.0255	0	0	0.0255	0.0180	0.0104	0.0034	0.0318
MS(a)	0	0.0009	0.0004	0.0013	0	0.0010	0.0007	0.0017
NC	0.1669	0.0251	0.0050	0.1970	0.2257	0.0148	0.0062	0.2467
ND(a)					0	0.0011	0.0016	0.0027
NE(a)	0.0038	0	0	0.0038	0.0023	0	0.0009	0.0032
NH	0.0010	0.0001	0.0002	0.0012	0.0013	5.3E-05	0.0002	0.0016
NJ	0.0102	0.0018	0.0046	0.0166	0.0119	0.0022	0.0071	0.0212
NY	0.0350	0.0027	0.0141	0.0519	0.0468	0.0141	0.0167	0.0776
OH	0.4678	0.0256	0.0027	0.4960	0.6483	0.1088	0.0114	0.7685
OK(a)	0.0080	0	0	0.0080	0.0081	0.0016	0.0009	0.0105
PA	0.2774	0.0354	0.0214	0.3342	0.4517	0.0318	0.0247	0.5082
RI	0	0	0.0004	0.0004	3.1E-07	2.9E-05	0.0002	0.0002
SC	0.0242	0.0117	0.0041	0.0401	0.0232	0.0093	0.0035	0.0359
SD(a)	0.0011	0	0	0.0011	0.0011	4.0E-05	0.0014	0.0025
TN	0.0781	0.0207	0.0073	0.1061	0.0929	0.0304	0.0086	0.1319
TX(a)	0	0	0	0	1.7E-07	0	3.2E-05	3.2E-05
VA	0.1102	0.0398	0.0047	0.1547	0.1124	0.0469	0.0263	0.1856
VT	0	0	0.0006	0.0007	3.6E-07	2.6E-05	0.0001	0.0002
WI	0.0259	0.0311	0.0007	0.0577	0.0289	0.0096	0.0026	0.0410
WV	0.2691	0.0259	0.0045	0.2995	0.4657	0.0402	0.0111	0.5170
Canada(b)	0	0.0781	0	0.0781				
Totals	**2.271**	**0.412**	**0.106**	**2.789**	**2.98**	**0.46**	**0.22**	**3.66**

Notes:

(a) Only sources in that portion of the state within the RPO modeling domain were modeled.

(b) 52 Canadian point sources > 250 tons/yr SO_2 emissions during 2002 (from Canadian NPRI).

Figure 7-3a. Ranked state percent sulfate contributions to Northeast Class I receptors based on observation-based (VT) CALPUFF results

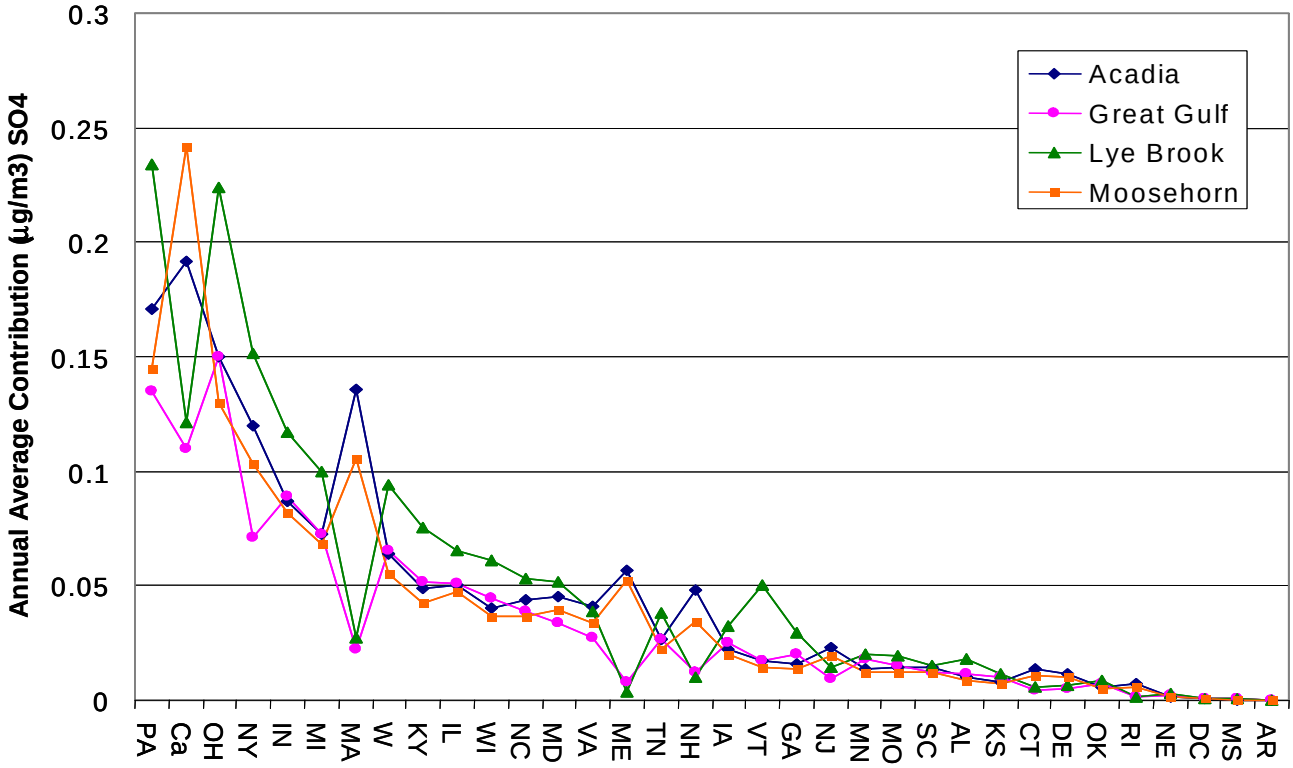

Figure 7-3b. Ranked state percent sulfate contributions to Mid-Atlantic Class I receptors based on observation-based (VT) CALPUFF results

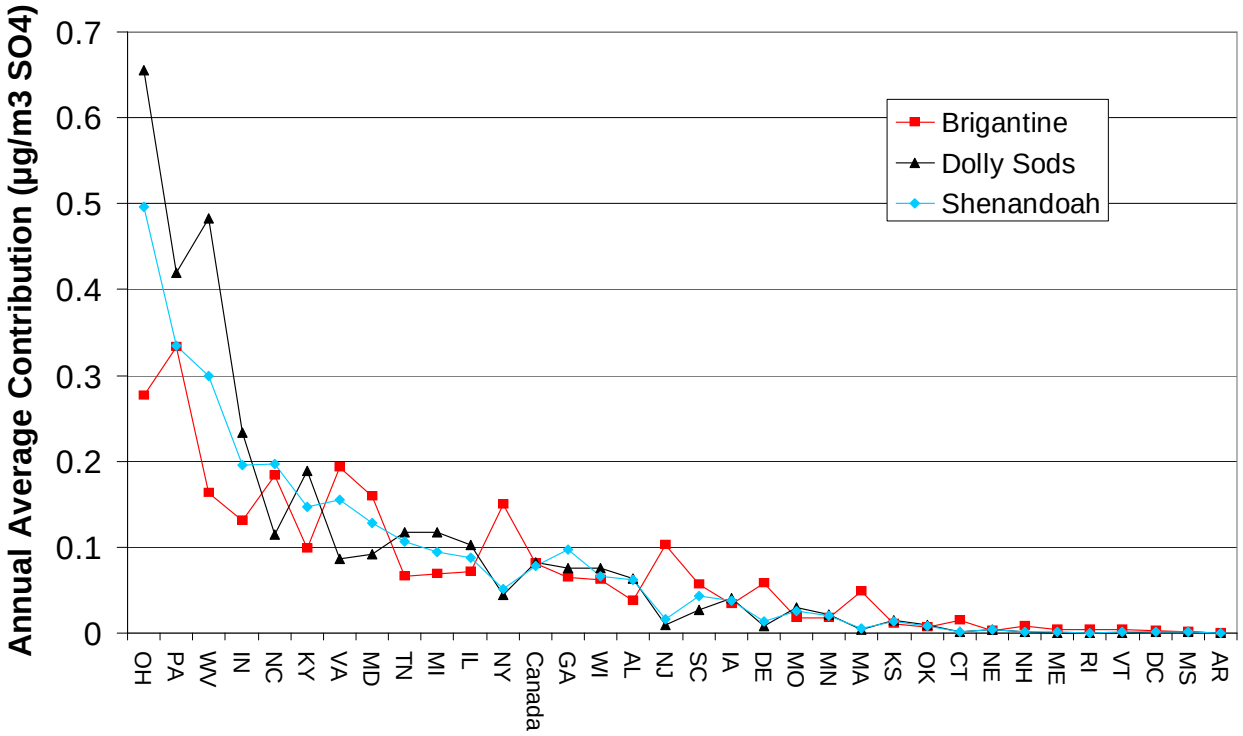

Figure 7-4a. Ranked state percent sulfate contributions to Northeast Class I receptors based on MM5-based (MD) CALPUFF results

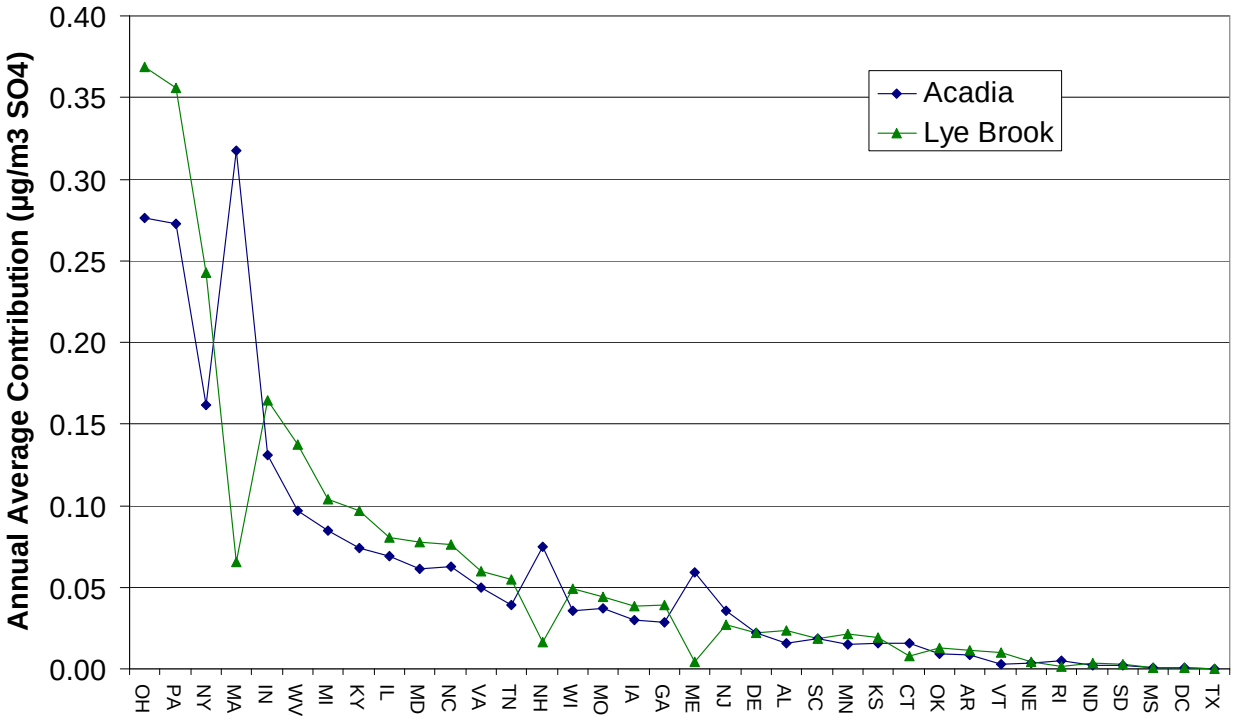

Figure 7-4b. Ranked state percent sulfate contributions to Mid-Atlantic Class I receptors based on MM5-based (MD) CALPUFF results

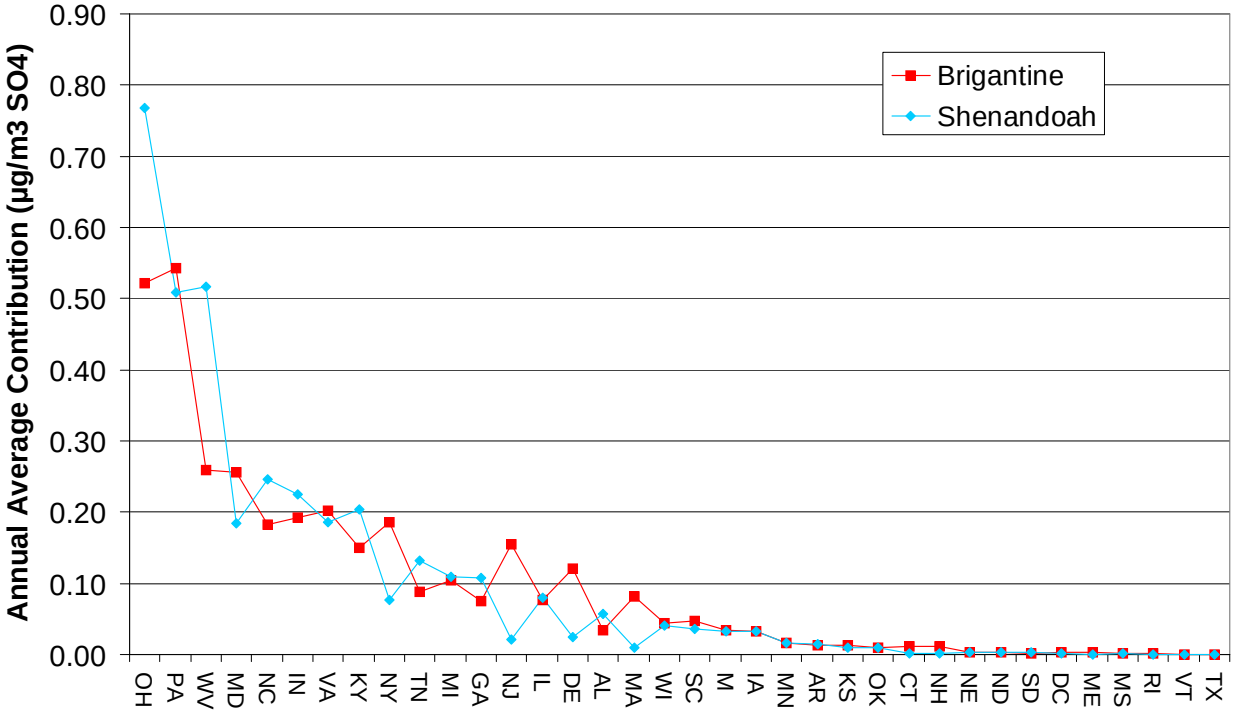

7.5. Future work and potential uses of CALPUFF results for BART determinations

Modeling efforts to date have provided a solid basis for contributing to a weight-of-evidence assessment of state contributions. In addition, the two CALPUFF platforms can be used to evaluate the relative contributions to fine PM and visibility impacts of individual sources in the MANE-VU region. It is anticipated that MANE-VU will provide all states with a consistent set of modeling results from each of these platforms to serve as a preliminary basis for BART visibility determinations and states will have several options with regard to how these results are used:

- States may accept the MANE-VU modeling as an adequate basis for determining whether BART controls at a facility are justified by its contribution to visibility degradation.

- States may conduct additional modeling on their own to determine whether BART controls at a facility are justified by its contribution to visibility degradation.

- States may require a source to conduct additional modeling to determine whether BART controls at a facility are justified by its contribution to visibility degradation.

These options and the use of modeling results for BART determinations are discussed in more detail in the *MANE-VU BART Resource Book* (NESCAUM, 2006), and the reader is referred to that resource for additional information.

References

NESCAUM, *BART Resource Guide*, Northeast States for Coordinated Air Use Management, 2006.

USEPA, CALPUFF Modeling System, Available at: http://www.epa.gov/ttn/scram, 2006.

8. SYNTHESIS OF RESULTS USING DIFFERENT SOURCE ASSESSMENT TECHNIQUES

By synthesizing results from a variety of data sources and analysis techniques MANE-VU has taken a first step toward identifying sources of visibility impairment in the Northeast generally, and toward understanding the role of transported sulfate in particular. The variety of approach and complexity of analytical tools utilized for this purpose provides numerous metrics and means of comparison into how SO_2 emissions are chemically transformed, transported and combined with various local constituents of fine particle pollution in the MANE-VU region. Beyond reviewing these results, additional sections of this chapter describe opportunities for further synthesizing the available data to solidify a weight-of-evidence approach to implementing the contribution assessment and pollution apportionment requirements of the Haze Rule

8.1. Ranked Contribution

Chapter 4 of this report describes two crude methods of ranking state contributions based on the ratio of source emissions to source-receptor distance as well as the gridded product of emissions and upwind residence time probability. Chapter 5 describes the qualitative evidence available from several different trajectory-based techniques and source apportionment studies. These include source region comparisons, source profile examinations, and the development of other techniques and metrics to support the more quantitative ranking techniques. Chapter 6 describes results obtained using Eulerian grid models such as the Regulatory Modeling System for Aerosols and Deposition (REMSAD) and the Community Multi-scale Air Quality (CMAQ) model. Ultimately these types of models are likely to yield the most definitive assessments of contribution from different sources. Chapter 7 explores the use of lagrangian puff dispersion models such as CALPUFF for estimating source contributions and compares two related but distinct versions of the CALPUFF modeling system that demonstrate the sensitivity of this tool to emissions and meteorology inputs.

In Table 8-1 through Table 8-5 (and graphically in Figure 8-1), we have normalized the results obtained using five techniques for assessing state contribution by calculating the percentage contribution and plotted them on a common graph. The figure shows substantial consistency across a variety of independent analyses using techniques that are themselves based on the application of disparate chemical, meteorological and physical principles. Together, these findings create a strong weight-of-evidence case for identifying the most significant contributors to visibility impairment in MANE-VU Class I areas.

In Figure 8-1, several features of the normalized results bear notice. First, we note that the apparent perfect agreement among the techniques for the “other” contribution that represents all emissions from outside the domain of study is a result of having substituted the REMSAD calculated “other” contribution for all of the other methods. REMSAD is the only method that has a means of developing a comprehensive estimate of the total out-of-domain contribution because the boundary condition used was derived from a global model run using global SO_2 emissions estimates. It is also worth noting how high the “other,” or out-of-domain, contribution is to observed sulfate at

Acadia National Park. This is not surprising given how close Acadia is to the domain boundaries on both the northern and eastern edge. There may be some recirculation of in-domain SO_2 emissions that leave the modeling domain and re-enter through the dynamic boundary condition, but lose their tag in the process.

It is also worth noting the differences between the methods for certain states and Canada, such as Massachusetts and Maine in the case of Acadia, Maryland and Canada for Brigantine, Canada for Lye Brook, and Ohio and West Virginia for Shenandoah. Those states and Canada that are directly upwind a large fraction of the time, either because they are very large geographically or because they are very nearby, are likely to be treated differently by the percent-time-upwind method relative to the other methods. In addition, the CALPUFF models appear to underestimate the contribution from Canada relative to other methods. This is likely to result from an incomplete characterization of the total SO_2 inventory for Canada relative to other methods that are based on the entire MANE-VU Canadian inventory.

Table 8-1. Annual Average Sulfate Impact from REMSAD (%)

RPO	STATE	ACADIA	BRIGANTINE	DOLLY SODS	GREAT GULF	LYE BROOK	MOOSEHORN	SHENANDOAH
CANADA		**8.69**	**7.11**	**3.90**	**14.84**	**12.43**	**7.85**	**4.75**
CENRAP		**0.88**	**1.12**	**1.58**	**1.65**	**1.67**	**0.82**	**1.48**
MANE-VU		**36.17**	**34.83**	**14.81**	**27.83**	**31.78**	**30.08**	**20.59**
MANE-VU	Connecticut	0.76	0.53	0.04	0.48	0.55	0.56	0.08
	Delaware	0.96	3.20	0.30	0.63	0.93	0.71	0.61
	District of Columbia	0.01	0.04	0.01	0.01	0.02	0.01	0.04
	Maine	6.54	0.16	0.01	2.33	0.31	8.01	0.02
	Maryland	2.20	4.98	2.39	1.92	2.66	1.60	4.84
	Massachusetts	10.11	2.73	0.18	3.11	2.45	6.78	0.35
	New Hampshire	2.25	0.60	0.04	3.95	1.68	1.74	0.08
	New Jersey	1.40	4.04	0.27	0.89	1.44	1.03	0.48
	New York	4.74	5.57	1.32	5.68	9.00	3.83	2.03
	Pennsylvania	6.81	12.84	10.23	8.30	11.72	5.53	12.05
	Rhode Island	0.28	0.10	0.01	0.11	0.06	0.19	0.01
	Vermont	0.13	0.06	0.00	0.41	0.95	0.09	0.01
MIDWEST		**11.98**	**18.16**	**30.26**	**20.10**	**21.48**	**10.40**	**26.84**
MIDWEST	Illinois	1.37	1.82	2.56	2.52	2.42	1.30	2.47
	Indiana	2.13	3.29	5.40	3.94	3.93	2.02	5.23
	Michigan	2.02	2.77	3.24	3.88	3.67	1.74	3.20
	Ohio	5.62	9.11	17.98	8.33	9.96	4.62	14.87
	Wisconsin	0.85	1.16	1.08	1.42	1.49	0.72	1.07
VISTAS		**8.49**	**21.99**	**36.75**	**12.04**	**13.65**	**6.69**	**33.86**
VISTAS	Alabama	0.32	1.07	2.13	0.65	0.81	0.25	1.77
	Georgia	0.67	2.32	3.71	1.27	1.31	0.56	3.47
	Kentucky	1.17	2.22	4.89	1.99	2.22	0.98	4.34
	Mississippi	0.01	0.04	0.08	0.03	0.04	0.01	0.07
	North Carolina	1.45	4.19	4.29	1.88	1.89	1.14	4.78
	South Carolina	0.43	1.69	1.04	0.64	0.56	0.36	1.30
	Tennessee	0.61	1.56	3.41	1.11	1.23	0.50	2.73
	Virginia	1.48	4.30	2.82	1.52	1.95	1.13	6.20
	West Virginia	2.35	4.59	14.38	2.96	3.64	1.75	9.19
OTHER		**33.79**	**16.78**	**12.70**	**23.54**	**18.99**	**44.17**	**12.48**
TOTAL ($\mu g/m^3$)		**2.026**	**3.444**	**3.867**	**1.780**	**2.137**	**1.767**	**3.919**

Table 8-2. Annual Average Sulfate Impact from Q/D (%)

RPO	STATE	ACADIA	BRIGANTINE	DOLLY SODS	GREAT GULF	LYE BROOK	MOOSEHORN	SHENANDOAH
CANADA		**11.91**	**6.01**	**0.00**	**8.97**	**12.00**	**18.77**	**6.76**
CENRAP		**1.74**	**1.64**	**1.59**	**2.33**	**1.99**	**1.35**	**1.72**
CENRAP	Arkansas	0.13	0.15	0.13	0.08	0.17	0.09	0.26
	Iowa	0.29	0.19	0.24	0.40	0.32	0.24	0.24
	Louisiana	0.02	0.03	0.02	0.02	0.03	0.02	0.04
	Minnesota	0.22	0.13	0.16	0.30	0.24	0.13	0.19
	Missouri	1.08	1.15	1.03	1.53	1.23	0.87	1.00
MANE-VU		**20.13**	**32.53**	**20.10**	**21.48**	**25.69**	**12.84**	**24.50**
MANE-VU	Connecticut	0.34	0.33	0.11	0.74	0.38	0.21	0.31
	Delaware	0.59	3.01	0.46	0.51	0.67	0.36	1.07
	District of Columbia	0.01	0.05	0.02	0.01	0.02	0.01	0.09
	Maine	1.74	0.15	0.08	0.71	0.15	1.13	0.15
	Maryland	1.83	7.26	3.86	0.43	2.67	1.27	5.27
	Massachusetts	2.89	0.95	0.46	4.61	1.06	1.33	1.22
	New Hampshire	1.07	0.30	0.14	0.42	0.08	0.60	0.18
	New Jersey	0.76	4.22	0.43	3.11	0.75	0.48	1.82
	New York	4.02	4.61	1.93	3.67	6.71	2.83	3.30
	Pennsylvania	6.64	11.57	12.58	6.62	13.07	4.50	11.00
	Rhode Island	0.12	0.05	0.02	0.08	0.04	0.06	0.06
	Vermont	0.10	0.03	0.02	0.57	0.10	0.07	0.04
MIDWEST		**16.99**	**17.48**	**26.30**	**25.38**	**22.84**	**12.49**	**22.46**
MIDWEST	Illinois	2.53	2.16	2.60	3.64	2.98	2.11	2.61
	Indiana	3.94	4.24	5.17	6.01	5.01	2.91	4.50
	Michigan	2.69	1.95	2.46	4.08	3.50	2.16	2.49
	Ohio	6.63	8.34	15.06	9.94	9.98	4.51	11.85
	Wisconsin	1.19	0.79	1.00	1.71	1.38	0.80	1.01
VISTAS		**15.44**	**25.55**	**39.32**	**18.30**	**18.48**	**10.39**	**32.08**
VISTAS	Alabama	1.24	1.69	1.66	1.45	1.60	0.91	1.65
	Georgia	2.36	3.28	3.18	2.62	2.82	1.63	3.30
	Kentucky	2.07	3.36	3.99	3.18	2.79	1.50	3.54
	Mississippi	0.19	0.24	0.22	0.22	0.24	0.14	0.37
	North Carolina	2.27	4.16	9.03	2.59	2.69	1.44	6.60
	South Carolina	1.29	1.62	0.95	1.14	0.94	0.70	1.69
	Tennessee	1.45	2.14	2.49	1.74	1.92	1.06	2.40
	Virginia	1.93	4.36	2.49	1.97	1.78	1.12	4.25
	West Virginia	2.64	4.71	15.33	3.39	3.71	1.88	8.27
OTHER[36]		**33.79**	**16.78**	**12.70**	**23.54**	**18.99**	**44.17**	**12.48**
TOTAL (µg/m^3)		**1.920**	**2.740**	**3.455**	**1.305**	**1.858**	**1.977**	**3.417**

[36] OTHER is % from REMSAD result; Florida is considered within OTHER

Table 8-3. Annual Average Sulfate Impact from CALPUFF (NWS Observations) (%)

RPO	STATE	ACADIA	BRIGANTINE	DOLLY SODS	GREAT GULF	LYE BROOK	MOOSEHORN	SHENANDOAH
CANADA		**8.07**	**2.65**	**2.30**	**7.22**	**5.77**	**9.45**	**2.45**
CENRAP		**2.76**	**2.98**	**3.34**	**5.06**	**4.50**	**2.30**	**3.42**
CENRAP	Iowa	0.93	1.09	1.13	1.65	1.55	0.80	1.17
	Kansas	0.34	0.37	0.41	0.64	0.55	0.28	0.43
	Louisiana	0.00	0.00	0.00	0.00	0.00	0.00	0.00
	Minnesota	0.58	0.60	0.62	1.16	0.95	0.49	0.65
	Missouri	0.59	0.59	0.81	1.00	0.91	0.49	0.80
	Nebraska	0.07	0.10	0.11	0.14	0.13	0.06	0.12
	Oklahoma	0.25	0.22	0.26	0.47	0.41	0.20	0.25
MANE-VU		**27.41**	**29.17**	**16.21**	**20.91**	**26.52**	**21.11**	**17.47**
MANE-VU	Connecticut	0.58	0.50	0.03	0.26	0.27	0.41	0.06
	Delaware	0.48	1.90	0.21	0.31	0.32	0.38	0.44
	District of Columbia	0.02	0.07	0.02	0.03	0.02	0.02	0.05
	Maine	2.40	0.12	0.01	0.53	0.18	2.04	0.02
	Maryland	1.90	5.22	2.54	2.19	2.47	1.55	4.01
	Massachusetts	5.73	1.58	0.12	1.44	1.29	4.13	0.19
	New Hampshire	2.02	0.26	0.02	0.79	0.47	1.36	0.04
	New Jersey	0.98	3.37	0.28	0.63	0.67	0.75	0.52
	New York	5.06	4.92	1.24	4.67	7.20	4.03	1.63
	Pennsylvania	7.19	10.97	11.71	8.86	11.16	5.65	10.48
	Rhode Island	0.31	0.14	0.01	0.08	0.06	0.22	0.01
	Vermont	0.73	0.12	0.01	1.13	2.41	0.56	0.02
MIDWEST		**16.85**	**19.99**	**33.09**	**26.68**	**26.98**	**14.21**	**29.46**
MIDWEST	Illinois	2.12	2.37	2.86	3.36	3.11	1.84	2.74
	Indiana	3.67	4.28	6.52	5.83	5.57	3.19	6.11
	Michigan	3.06	2.25	3.28	4.74	4.74	2.67	2.97
	Ohio	6.31	9.07	18.33	9.82	10.66	5.07	15.55
	Wisconsin	1.69	2.03	2.10	2.93	2.90	1.44	2.09
VISTAS		**11.12**	**28.43**	**32.35**	**16.59**	**17.24**	**8.76**	**34.72**
VISTAS	Alabama	0.43	1.26	1.77	0.77	0.85	0.32	1.96
	Georgia	0.65	2.13	2.12	1.30	1.41	0.52	3.06
	Kentucky	2.05	3.23	5.29	3.39	3.59	1.64	4.59
	Mississippi	0.01	0.03	0.04	0.03	0.03	0.01	0.04
	North Carolina	1.84	6.03	3.20	2.52	2.51	1.42	6.18
	South Carolina	0.61	1.87	0.75	0.80	0.71	0.49	1.33
	Tennessee	1.10	2.19	3.27	1.72	1.80	0.86	3.33
	Virginia	1.72	6.33	2.42	1.80	1.86	1.32	4.85
	West Virginia	2.71	5.37	13.49	4.26	4.48	2.17	9.39
OTHER[36]		**33.79**	**16.78**	**12.70**	**23.54**	**18.99**	**44.17**	**12.48**
TOTAL ($\mu g/m^3$)		**1.571**	**2.533**	**3.125**	**1.167**	**1.701**	**1.429**	**2.793**

Table 8-4. Impact from CALPUFF (MM5) (%)

RPO	STATE	ACADIA	BRIGANTINE	DOLLY SODS	GREAT GULF	LYE BROOK	MOOSEHORN	SHENANDOAH
CANADA		**8.05**	**2.65**			**5.76**		**2.46**
CENRAP		**3.26**	**2.85**			**5.08**		**2.74**
CENRAP	Arkansas	0.23	0.32			0.39		0.33
	Iowa	0.82	0.75			1.28		0.74
	Kansas	0.43	0.29			0.65		0.24
	Louisiana							
	Minnesota	0.41	0.39			0.71		0.37
	Missouri	1.01	0.80			1.48		0.74
	Nebraska	0.10	0.08			0.15		0.07
	Oklahoma	0.25	0.23			0.42		0.24
	Texas	0.00	0.00			0.00		0.00
MANE-VU		**28.09**	**31.83**			**27.69**		**19.31**
MANE-VU	Connecticut	0.43	0.27			0.25		0.04
	Delaware	0.60	2.81			0.73		0.57
	District of Columbia	0.01	0.07			0.02		0.03
	Maine	1.62	0.06			0.14		0.01
	Maryland	1.68	5.95			2.59		4.27
	Massachusetts	8.67	1.87			2.18		0.23
	New Hampshire	2.05	0.26			0.56		0.04
	New Jersey	0.97	3.60			0.91		0.49
	New York	4.41	4.30			8.08		1.79
	Pennsylvania	7.44	12.57			11.86		11.83
	Rhode Island	0.14	0.04			0.04		0.00
	Vermont	0.08	0.02			0.33		0.00
MIDWEST		**16.28**	**21.79**			**25.58**		**28.43**
MIDWEST	Illinois	1.89	1.78			2.68		1.85
	Indiana	3.57	4.46			5.48		5.22
	Michigan	2.30	2.41			3.47		2.53
	Ohio	7.53	12.11			12.30		17.88
	Wisconsin	0.98	1.04			1.65		0.95
VISTAS		**10.53**	**24.10**			**16.90**		**34.57**
VISTAS	Alabama	0.43	0.79			0.79		1.32
	Georgia	0.78	1.74			1.30		2.50
	Kentucky	2.02	3.47			3.22		4.73
	Mississippi	0.01	0.03			0.04		0.04
	North Carolina	1.72	4.23			2.53		5.74
	South Carolina	0.50	1.10			0.62		0.84
	Tennessee	1.07	2.04			1.82		3.07
	Virginia	1.36	4.70			1.99		4.32
	West Virginia	2.64	6.00			4.58		12.03
OTHER		**33.79**	**16.78**	**12.70**	**23.54**	**18.99**	**44.17**	**12.48**
TOTAL (ug/m3)		**2.424**	**3.589**			**2.430**		**3.761**

Table 8-5. Annual Average Sulfate Impact from percent time upwind method (%)

RPO	STATE	ACADIA	BRIGANTINE	DOLLY SODS	GREAT GULF	LYE BROOK	MOOSEHORN	SHENANDOAH
CANADA		**15.24**	**6.70**		**19.29**	**15.91**	**13.45**	**4.33**
CENRAP		**1.89**	**1.77**		**1.73**	**1.66**	**1.52**	**1.72**
CENRAP	Arkansas	0.12	0.24		0.15	0.15	0.15	0.20
	Iowa	0.38	0.27		0.27	0.28	0.28	0.25
	Kansas	0.00	0.00		0.00	0.00	0.00	0.00
	Louisiana	0.04	0.08		0.06	0.04	0.04	0.09
	Minnesota	0.56	0.33		0.38	0.44	0.44	0.22
	Missouri	0.80	0.85		0.87	0.75	0.62	0.95
	Texas	0.00	0.00		0.00	0.00	0.00	0.00
MANE-VU		**18.33**	**25.83**		**20.64**	**25.38**	**15.23**	**11.38**
MANE-VU	Connecticut	0.51	0.27		0.52	0.59	0.40	0.10
	Delaware	0.30	1.36		0.34	0.42	0.28	0.24
	District of Columbia	0.12	0.29		0.11	0.14	0.12	0.24
	Maine	1.49	0.08		0.68	0.26	1.53	0.05
	Maryland	1.32	3.06		1.31	1.31	0.96	2.29
	Massachusetts	1.10	0.33		0.86	0.81	0.90	0.12
	New Hampshire	1.21	0.17		1.48	0.72	0.77	0.06
	New Jersey	1.02	6.01		0.99	1.39	0.78	0.49
	New York	4.80	3.49		6.80	9.08	4.23	1.44
	Pennsylvania	6.21	10.71		7.10	10.36	5.07	6.33
	Rhode Island	0.11	0.05		0.08	0.08	0.09	0.02
	Vermont	0.14	0.03		0.37	0.23	0.10	0.01
MIDWEST		**17.35**	**19.55**		**20.67**	**21.63**	**15.56**	**22.03**
MIDWEST	Illinois	3.79	3.47		3.31	3.74	3.22	3.76
	Indiana	3.37	4.36		4.33	4.13	3.21	5.08
	Michigan	2.73	2.07		3.03	3.27	2.34	1.80
	Ohio	6.10	8.65		8.73	9.23	5.77	10.64
	Wisconsin	1.36	1.00		1.28	1.25	1.02	0.76
VISTAS		**13.40**	**29.37**		**14.14**	**16.43**	**10.07**	**48.06**
VISTAS	Alabama	0.72	1.32		0.63	0.71	0.39	2.14
	Georgia	1.40	3.21		1.06	1.54	0.72	4.73
	Kentucky	2.65	4.71		3.59	3.83	2.31	7.82
	Mississippi	0.04	0.10		0.06	0.06	0.03	0.12
	North Carolina	1.29	4.35		0.92	0.99	1.18	6.11
	South Carolina	0.72	1.64		0.42	0.41	0.44	1.62
	Tennessee	1.05	1.91		1.04	1.16	0.86	3.67
	Virginia	1.80	4.83		1.48	1.67	1.32	5.45
	West Virginia	3.74	7.31		4.94	6.05	2.81	16.39
OTHER[36]		**33.79**	**16.78**	**12.70**	**23.54**	**18.99**	**44.17**	**12.48**

MANE-VU will continue to explore these differences, but it remains encouraging that the use of different platforms and approaches results in more agreement across the various techniques than difference. With the few, specific exceptions mentioned above, it is relatively easy — using the normalized results from multiple techniques shown in Figure 8-1(a-d) — to identify those states that have the largest influence on sulfate levels at each Class I site. MANE-VU believes that this information can provide a solid basis for initiating consultation and planning efforts between upwind and downwind states and RPOs.

Figure 8-1(a-d). Comparison of normalized (percent contribution) results using different techniques for ranking state contributions to sulfate levels at the MANE-VU Class I sites (a) Acadia National Park, ME, (b) Brigantine Wilderness Area, NJ, (c)Lye Brook Wilderness Area, VT, and (d) Shenandoah National Park, VA.

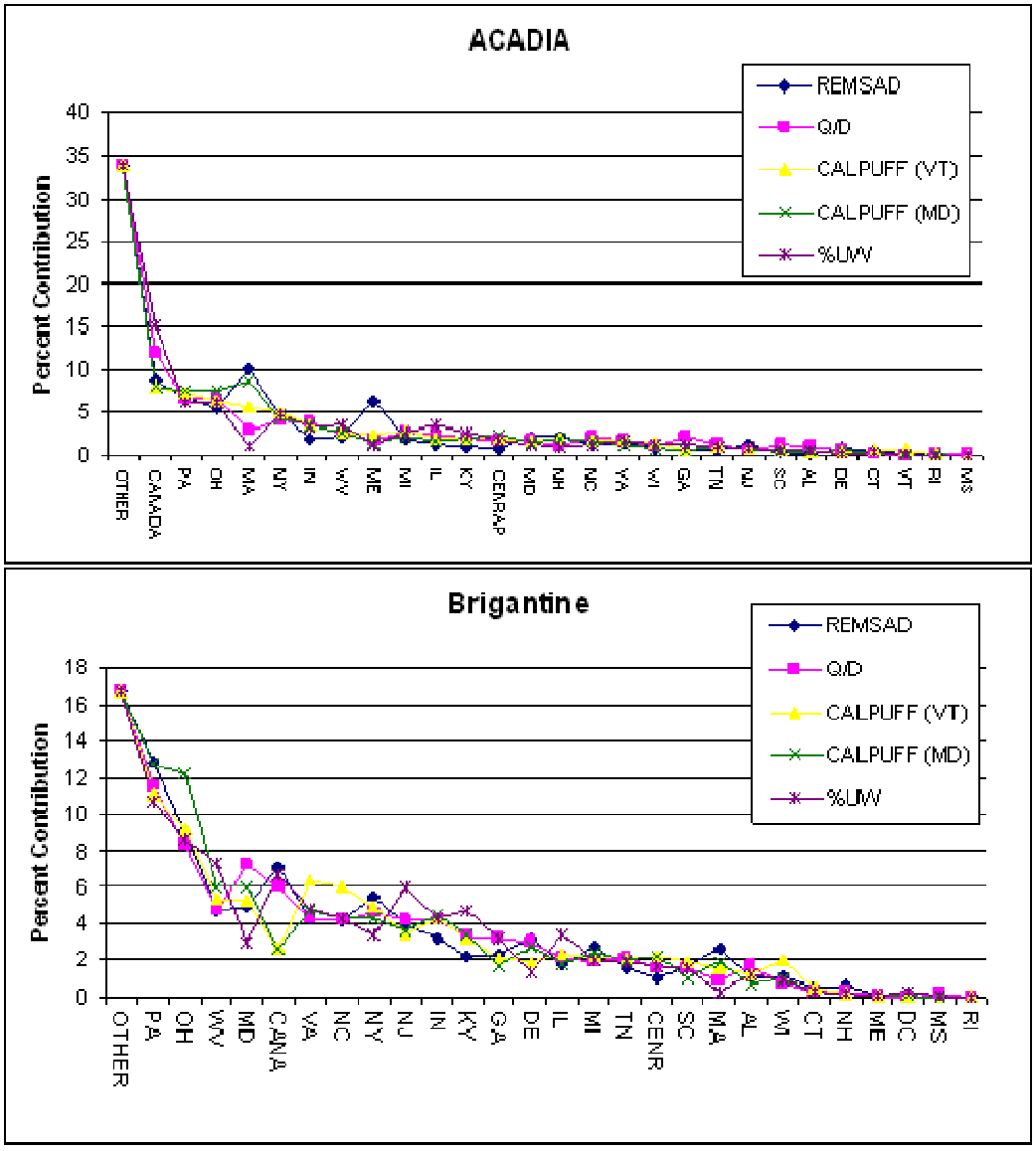

Figure 8-1(a-d). Continued

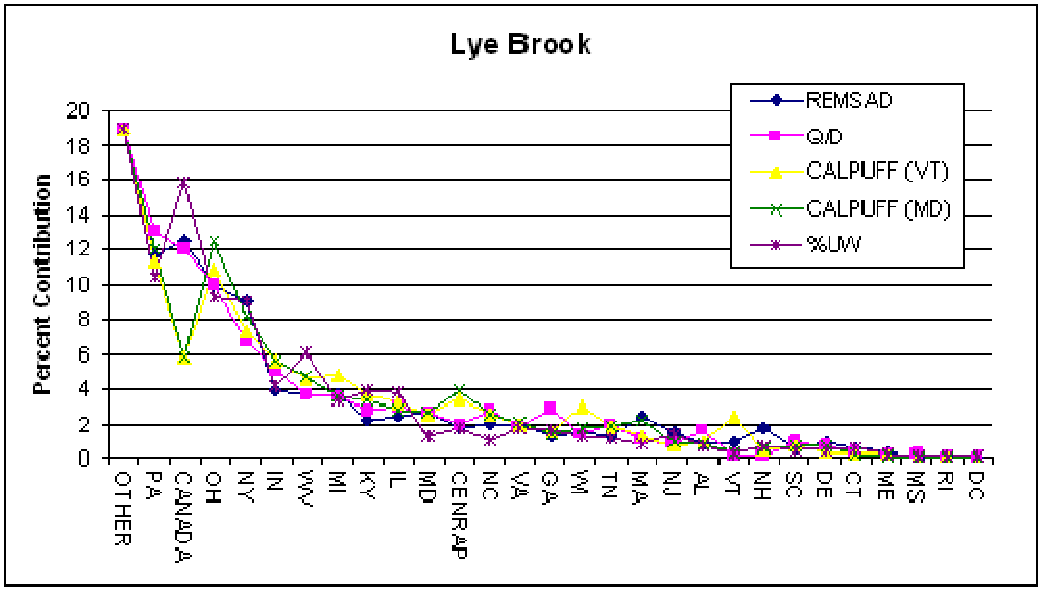

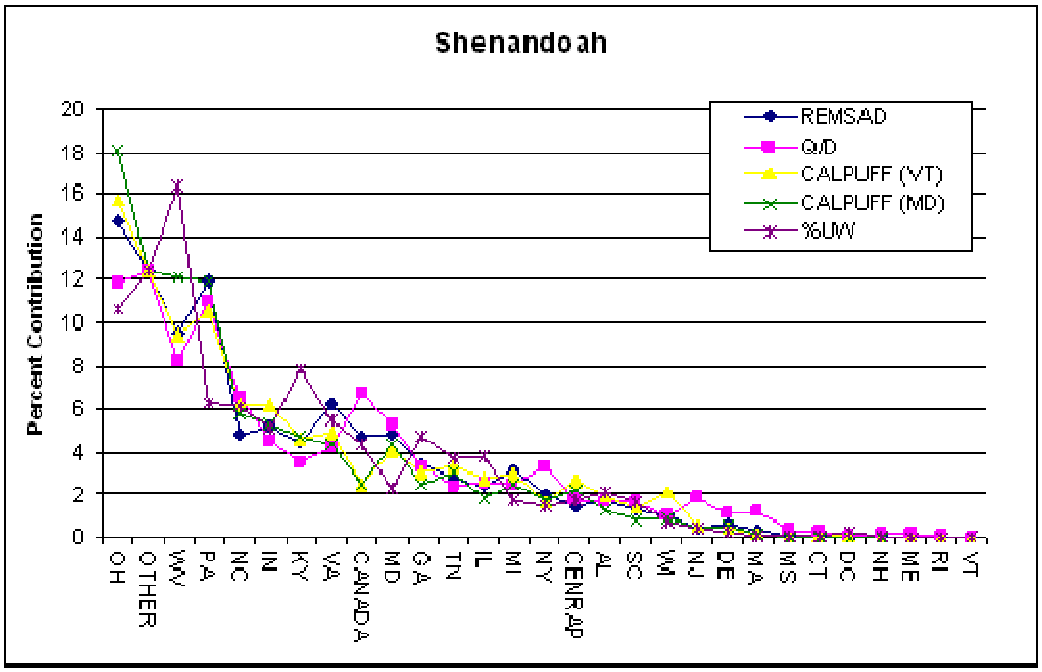

An alternative means of displaying the above results is in Table 8-6, which shows the individual state rankings produced by different assessment techniques for Acadia National Park, Maine. In the left-side column of Table 8-6, states are colored according to their average ranking across the different assessment methods. Those states that are ranked in the top five on average, across all techniques are colored red, while states ranked in the top six through ten are colored magenta, and so on for each group of five going down the left-side column. Through this color scheme, one can see how the states' average ranking compares to their rankings under each individual assessment method given in the other columns of the table. The fact that all techniques tend to come to

consistent conclusions about which states are top contributors provides some confidence that the source regions with the most influence on sulfate levels at MANE-VU Class I sites can be correctly identified. Note that the CENRAP states and several other states along the border of the analysis domain represent only partial state contributions.

Table 8-6. Ranked Contributing States to Acadia Sulfate

Average	REMSAD	Q/d	CALPUFF (VT)	CALPUFF (MD)	E x RTP
CANADA	MA	CANADA	CANADA	MA	CANADA
PA	CANADA	PA	PA	CANADA	PA
OH	PA	OH	OH	OH	OH
MA	ME	NY	MA	PA	NY
NY	OH	IN	NY	NY	IL
IN	NY	MA	IN	IN	WV
WV	WV	MI	MI	WV	IN
ME	NH	WV	WV	CENRAP	MI
MI	MD	IL	ME	MI	KY
IL	IN	GA	IL	NH	CENRAP
KY	MI	NC	CENRAP	KY	VA
CENRAP	VA	KY	KY	IL	ME
MD	NC	VA	NH	NC	GA
NH	NJ	MD	MD	MD	WI
NC	IL	CENRAP	NC	ME	MD
VA	KY	ME	VA	VA	NC
WI	DE	TN	WI	TN	NH
GA	CENRAP	SC	TN	WI	MA
TN	WI	AL	NJ	NJ	TN
NJ	CT	WI	VT	GA	NJ
SC	GA	NH	GA	DE	AL
AL	TN	NJ	SC	SC	SC
DE	SC	DE	CT	AL	CT
CT	AL	CT	DE	CT	DE
VT	RI	MS	AL	RI	VT
RI	VT	RI	RI	VT	DC
MS	MS	VT	DC	DC	RI
DC	DC	DC	MS	MS	MS

Yet one more way of combining the ranked contributions is shown in Figure 8-2, which summarizes the relative contributions of four RPOs, Canada, and "outside domain" regions to ambient sulfate concentrations at several Class I areas using four different assessment techniques. The techniques considered here include: tagged REMSAD modeling, two CALPUFF platforms (MM5-based meteorology used by MDE and NWS observation-based meteorology used by VT DEC), the empirical emissions divided by distance approach (Q/d), and emissions times residence time probability. The estimates of state-by-state sulfate mass contributions ($\mu g/m^3$) from each method have been aggregated by RPO, both in terms of their absolute contribution (these values are displayed within the bars shown in the graphic) and in terms of their proportional contribution relative to other RPOs. It should be noted that the "outside domain"

contribution shown for each analysis method was derived exclusively from the REMSAD result. Averaging estimated impacts at the Acadia, Brigantine, and Lye Brook sites over the four assessment techniques utilized, MANE-VU states account for about 20 to 30 percent of sulfate impacts in these three MANE-VU Class I areas, while the Midwest RPO and VISTAS states each account for about 20 to 25 percent of the total sulfate contribution at Brigantine and Lye Brook and about 10 to 15 percent each at Acadia. The CENRAP states, Canada and "outside domain" add the remainder. Although variation exists across estimates of contribution for different sites and using different techniques, the overall pattern is generally consistent. Relative contributions are somewhat reversed at Shenandoah, which is a VISTAS Class I area. There, VISTAS states and Midwest RPO states account for roughly 20 to 30 percent of overall sulfate impacts, with MANE-VU states contributing roughly 15 to 20 percent.

Figure 8-2. Estimated RPO contributions to sulfate concentrations at Class I areas using different assessment techniques

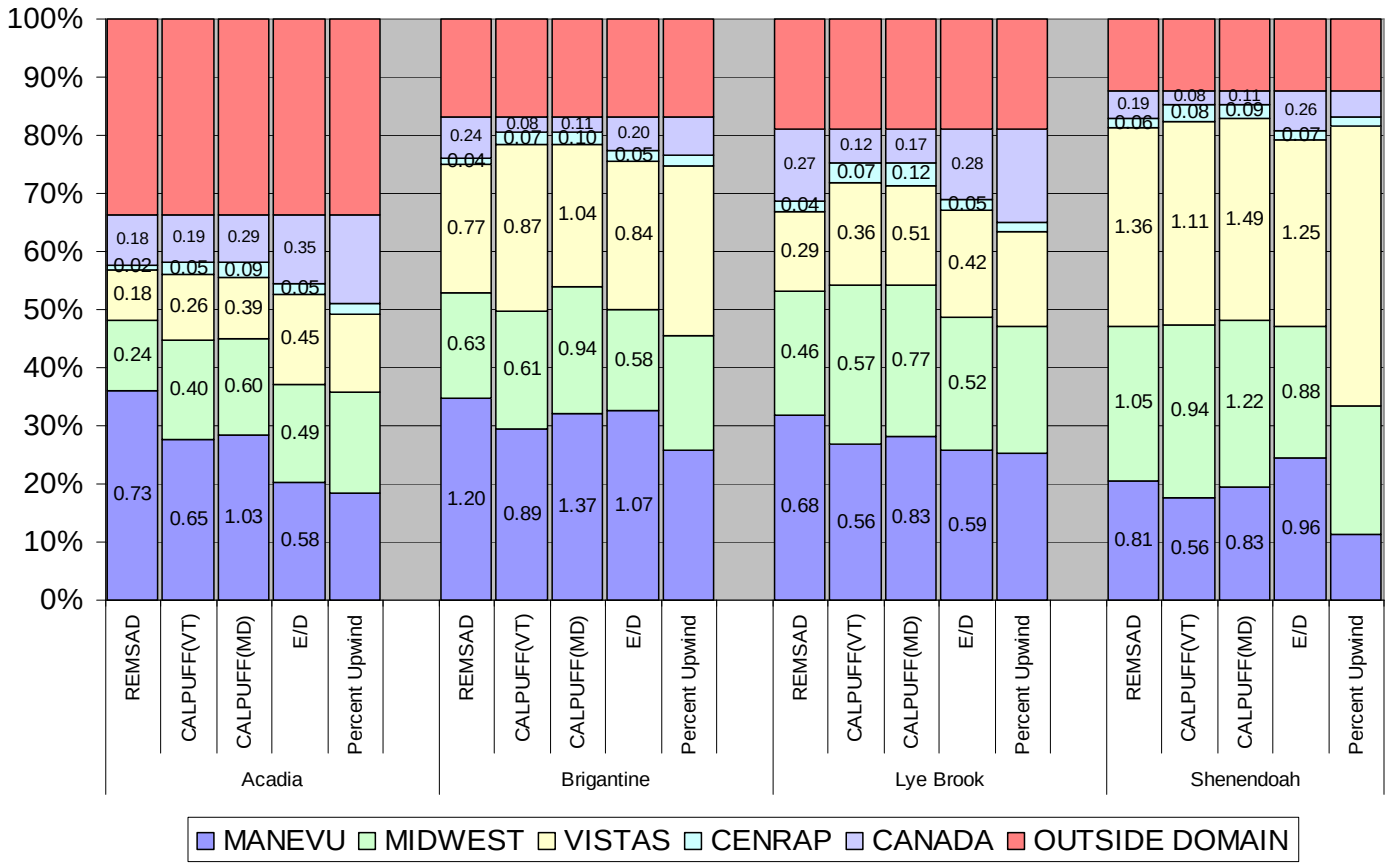

While the foregoing discussion has focused on quantitative methods for comparing contributions from individual states and regions, additional analyses have been conducted to verify and support these results using more qualitative means of identifying "regions of influence" for each Class I area. One such qualitative approach to synthesizing and interpreting the results obtained through different assessment techniques is illustrated in Figure 8-3 and Figure 8-4 below, which show a series of maps shaded to indicate different levels of contribution from different states and regions as determined by the analysis platforms already discussed. In these maps, states are shaded darker the higher they rank in terms of percent contribution to sulfate at a Class I site. For example, in Figure 8-3, states in a line from Indiana through Massachusetts are calculated to have the greatest impact on sulfate at Acadia. Overlaid on top of these maps are contours of

Figure 8-3. Ranked contributions of states to ambient sulfate concentrations at Acadia National Park, Maine.

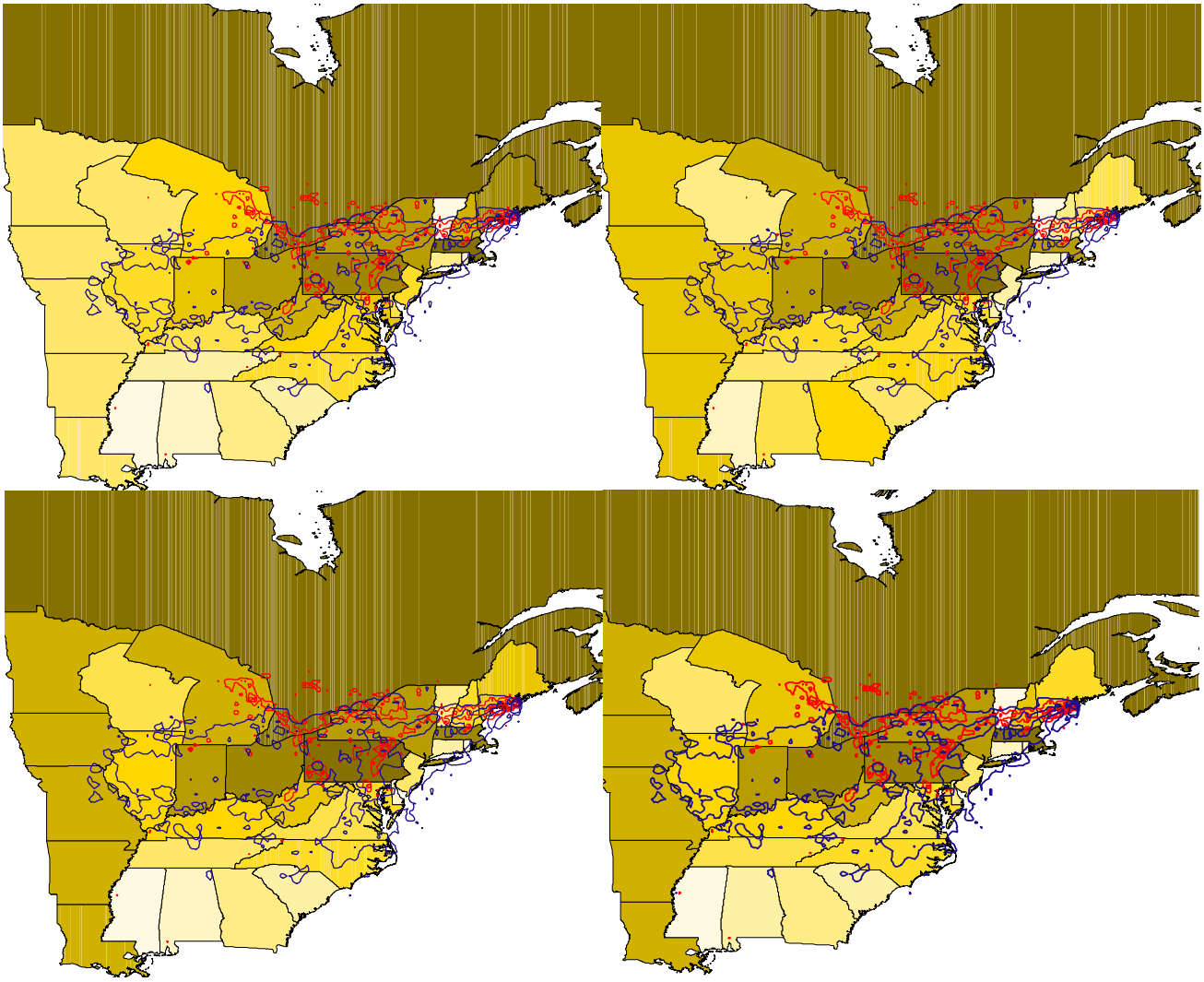

Note: Shaded maps show contributions as estimated by REMSAD, Emissions divided by Distance, CALPUFF VT, and CALPUFF MD. Red and blue contours representing regions of high incremental probability (IP) and high cluster-weighted probability (CWP) are overlaid onto the shaded state maps to indicate similarity of regional contributions as calculated by these independent receptor-based methods.

Incremental Probability (red) and Cluster Weighted Probability (blue) of contributing to sulfate on the highest days. The substantial consistency in the patterns support and bolster the quantitative results. The importance of this finding is that the receptor-based results portrayed by the contours rely on methods that are completely independent of the source-based modeling approaches used to calculate the underlying ranks. This sort of internal consistency among approaches gives considerable strength to the weight-of-evidence approach that MANE-VU has adopted for identifying sulfate source regions.

Figure 8-4. Ranked contributions of states to ambient sulfate concentrations at Brigantine Wilderness Area, New Jersey.

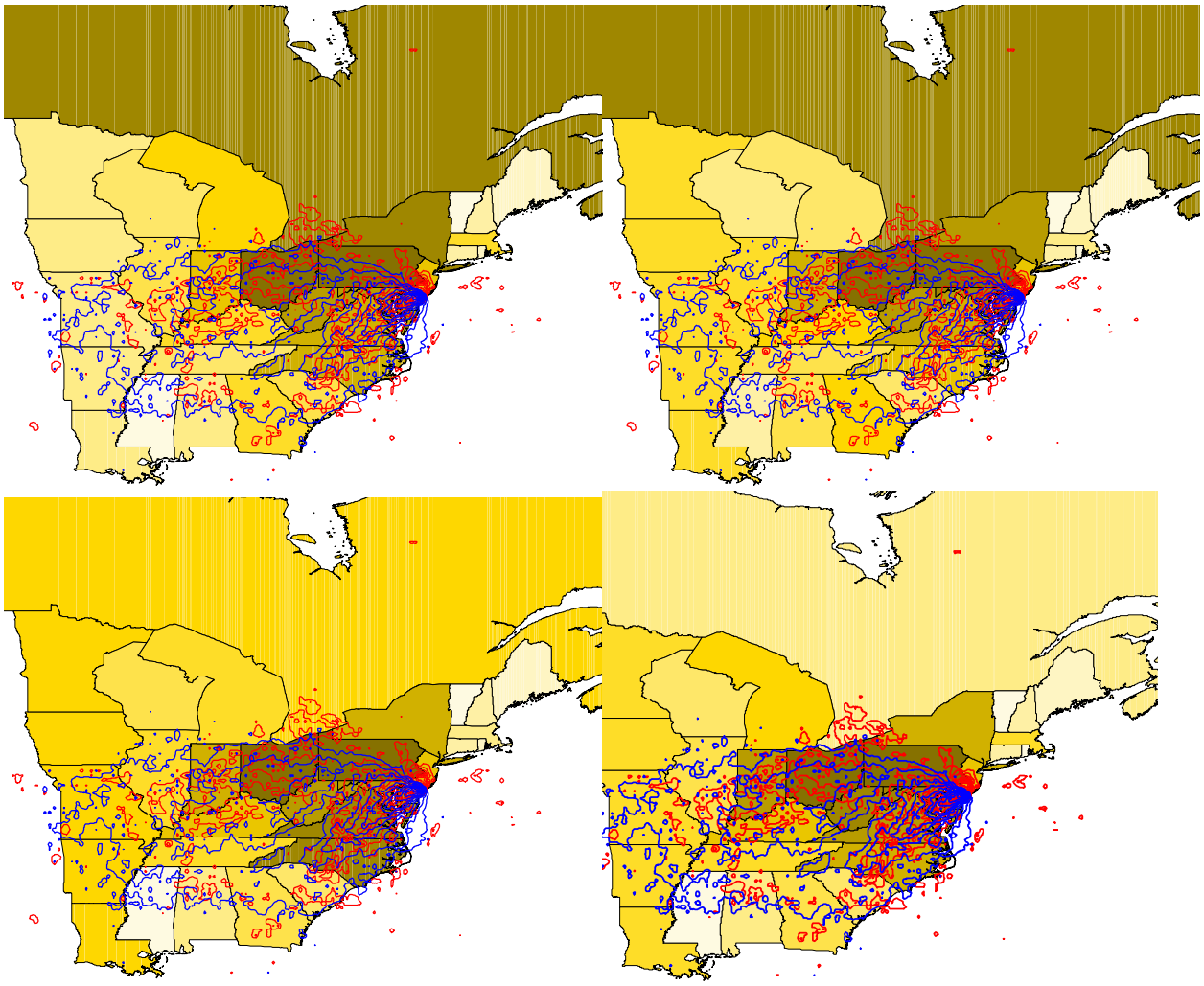

Note: Shaded maps show contributions as estimated by REMSAD, Emissions divided by Distance, CALPUFF VT, and CALPUFF MD. Red and blue contours representing regions of high incremental probability (IP) and high cluster-weighted probability (CWP) are overlaid onto the shaded state maps to indicate similarity of regional contributions as calculated by these independent receptor-based methods.

9. CONCLUSION

As MANE-VU prepares to implement the requirements of the Regional Haze Rule, a significant technical effort has focused on developing multiple analysis tools for assessing contributions to fine particle pollution and thus visibility impairment at Class I areas in the eastern United States. These analysis tools span the discipline of atmospheric science and include traditional Eulerian "source" or "grid" models, Lagrangian dispersion models, back trajectory receptor techniques, source apportionment models, and simple approximations based on empirical relationships between emissions and geography.

A review of the literature and of recent monitoring data has yielded a conceptual model of visibility impairment in the MANE-VU region that attributes a dominant role, on the worst visibility days, to the sulfate component of fine particle matter. This model in turn suggests that the most effective near-term strategy for reducing fine particle pollution and visibility impairment in the East is to continue reducing anthropogenic emissions of SO_2. Reductions in both NO_X and VOCs should also be considered. Given that sulfate, in particular, plays a dominant role in causing visibility impairment throughout the East, MANE-VU has focused on multiple methods of apportioning the sulfate mass found in ambient air at Class I sites to contributing states and regions. This weight-of-evidence approach is intended to overcome large uncertainties that would otherwise undermine confidence in the results obtained using any one modeling or analysis technique in isolation.

The assessment techniques described in this report use numerous approaches to develop ranked lists of individual state contributions to sulfate levels in MANE-VU Class I areas. When these results are normalized and compared, we find broad general agreement concerning the top contributing states at each site as well as some differences that suggest the magnitude of uncertainty inherent in these results.

The conclusions that emerge from this report regarding the relative contributions of different upwind RPOs to downwind sulfate concentrations at MANE-VU Class I areas appear quite robust and the modest differences presented here relative to the preliminary results presented in Spring of 2005 are a further indication that the general patterns of contribution presented here are unlikely to change due to further refinements of the emissions and meteorological inputs. This suggests that the MANE-VU findings are sufficiently robust to serve as a basis for inter-RPO consultations and the regional haze planning process. Given that as much as 30 to 50 percent of the ambient sulfate found at northeastern Class I sites on hazy days appears to originate within neighboring RPOs, coordination and consultation is likely to be critical if MANE-VU is to achieve its visibility goals for 2018 and beyond.

Appendix A: Application of Trajectory Analysis Methods to Sulfate Source Attribution Studies in the Northeast U.S.

Appendix B: Source Attribution by Receptor-Based Methods

Appendix C: Chemical Transport Model Results for Sulfate Source Attribution Studies in the Northeast U.S.

Appendix D: Development of Parallel CALPUFF Dispersion Modeling Platforms for Sulfate Source Attribution Studies in the Northeast U.S.